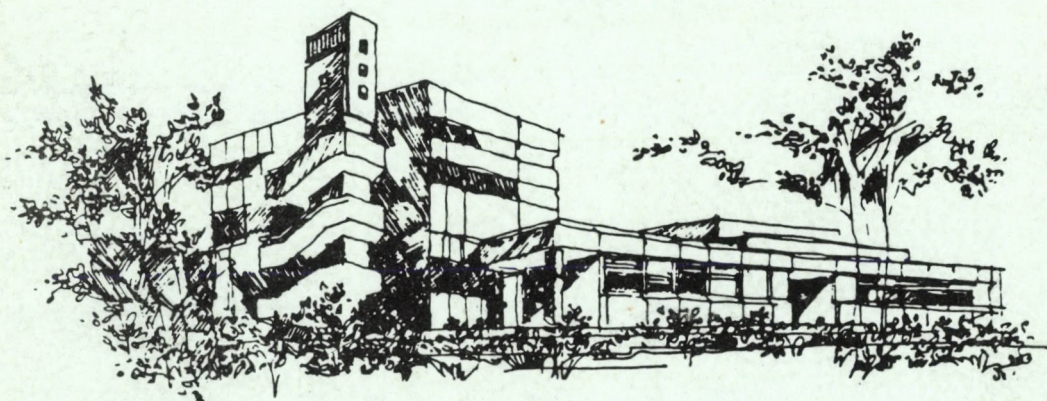


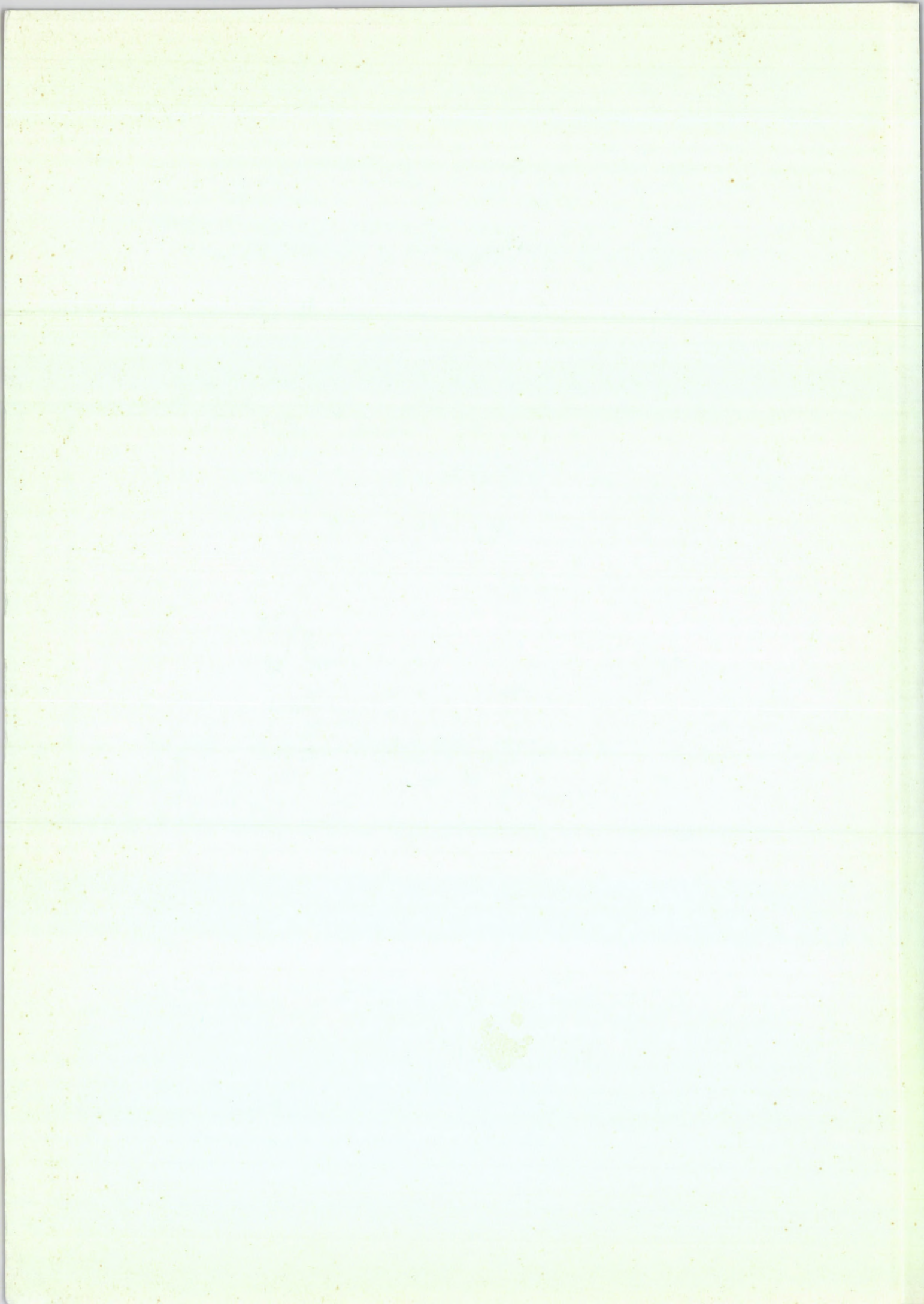
ATOMKI

ANNUAL REPORT

1988



INSTITUTE OF NUCLEAR RESEARCH
OF THE HUNGARIAN ACADEMY OF SCIENCES
DEBRECEN, HUNGARY



INSTITUTE OF NUCLEAR RESEARCH
OF THE HUNGARIAN ACADEMY OF SCIENCES
DEBRECEN, HUNGARY

ANNUAL REPORT

1988

ATOMKI

Postal address:

Debrecen

P. O. Box 51

H-4001

Hungary

Edited by Z. Gácsi

J. Tóth

HU ISSN 0231-3596

P R E F A C E

The contributions included in the present Annual Report 1988 as usual are of progress report character. Looking at the contents of the Annual Report, however, some changes can be observed in the grouping of the contributions.

This Institute (founded in 1954) developed out of the Experimental Physics Department of the Kossuth Lajos University. Formerly (before 1949) this department belonged to the Faculty of Medicine of the Debrecen University. The horizon and interest of the director of Physics Department that time, Professor S. Szalay, the founder of ATOMKI was broad and of interdisciplinary character. This fact determined the research field of the Physics Department, and the research activity of ATOMKI as well from the very beginning.

In the first years of the Institute, in addition to the traditional nuclear physics research, the applications in different fields (medicine, geology, uranium prospecting, etc.) had been started, but that time the applications were overwhelmingly those of **nuclear methods**.

As the years passed away, more and more different, not only nuclear, but several other methods (vacuum techniques, cryogenics, etc.) were also used in the solution of the research tasks. These additional methods originally were applied and improved in the Institute in nuclear physics experiments.

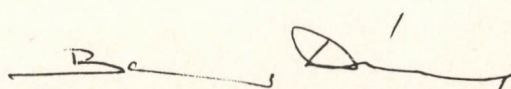
At present, however, other research fields have similar rank and importance as nuclear physics has in the activity of ATOMKI. Thus the sections of the present Annual Report represent the main research fields of the Institute, namely

- nuclear physics
- atomic physics
- materials science and analysis
- earth and cosmic sciences, environmental research
- biological and medical sciences
- development of methods and instruments.

Like in the former volumes of the Annual Reports, the list of publications, the conference contributions and talks of the staff members of ATOMKI are given in the same grouping as the contributions. The titles of the completed theses are also included.

Finally, it is the first time that in the list of seminars not only the traditional hebdomadal seminars of the Institute and the monthly seminars of the Debrecen Physics Centre, but some of the divisional and sectional seminars are also included.

Debrecen, February 28, 1989.


Professor Dénes Berényi
Director

C O N T E N T S

Nuclear Physics	1
Atomic Physics	43
Materials Science and Analysis	69
Earth and Cosmic Sciences, Environmental Research	82
Biological and Medical Research	92
Development of Methods and Instruments	108
Papers Published	127
Conference Contributions and Talks	133
Theses Completed	146
Seminars in the ATOMKI	147
Author Index	153

NUCLEAR PHYSICS

DSA LIFETIMES IN ^{29}P FROM THE REACTION
 $^{28}\text{Si}(p,\gamma)^{29}\text{P}$

Á.Z. Kiss, P. Tikkanen⁺, J. Keinonen⁺, E. Koltay, É. Pintye⁺⁺

The present work contains the first part of a comparative study of the $^{29}\text{P} - ^{29}\text{Si}$ mirror nuclei under course, in which ^{29}P and ^{29}Si are being investigated in reactions $^{28}\text{Si}(p,\gamma)^{29}\text{P}$ and $^{15}\text{N}(^{16}\text{O},pn)^{29}\text{Si}$, respectively.

Previous to this experiment several studies have been reported in the literature on the lifetime values in ^{29}P [1]. However because of the use of thin evaporated targets (Si or SiO_2) on heavier backings or natural thick Si and because of the application of the slowing-down theory without sufficient experimental confirmation, the reported values have large un-

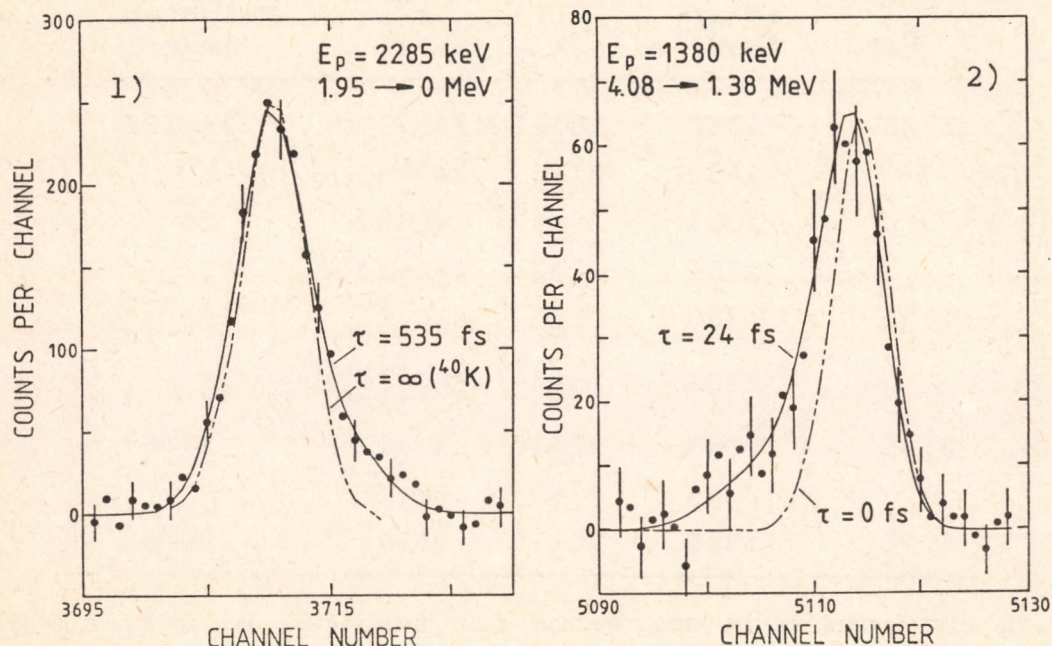


Fig. 1. Portion of γ -ray spectra recorded in the DSA measurement of the 1.95 MeV state. The solid line is the Monte Carlo simulation of the γ -ray line shape at 0° . The fit is shown for the lifetime 535 fs. As a comparison, the line shape of the ^{40}K laboratory background line ($\tau = \infty$) is shown by the dotted curve. The dispersion is 0.53 keV/channel.

Fig. 2. As for Fig. 1, but for the 4.08 MeV unbound state. The fit is shown for the lifetime 24 fs. The dotted curve shows the Monte Carlo simulated line shape for $\tau = 0 \text{ fs}$.

⁺ University of Helsinki, Accelerator Laboratory, Helsinki, Finland

⁺⁺ Department of Radiation Therapy, University Medical School, Debrecen

Certainties and mutual inconsistencies. The above mentioned facts necessitate the remeasurement of lifetimes in ^{29}P applying an improved Doppler shift attenuation (DSA) method [2].

The measurements were performed at the 5 MV Van de Graaff accelerator of the Institute and at the 2.5 MV VdG accelerator of the University of Helsinki Accelerator Laboratory using 10 to 25 μA proton beams. Use was made of implanted ^{28}Si targets prepared by a 15 $\mu\text{g}/\text{cm}^2$ fluence of 60 keV ^{28}Si bombarding 0.4 mm thick Ta plate. Charges of 0.1 - 0.5 C were collected in the recorded γ -ray spectra.

As an example plots of spectra measured at 0° to the beam direction for the 1.9 MeV bound and 4.08 MeV unbound states are presented in Figs. 1 and 2, respectively.

The resulted lifetime values are summarized in Table 1.

Table 1.

E_x (MeV)	Measurement		$F(\tau)$ (%)	$\tau^b)$ (fs)	Weighted ^{d)} mean
	at E_p (keV)				
1.38	1380		20 \pm 7 ^{a)}	248 \pm 100	244 \pm 32
	1652		21 \pm 6	240 \pm 80	
	2083		23 \pm 6 ^{a)}	240 \pm 80	
	2285		21 \pm 2	245 \pm 23 ^{c)}	
1.95	1380		8 \pm 5	610 $\begin{smallmatrix} +500 \\ -260 \end{smallmatrix}$	590 $\begin{smallmatrix} +190 \\ -130 \end{smallmatrix}$
	2285		11 \pm 3	580 $\begin{smallmatrix} +190 \\ -130 \end{smallmatrix}$ ^{c)}	
2.42	2083		82 \pm 11	17 \pm 12	27 \pm 6
	2285		71 \pm 5	30 \pm 6 ^{c)}	
4.08	1380		71 \pm 7	26 \pm 7 ^{c)}	26 \pm 8

a) Values have not been corrected for feeding. b) Only statistical uncertainty is shown. c) Value given is based on the $F(\tau)$ value and line shape analysis. d) Values include uncertainty of 10% in the experimental stopping power.

References

- [1] P. M. Endt and C. van der Leun, Nucl. Phys. A310 (1978) 1
 [2] J. Keinonen, Capture γ -ray spectroscopy and related topics-1984, ed. S. Raman (A.I.P. New York, 1985) p.557.

EXCITATION FUNCTIONS FOR PROTON AND DEUTERON INDUCED
NUCLEAR REACTIONS ON $^{66,67,68}\text{Zn}$

F. Szelecsényi, F. Tárkányi, Z. Kovács, L. Andó, S. Sudár⁺

For investigation of the production possibilities of medically important ^{67}Ga radioisotope with the Debrecen MGC compact cyclotron, (p,xn) and (d,xn) reaction cross sections were studied on enriched $^{66,67,68}\text{Zn}$ [1], [2].

Excitation functions have been measured with stacked-foil technique for $^{66}\text{Zn}(p,n)^{66}\text{Ga}$, $^{67}\text{Zn}(p,n)^{67}\text{Ga}$, $^{67}\text{Zn}(p,2n)^{66}\text{Ga}$, $^{68}\text{Zn}(p,n)^{68}\text{Ga}$ and $^{68}\text{Zn}(p,2n)^{67}\text{Ga}$ reactions up to 18 MeV protons and for $^{66}\text{Zn}(d,n)^{67}\text{Ga}$, $^{67}\text{Zn}(d,n)^{68}\text{Ga}$, $^{67}\text{Zn}(d,2n)^{67}\text{Ga}$ and $^{68}\text{Zn}(d,2n)^{68}\text{Ga}$ reactions up to 10 MeV deuterons.

The obtained results have been compared with previous measurements and with the predictions of the statistical/precompound reaction models. Our data in general are in good agreement with the existing previous results. In several cases, however, the position of maximum of excitation function lies lower than it was reported. The calculated absolute cross sections are also in good agreement with our measured data.

It was found that in our available low energy range the $^{67}\text{Zn}(p,n)^{67}\text{Ga}$ and the $^{68}\text{Zn}(p,2n)^{67}\text{Ga}$ reactions are the major process of interest. The results for the $^{67}\text{Zn}(p,n)^{67}\text{Ga}$, $^{67}\text{Zn}(p,2n)^{66}\text{Ga}$ and the $^{68}\text{Zn}(p,2n)^{67}\text{Ga}$ reactions are given in Fig. 1 and 2 in comparison with earlier reported experimental data [3].

References

- [1] I. Mahunka, F. Tárkányi, L. Andó, F. Szelecsényi, A. Fenyvesi, F. Ditrói, S. Takács, Medical Application of Cyclotrons IV, Ann. Univ. Turkuensis D: 27 1988. p. 137.
- [2] I. Mahunka, F. Szelecsényi, F. Tárkányi, The Abo Akademi Accelerator Biennial Report 1983-84, p. 153.
- [3] F.E. Little, M.C. Lagunas-Solar, Int. J. Appl. Radiat. Isot. 34 (1983)34.

⁺Inst. Experimental Phys., L. Kossuth University, Debrecen

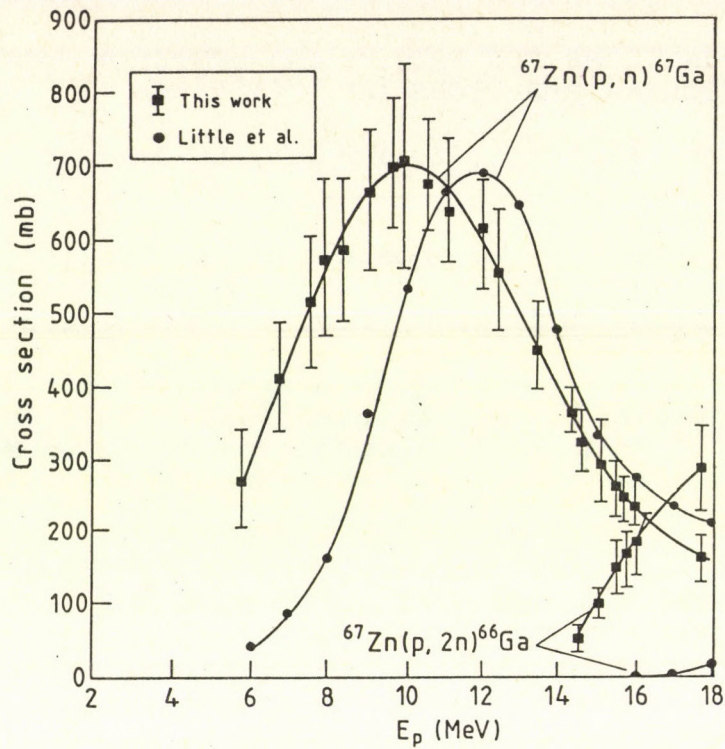


Fig.1. Excitation functions of $^{67}\text{Zn}(p, n)^{67}\text{Ga}$ and $^{67}\text{Zn}(p, 2n)^{66}\text{Ga}$ reactions.

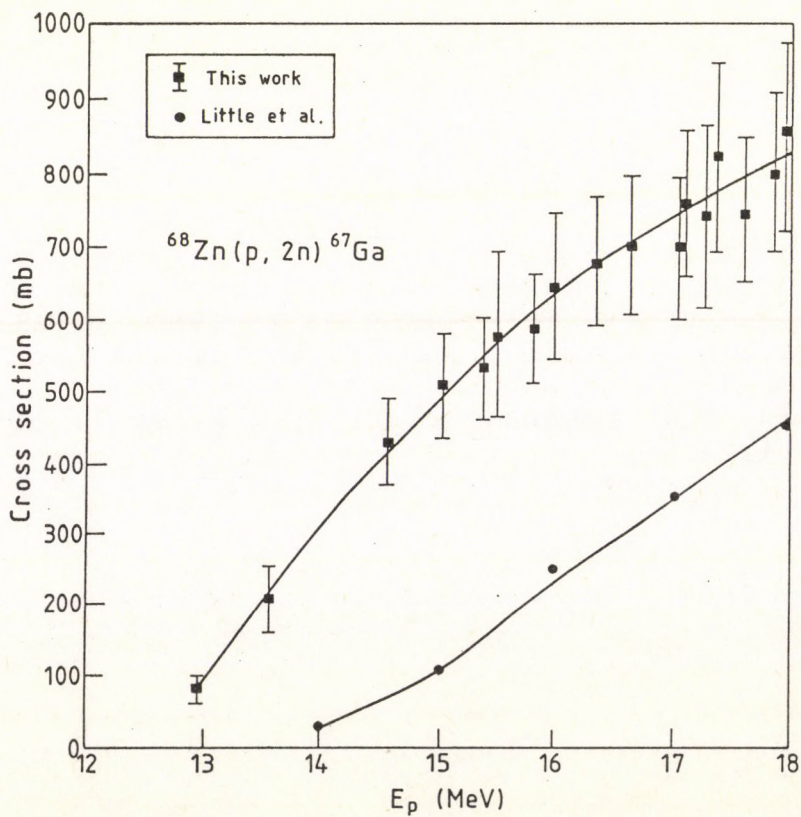


Fig.2. Excitation functions of $^{68}\text{Zn}(p, 2n)^{67}\text{Ga}$ reaction.

IN-BEAM SPECTROSCOPY OF ^{106}In

J. Gulyás, Zs. Dombrádi, T. Fényes, J. Timár, A. Passoja*,
J. Kumpulainen** and R. Julin**

Gamma-ray and internal conversion electron singles spectra of the $^{106}\text{Cd}(p,n\gamma)^{106}\text{In}$ reaction were measured with Ge(HP), Ge(Li), LEPS and combined intermediate-image magnetic plus Si(Li), as well as superconducting magnetic lens plus Si(Li) spectrometers at various bombarding proton energies between 8.0 and 9.0 MeV. Gamma-gamma coincidence and angular distribution of gamma rays were also measured. More than 120 (among them 95 new) gamma transitions have been assigned to ^{106}In . From the conversion electron measurements internal conversion coefficients of 18 gamma-transitions have been determined for the first time.

A more complete level scheme of ^{106}In has been constructed, which contains about 40 levels below 1600 keV excitation energy. On the basis of the internal conversion coefficients of transitions, Hauser-Feshbach analysis of (p,n) reaction cross sections, gamma-ray angular distributions and other arguments spin and parity assignments to several levels have been made. Gamma branching ratios have also been deduced. Energies of several ^{106}In proton-neutron multiplets were calculated on the basis of the parabolic rule derived from the cluster-vibration model. Interacting boson-fermion-fermion / odd-odd truncated quadrupole phonon model calculations are in progress.

* University of Joensuu, Department of Physics, Finland
** University of Jyväskylä, Department of Physics, Finland

NUCLEAR STRUCTURE OF ^{108}In

A. Krasznahorkay, Zs. Dombrádi, J. Timár, T. Fényes, J. Gulyás,
J. Kumpulainen⁺ and E. Verho⁺

The structure of ^{108}In has been studied with in-beam γ - and e^- -spectroscopic methods [1]. A more complete level scheme of ^{108}In has been deduced which contains 54 levels below 1630 keV excitation energy (including 42 new ones). On the basis of the internal conversion coefficients of transitions, Hauser-Feshbach analysis of (p,n) reaction cross sections, γ -ray angular distributions and other arguments spin and parity assignments were made to 24 excited ^{108}In levels. Lifetime measurements were performed by delayed coincidence method. The energies of several ^{108}In proton-neutron multiplets were calculated on the basis of the parabolic rule derived from the quasi-cluster-vibration model (QCVM) /fig. 1/. In order to facilitate the configuration assignments the electromagnetic decay properties of the nuclear levels were also analysed. Members of different proton-neutron multiplets have been identified.

An interesting result is that the energy splitting of the $\pi\tilde{g}_{9/2}\nu\tilde{g}_{7/2}$ multiplet is much larger than expected, and the "parabola" is far not perfect. In order to get a better description for the nuclear structure interacting boson-fermion-fermion/ odd-odd truncated quadrupole phonon model calculations were also performed. The particle - vibration exchange interaction was included also in the calculations, and a reasonable description of the level energy spectrum /fig. 2/ and electromagnetic properties of ^{108}In was obtained. The inclusion of the particle-vibration exchange interaction resulted in a W type energy splitting of the $\pi\tilde{g}_{9/2}\nu\tilde{g}_{7/2}$ multiplet as a function of $J(J+1)$, where J is the spin of the nuclear state.

This work was supported partly by the National Scientific Research Foundation /OTKA/.

Reference:

1. A. Krasznahorkay et al., ATOMKI Ann. Rep. 1987, p. 41

⁺University of Jyväskylä, Department of Physics, Finland

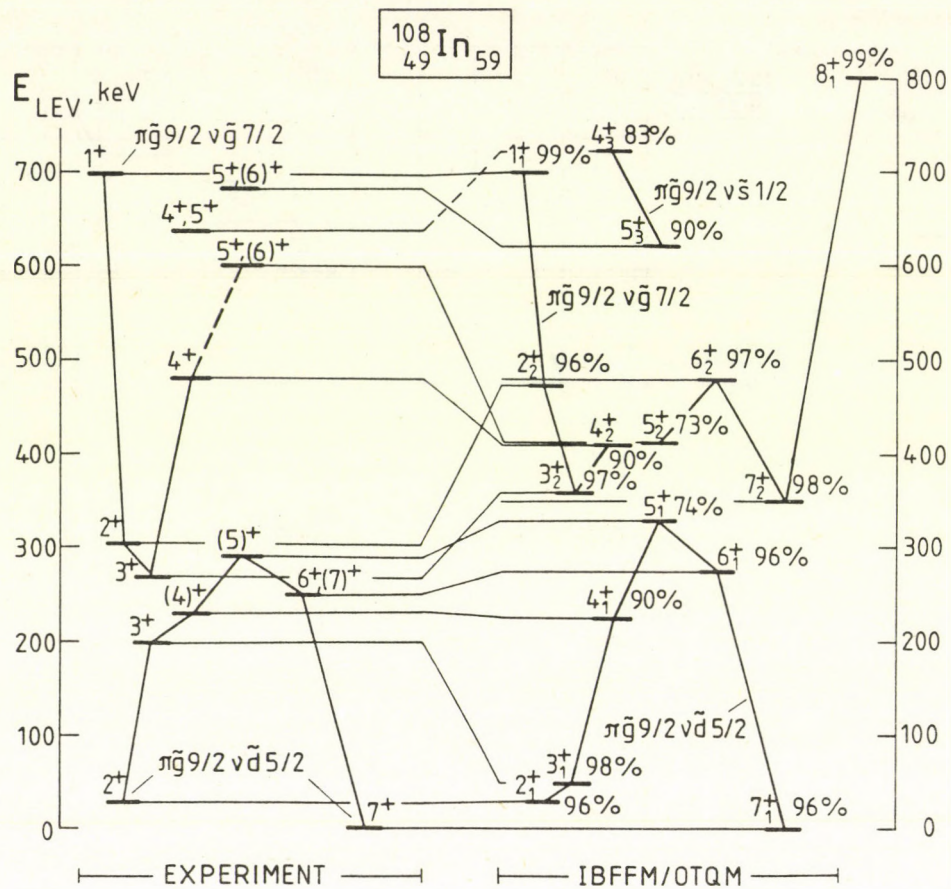


Fig. 2. IBFFM/OTQM energy spectrum of ^{108}In in comparison with experimental data. After the spin and parity of the state "purity" is shown (in %), which characterizes the total strength of the indicated configuration in the wave function. States having identical main components are connected with solid lines.

NUCLEAR STRUCTURE OF ^{110}In

A. Krasznahorkay, Zs. Dombrádi, J. Tímár, Z. Gácsi, T. Kibédi

A. Passoja*, R. Julin*, J. Kumpulainen*, S. Brant** and V. Paar**

In our earlier work on ^{108}In [1] we observed some indications on deviation of the pattern of the $\pi(g_{9/2}^{-1})\nu(\tilde{g}_{7/2})$ multiplet from the one predicted by the parabolic rule. To obtain more information on this interesting multiplet splitting and to test the validity of predictions for the ^{110}In nucleus, where a similar deviation is expected, the nucleus ^{110}In has been studied via the reactions $^{107}\text{Ag}(\alpha, n\gamma)^{110}\text{In}$ and $^{110}\text{Cd}(p, n\gamma)^{110}\text{In}$.

γ -ray and $\gamma\gamma$ -coincidence measurements have been performed. Energies and relative intensities of 137 transitions in ^{110}In have been determined. A more complete level scheme, containing 53 levels, has been deduced. The energy separation of the $J^\pi=7_1^+$ ($T_{1/2}=4.9$ h) ground state and the $J^\pi=2_1^+$ ($T_{1/2}=69.1$ min) isomer has been deduced: $E(2_1^+)=62.08\pm 0.04$ keV. The electron spectrum of the reaction was measured with a superconducting magnetic spectrometer. Internal conversion coefficients of 30 transitions have been determined. Spins and parities have been deduced on the basis of the multipolarity of γ -transitions, and other arguments. Lifetime measurements were performed by delayed coincidence and DSA methods.

The energies and electromagnetic properties of the ^{110}In states were calculated using the interacting boson-fermion-fermion/odd-odd truncated quadrupole phonon model. Several approximate proton-neutron multiplet states were identified, the W-like energy splitting of the $\pi(g_{9/2}^{-1})\nu(\tilde{g}_{7/2})$ multiplet was reproduced, and the importance of the exchange interaction in spherical odd-odd nuclei was pointed out.

* University of Jyväskylä, Department of Physics, Finland

** Prirodoslovno-Matematički Fakultet, University of Zagreb, Yugoslavia

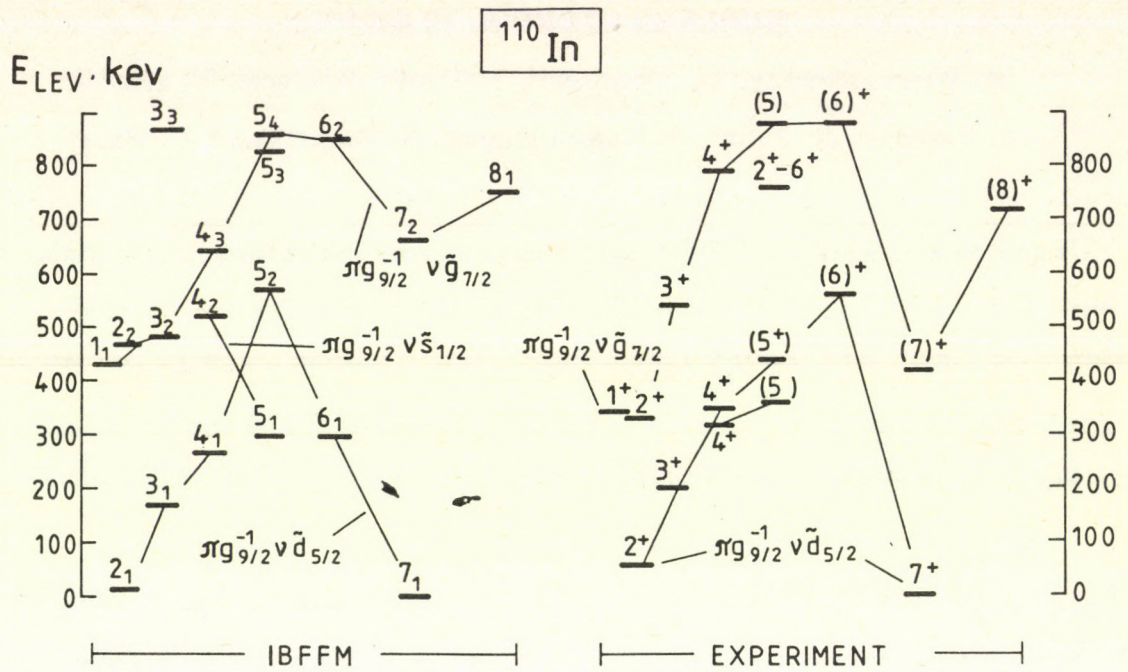


Fig. 6. Low-lying positive parity levels of ^{110}In below 0.9 MeV. The calculated and experimental states are denoted by IBFFM and EXPERIMENT, respectively. In addition to the states assigned to proton-neutron multiplets, there appear two additional ones in the IBFFM calculation: the 3_3 and the 5_3 level.

References:

- [1] A. Kasznahorkay et al., Nucl. Phys. A, in press

NUCLEAR ELECTRIC MONOPOLE STRENGTHS AND BRANCHING RATIOS IN ^{116}Sn

Z. Gácsi

This contribution eliminates a discrepancy of a factor of three apparent in the compiled and former experimental data¹ on the branching ratios of the first 5^- level at 2366 keV excitation energy in ^{116}Sn (See Fig.1) and suggests strong mixing between its low-lying 0^+ states of different radii.

Gamma-ray and internal conversion electron spectra were recorded with Ge(Li) and superconducting magnetic lens plus Si(Li) spectrometers in $^{113}\text{In}(\alpha, n\gamma)^{116}\text{Sb} \rightarrow ^{116}\text{Sn}$, $E = 14.5$ MeV and in $^{116}\text{Sn}(p, p'\gamma e^-)^{116}\text{Sn}$, $E_p = 7.2$ MeV reactions, respectively.

0^+ states

Internal conversion electron branching ratios

$$I_e(0_2^+ \rightarrow 0_1^+) / I_e(0_2^+ \rightarrow 2_1^+) = 0.33(5)$$

and

$$I_e(0_3^+ \rightarrow 0_2^+) / I_e(0_3^+ \rightarrow 2_1^+) \geq 4.9$$

have been determined. Combined with the absolute $B(E2)$ values of Ref.2, nuclear electric monopole strength values of

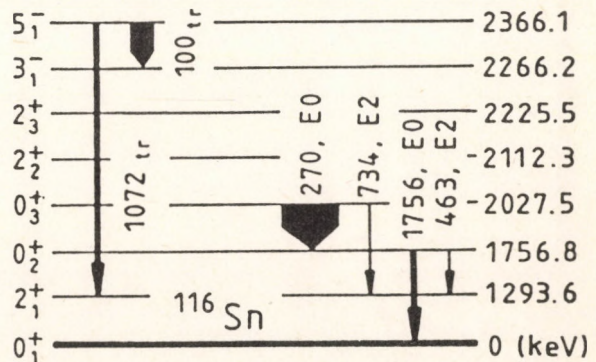
$$\rho^2(0_2^+ \rightarrow 0_1^+) = 3.8(6) \times 10^{-3}$$

which agrees well with $4.3(13) \times 10^{-3}$ (Ref.2), and of

$$\rho^2(0_3^+ \rightarrow 0_2^+) \geq 28.3 \times 10^{-3}$$

which does not contradict the value of $103(21) \times 10^{-3}$ (Ref.2), have been deduced. The present results confirm and support the previously revealed structural features of the first two excited 0^+ states, which can now be supplemented, based on a recent study³, that such a large value of $\rho^2(0_3^+ \rightarrow 0_2^+)$ indicates strong mixing of the two 0^+ states with different radii and possibly also mixture between states with different shapes: the 0_2^+ level at 1756.8 keV excitation energy is related to the intruder deformed state and the 0_3^+ level at 2027.5 keV corresponds to the spherical one: as the unperturbed configurations.

Fig.1. Low-lying levels of ^{116}Sn . The line-thickness represents relative transition intensity at the 5^- level and relative values of the monopole strengths for the $E0$ transitions.



5₁⁻ State

The 2366.1 keV, 5₁⁻ state in ¹¹⁶Sn decays to the one quadrupole phonon state of 1293.6 keV, 2₁⁺ and to the one octupole phonon state of 2266.2 keV, 3₁⁻. In understanding the structural relation of the 5₁⁻ state to these phonon states, it is crucial to know its branching ratio. Using the gamma-ray relative intensities in this work, we obtained:

$$R_{\gamma} = I_{\gamma}(99.9 \text{ keV}) / I_{\gamma}(1072.5 \text{ keV}) = 100(4) / 96(6).$$

When combined with the total internal conversion coefficients¹, we get the transition branching ratio:

$$R_{\text{tr}} = 100(4) / 37(3).$$

These values agree very well with previous results. There is, however, a factor of about three discrepancy between the gamma branching ratios in the adopted value in Ref.1. and in this work. This is due only to a mistaken adoption of transition intensities as gamma intensities in the compilation¹, and the discrepancy can be eliminated by a clear distinction between them.

References:

- ¹ J. Blachot et al., Nucl. Data Sheets 32 (1981)267 and references therein
- ² J. Kantele et al., Z. Physik A289 (1979) 157
- ³ K. Heyde and R.A. Meyer, Phys. Rev. C37 (1988)2170

BAND STRUCTURES IN THE ODD - ODD NUCLEUS ^{126}La

B.M. Nyakó^o, J. Gizon*, D. Barneoud*, A. Gizon*, M. Józsa,
W. Klamra⁺, F.A. Beck[∇] and J. C. Merdinger[∇]

The high spin structure of odd-odd $A \approx 130$ nuclei has recently become actively studied as it could give additional information on the role of the different shape-driving effects of low- Ω $h_{1/2}$ protons and high- Ω $h_{1/2}$ neutrons on the nuclear shape. The nucleus ^{126}La offers the possibility of extending our knowledge on heavier lanthanums [1] to a more neutron deficient one, where the effect of high- Ω neutron orbitals driving the nucleus towards more triaxial shape is expected to decrease. As little was known earlier [2] in this nucleus, we decided to further develop its decay scheme at high spins.

Two experiments were carried out to populate excited states of ^{126}La . The reactions used were $^{111}\text{Cd}(^{19}\text{F}, 4n)$ at 90 MeV and $^{93}\text{Nb}(^{37}\text{Cl}, p3n)$ at 155 MeV. Evaporated gold-backed ^{111}Cd and 4 stacked self-supporting ^{93}Nb targets were applied, respectively. The level scheme was established by taking γ - γ coincidence data by the "Chateau de Cristal" detector array at the MP tandem in CRN, Strasbourg. Compton-suppressed Ge detectors and, in the second experiment, 2 planar high purity Ge detectors were employed together with a BaF_2 "ball" measuring the total energy and multiplicity of the γ -cascades. Coincidence data were sorted into γ - γ and γ -X matrices, where X is used for γ -events in a planar Ge.

Three band structures have been identified in this nucleus as shown in figure 1. The bands are labelled according to their decreasing intensity. Bands 2 and 3 were assigned to ^{126}La on the basis of coincidence relations of the strongest M1 transitions with La X-rays and using information from β -decay of ^{126}Ce [3]. Bands 1 and 2 consist of M1 intraband and E2 cross-over transitions, with a relatively large signature splitting in the energy of the M1 transitions for band 1 and almost no signature splitting in band 2. The measured $B(\text{M1})/B(\text{E2})$ reduced transition probability ratios vary from ~ 2.5 to 1.1 with increasing spin for band 1. These ratios are close to unity in the negative parity band. No backbending is seen in the positive parity band, but a bandcrossing is clearly visible near $\hbar\omega \approx 0.4$ MeV in band 2. Such facts indicate different natures for these two bands. For band 3 only one signature member has been observed.

No spin and parity measurements are available for odd-odd nuclei in the considered mass region. Therefore the interpre-

^o On leave of absence in ISN, Grenoble

* Institut des Sciences Nucléaires, Grenoble, France

+ Manne Siegbahninstituttet för fysik, Stockholm, Sweden

∇ Centre de Recherches Nucléaires, Strasbourg, France

tations of the observed band structures are based on qualitative considerations and/or systematics. We proposed [4] $\pi h_{11/2} \nu h_{11/2}$ and $\pi h_{11/2} \nu g_{7/2}$ configurations for bands 1 and 2, respectively. This is based on similarities between the main characteristics of these bands and those of other odd-odd La isotopes [1] as well as on arguments drawn from signature splitting systematics derived from odd $A \approx 125$ nuclei [5]. For these configurations the spin and parity of the band heads are proposed to be 4^+ and 3^- (band 1 and 2), using predictions of the Gallagher-Moszkowski coupling rule. The interpretation of band 3 and its coupling to band 2 is not yet understood and therefore we intend to continue our work in this direction.

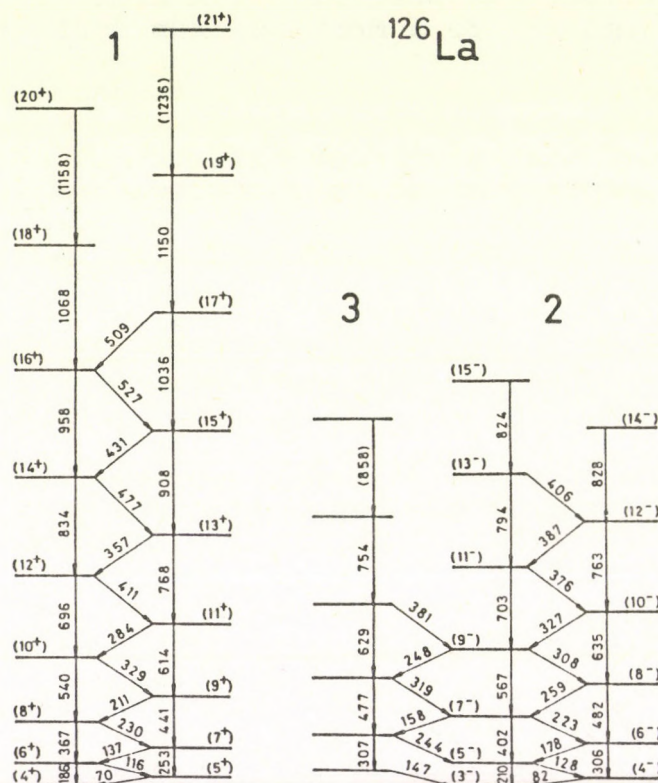


Fig. 1. Collective band structures in ^{126}La . Transition energies (in keV) and tentative spin/parity values are given. The energy of the band heads is unknown.

References

- [1] P.J. Nolan et al.: J. Phys. G: Nucl. Phys. 13 (1987) 1555
M.J. Godfrey et al.: to be published.
- [2] M.A. Quader et al.: Phys. Rev. C33 (1986) 1109
- [3] J. Genevey et al.: Proc. of Fifth Int. Conf. of Nuclei far from Stability. Rosseau Lake, Canada (1987)
- [4] B.M. Nyakó et al.: Z. Phys. accepted for publication
- [5] F.S. Stephens et al.: Phys. Rev. Lett. 29(1972) 438
J. Gizon, A. Gizon: Z. Phys. A285(1978) 259

IDENTIFICATION OF COLLECTIVE STRUCTURES IN ^{127}Ce

B.M. Nyakó^o, J. Gizon^{*}, D. Barneoud^{*}, A. Gizon^{*}, W. Klamra⁺
 F.A. Beck[∇] and J.C. Merdinger[∇]

The neutron-deficient cerium isotopes have been the subject of studies concerning the γ -softness of nuclei near $A \approx 130$ [1,2]. Recently more attention has been paid to $A \approx 125$ ceriums [3] but no data was available for the high spin states of ^{127}Ce .

Excited states in this nucleus were populated via the $^{93}\text{Nb}(^{37}\text{Cl}, 3n)$ nuclear reaction. Experimental details are given in our Report for ^{126}La in this booklet. Two rotational structures have been identified in ^{127}Ce as shown in fig.1. Their assignment to this nucleus is based on a recoil- γ coincidence experiment [4] and on γ -(Ce X-ray) coincidences. The tentative spin and parity of the states were derived from level energy systematics of neighbouring odd-neutron Ce isotopes: The negative parity band shows a signature splitting comparable to those of the $h_{11/2}$ neutron hole band in $^{125}, ^{129}\text{Ce}$ [1-3], the positive parity band shows no splitting, similarly to the $g_{7/2}$ neutron hole band in these nuclei. A backbending starts to develop in both the positive and negative parity bands as seen from additional transitions on top of those indicated in fig.1. The ordering of these transitions was difficult due to lack of statistics, but it seems obvious that these backbendings are caused by the alignment of $h_{11/2}$ protons. The aim of further works in progress is to extend the observed bands to higher spin.

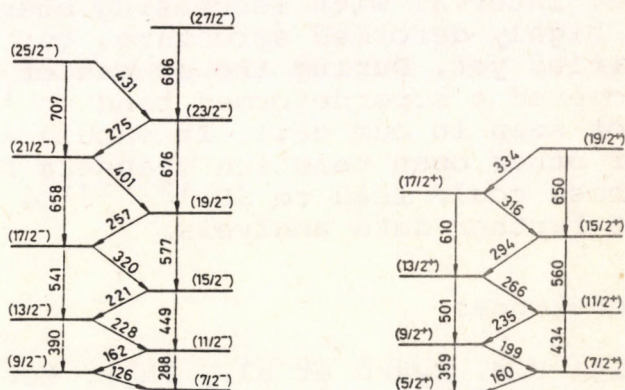


Figure 1. Proposed decay scheme of ^{127}Ce .

References

- [1] J. Gizon et al.: Nucl. Phys. A290 (1977) 272
- [2] P.J. Nolan et al.: Phys. Lett. 108B (1982) 269
 R. Aryaeinejad et al.: J. Phys. G: Nucl. Phys. 10(1984) 955
- [3] K.L. Ying et al.: Nucl. Structure Appendix to the Daresbury Ann. Rep. (1986/87) 27
- [4] A.N. James et al.: ibid (1985/86) 103

^o On leave of absence in ISN, Grenoble

^{*} Institut des Sciences Nucléaires, Grenoble, France

⁺ Manne Siegbahninstituttet för fysik, Stockholm, Sweden

[∇] Centre de Recherches Nucléaires, Strasbourg, France

SEARCH FOR SUPERDEFORMATION IN ^{129}La

B.M. Nyakó^o, S. André*, D. Barneoud*, F.A. Beck⁺, H. El-Samman[∇],
 C. Foin*, J. Genevey*, A. Gizon*, J. Gizon*, M. Józsa,
 J.C. Merdinger⁺ and L. Zolnai

The first observation of superdeformed (SD) nuclear shape with a major-to-minor axis ratio of 2:1 at high spins [1] was followed by the identification of several $A \approx 130$ SD nuclei [2] with an axis ratio of 3:2. Calculations made by Chasman [3] using the Strutinsky method show that the observation of 2:1 SD bands in $A \approx 150$ nuclei can be well accounted for by the appearance of a deep "valley" in the well-depth of the SD minima calculated as a function of Z and N for spin $I=50$. The observed cases for 3:2 superdeformation, however, do not correspond to the region predicted by a shallower valley along $Z \approx 57$ where nuclei are difficult or impossible to produce in heavy ion induced reactions. The nucleus ^{129}La is near the end of this second valley, therefore it seemed to be a good candidate to search for superdeformation in it.

High spin states of ^{129}La were excited via the reaction $^{100}\text{Mo} + ^{34}\text{S}$ at 165 MeV bombarding energy. Coincidence γ - γ events were taken with the "Chateau de Cristal" multidetector system at CRN, Strasbourg. Data were analysed using the γ -energy correlation method. Perpendicular cuts to the equal energy diagonal in the E_{γ_1} - E_{γ_2} matrix show the probable existence of a rotational structure for which the dynamic moment of inertia decreases from $I^{(2)} \approx 50 \hbar^2/\text{MeV}$ to $I^{(2)} \approx 35 \hbar^2/\text{MeV}$ in the $E_{\gamma} = 1100$ -1600 keV interval with increasing energy. This could correspond to a highly deformed structure, but no discrete band has been identified yet. During the course of this work Nolan et al [4] discovered a superdeformed band in ^{130}La . This band, however, was not seen in our data. It should also be noted, that the effect of other open reaction channels has to be checked as some of those could lead to SD $^{131,132}\text{Ce}$ [4], and this is the subject of further data analysis.

References

- [1] B.M. Nyakó et al., Phys. Rev. Lett. 52(1984)507
 P.J. Twin et al., Phys. Rev. Lett. 57(1986)811
- [2] P.J. Nolan and P.J. Twin, Ann. Rev. of Nucl. Part. Sci. 38(1988) in press (and references therein)
- [3] R.R. Chasman, Physics Letters B187(1987)219
- [4] P.J. Nolan et al., Workshop on Nuclear Structure, Copenhagen 1988 Slide Report p. 29.

^o On leave of absence in ISN, Grenoble

* Institut des Sciences Nucléaires, Grenoble, France

+ Centre de Recherches Nucléaires, Strasbourg, France

∇ Department of Physics, Menoufia University, Shebine El-Koom, Egypt

CALIBRATION OF THE ANALYZING MAGNET OF THE MGC CYCLOTRON

M. Józsa, Z. Máté, Z. Veress*, L. Zolnai

The nuclear reaction experiments at the MGC cyclotron of ATOMKI are performed with the use of a magnetic analyzer. The energy of the analyzed beam is determined from the NMR frequency ν by the well-known formula

$$E = K A \nu^2 / \left(1 + \frac{K A \nu^2}{2 E_0} \right). \quad (1)$$

Here K is a parameter characteristic for the magnet, the quantities A and E_0 are simply connected with the parameters of the accelerated ions. The energy calibration of the magnet, i.e. the determination of K is usually made by measuring the excitation function for a resonance state with well-known energy. However, for such a measurement it is necessary to have a rough value of K . We present here the result of a simple method that was used for the determination of such an approximate K -value.

The calibration was realized with the use of the $^{27}\text{Al}(p, \alpha)^{24}\text{Mg}$ reaction. The energy of the outgoing alpha particles was measured with five silicon detectors mounted in the scattering chamber at different angles. The detectors were calibrated with a radioactive alpha source (^{239}Pu , ^{241}Am , ^{244}Cm). The energy of the incoming protons was then calculated from the measured alpha energies using the appropriate kinematical formulae. Substituting the obtained proton energy (E) and the measured NMR frequency into formula (1) we extracted the value of K .

We performed such measurements at five different bombarding proton energies in the interval 5.5÷9.7 MeV. The data shows that K can be considered as a parameter not depending on ν . The averaged value of K was obtained as

$$(26.453 \pm 0.052) \text{ keV} / (\text{MHz})^2.$$

* Bajcsy-Zsilinszky Secondary School, Újfehértó

PROTON ELASTIC SCATTERING ON $^{114,122,124}\text{Sn}$
ISOTOPES NEAR THE COULOMB BARRIER

M. Józsa, Z. Máté, Z. Veress*, T. Vertse and L. Zolnai

In a previous paper [1] it was shown that the energy dependence of the real part of the volume integral of the proton optical potential has anomalous behaviour near the Coulomb barrier for the $p+^{116}\text{Sn}$ and $p+^{120}\text{Sn}$ systems. Similar result for the $p+^{124}\text{Sn}$ system has been published in ref. [2].

The aim of the recent measurements for $p+^{114}\text{Sn}$, $p+^{122}\text{Sn}$ and $p+^{124}\text{Sn}$ systems was to extend the investigation along the $Z=50$ isotopes. The measurements were done using the proton beam of the MGC cyclotron of the Atomki at energies different from those of the isobar analogue resonances. The measured angular distributions are being analysed in the frame of the optical model. An example is shown in fig. 1.

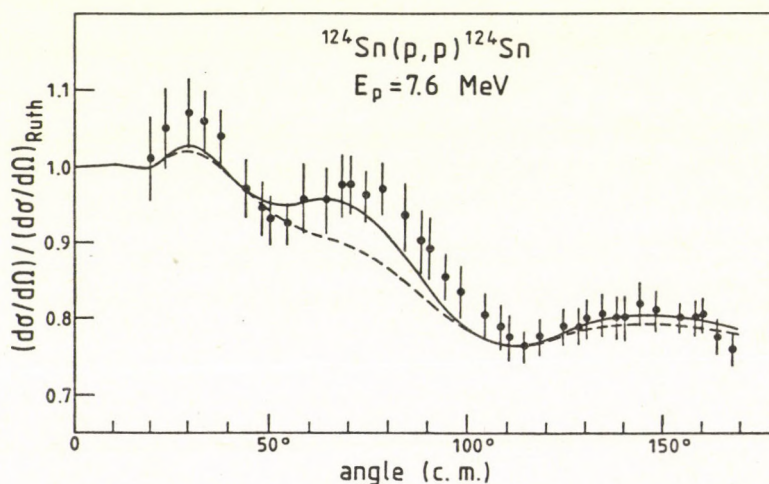


Fig. 1. Angular distribution of elastically scattered protons measured at the MGC cyclotron of Atomki. The full and broken lines are the optical model fits with Perey and Becchetti-Greenlees geometry, respectively.

References

- [1] B. Gyarmati, T. Vertse, L. Zolnai, A.I. Baryshnikov, A.F. Gurbich, N.N. Titarenko and E.L. Yadrovsky, J.Phys. G5 (1979)1225
- [2] A.F. Gurbich, V.P. Lunev, N.N. Titarenko, Yadernaya Fizika 40 (1984)310

* Bajcsy-Zsilinszky Secondary School, Újfehértó

"MICROP" - A CODE TO CALCULATE MACROSCOPIC JLM POTENTIALS

L. Zolnai

In ref. [1] Jeukenne, Lejeune and Mahaux presented a parametric expression for a theoretical microscopic optical potential (OMP) derived from nuclear matter calculations. The basic assumptions of the calculations were (1) the Reid's hard core interaction, (2) the Brueckner-Hartree-Fock approximation and (3) the improved local density approximation. However, this potential was limited to proton or neutron energies from 10 to 160 MeV. In ref. [2] Lejeune extended this potential below 10 MeV. Such energies are involved in (1) the study of nuclear processes in astrophysics and (2) in practical reactor calculations.

For practical cases the potentials above have to be folded with the mass density distribution of the target nuclei. For this purpose a code (MICROP) has been developed in the institute in FORTRAN-IV which makes it possible to calculate the different characteristics of the macroscopic potentials (rms radii, real and imaginary potential depths as well as the volume integrals). An illustrative example is shown in fig. 1.

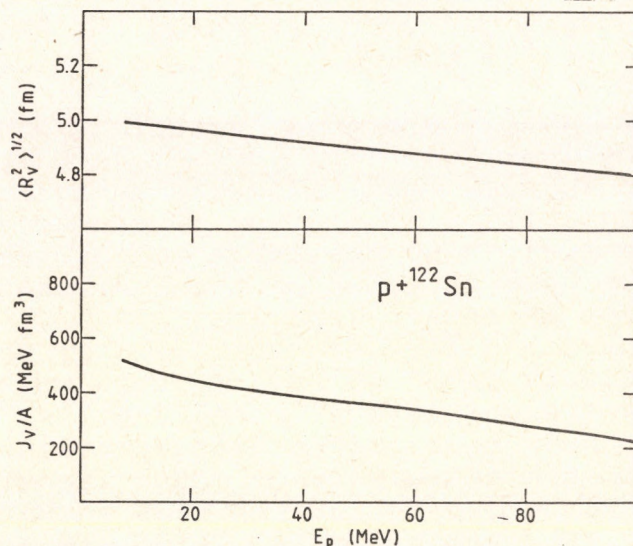


Fig.1. The full curves on the upper and lower parts represent the calculated values for the rms radius and the volume integral per nucleon of the real part of the proton OMP of ^{122}Sn .

References

- [1] J.P. Jeukenne, A. Lejeune and C. Mahaux, Phys.Rev. C16 (1977)80.
- [2] A. Lejeune., Phys. Rev. C21 (1980)1107.

OPTICAL MODEL ANALYSIS OF THE ${}^6\text{Ni}(\alpha, \alpha_0){}^6\text{Ni}$ PROCESS

Z. Máté, S. Szilágyi, L. Zolnai
and
Å. Bredbacka*, M. Brenner*, K.-M. Källman*, P. Manngård*

The observation of anomalous effects in the low energy behaviour of the optical potential (e.g. [1-3]) motivated us to investigate the alpha elastic scattering process at energies near the Coulomb barrier. Angular distribution experiments were carried out on target nuclei ${}^3\text{S}$, ${}^5\text{Cr}$ and ${}^6\text{Ni}$ at energies 12.8, 14.5, 16.3, 18.1 and 20.0 MeV using the ${}^4\text{He}$ beams of the 103 cm cyclotrons of Åbo Akademi (Turku) and Atomki (Debrecen) [4].

In the analysis of the angular distributions we obtained several sets of optical potential parameters that described the experimental data equally well (discrete ambiguity). In order to have better possibility in drawing conclusions on the features of the potential it is desirable to resolve this ambiguity. The method we used is based on the fact that the potential becomes unambiguous at higher energies.

We present here the case of ${}^6\text{Ni}$ for which we could use the results of an analysis given in [5]. In this work England et al. have found six equivalent optical model families for $\alpha+{}^6\text{Ni}$ at 25 MeV. Comparing their real volume integral values with the ones obtained at higher energies they could identify which family corresponded to the unique one at the high energies. The volume integral value of the chosen family was compared with our data as shown in fig.1. The cross at 25 MeV corresponds to the family found in [5] as the most appropriate one while the other symbols represent quantities extracted from our analysis. Approximating the $J_\alpha(E_\alpha)$ function by straight lines we can conclude that it is the $J_\alpha \approx 550 \text{ MeV} \times \text{fm}^3$ family which should be considered as the most appropriate one in our case.

* Department of Physics, Åbo Akademi, Turku, Finland

STRUCTURE OF ^{114}In NUCLEUS

Zs. Dombrádi and T. Fényes

The excited states of ^{114}In have been studied by our research group from $(p, n\gamma)$ reaction in a recent work [1]. In this paper the formerly published experimental and theoretical nuclear structure data on ^{114}In have been reviewed, too.

The aim of the present work was the calculation of the energy levels and electromagnetic properties of the low-lying positive parity states of ^{114}In within the framework of the interactive boson-fermion-fermion / odd-odd truncated quadrupole phonon model (IBFFM/OTQM). This model has proved formerly to be effective for the description of ^{116}In [2] and ^{112}In [3]. The energy spectrum of the negative parity, $\pi\tilde{g}_{9/2}v\tilde{h}_{11/2}$ multiplet has been reasonably described in our earlier work by means of the parabolic rule [1].

The Hamiltonian of the IBFFM/OTQM was described in refs. [4, 2, 3]. The computer code IBFFM/OTQM used in the calculations was written by Brant, Paar and Vretenar [5].

The core excitations were approximated with harmonic vibration. This is an acceptable approach, if we want to describe only low energy states. $\hbar\omega_2 = 1.3$ MeV effective phonon energy was used, which agrees with the energy of the 2_1^+ state of ^{114}Sn . We have used a reduced boson/phonon number $N_{\text{max}} = 2$. This strongly

reduced the scope of calculations, without sizeable effect on the properties of the low-lying states. The occupation probabilities were taken from the systematics of experimental data: $V^2(\pi\tilde{g}_{9/2}) = 0.87$, $V^2(v\tilde{d}_{5/2}) = 0.90$, $V^2(v\tilde{g}_{7/2}) = 0.78$, $V^2(v\tilde{s}_{1/2}) = 0.32$, $V^2(v\tilde{d}_{3/2}) = 0.20$. The quasiparticle energies were fitted to the experimental level energies of ^{114}In , but they are not far from the energies of the corresponding ^{115}Sn states: $E(v\tilde{s}_{1/2}) = 0$, $E(v\tilde{d}_{3/2}) = 0.37$, $E(v\tilde{g}_{7/2}) = 0.78$, $E(v\tilde{d}_{5/2}) = 0.91$ MeV. The boson-fermion interaction strengths were $\Gamma_0^p = 1.0$ and $\Gamma_0^n = 0.7$ MeV. The strengths of the exchange interactions: $\Lambda_0^p = 0$ and $\Lambda_0^n = 0.8$ MeV. The strengths of the residual force were the same as in the cases of ^{116}In [2] and ^{112}In [3]: $v_D = -0.4$ and $v_S = -0.1$ MeV.

For effective proton and neutron charges and gyromagnetic ratios the standard values have been used: $e_{s.p.}^p = 1.5 e$, $e_{s.p.}^n = 0.5 e$, $g_1^p = 1$, $g_1^n = 0$, $g_s^p = 0.5 g_s^p(\text{free})$, $g_s^n = 0.5 g_s^n(\text{free})$, $g_R = Z/A$. The boson charge: $e_{\text{vib}} = 2.6 e$ was fitted to the measured quadrupole moment of the 5_1^+ state of ^{114}In [6].

The calculated (from IBFFM/OTQM) and experimental energy spectra of the positive parity states of ^{114}In are shown in fig. 1. As seen, the main features of the energy spectrum have been reproduced. The wave functions of the states are usually very complex, but the 1_1^+ , 2_1^+ , 3_1^+ , 4_3^+ , 8_1^+ states are dominated by components with $\pi\tilde{g}_{9/2}v\tilde{g}_{7/2}$ quasiparticles, the 5_1^+ , 4_1^+ states

with $\pi\tilde{g}_{9/2}\nu\tilde{s}_{1/2}$, the 5_2^+ , 4_2^+ ones with $\pi\tilde{g}_{9/2}\nu\tilde{d}_{3/2}$, and the 7_1^+ level with $\pi\tilde{g}_{7/2}\nu\tilde{d}_{5/2}$ quasiparticles, in accordance with approximative classification of the parabolic rule [1] and with the experimental data. These data were obtained mainly from (d,p) and (d,t) neutron transfer experiments.

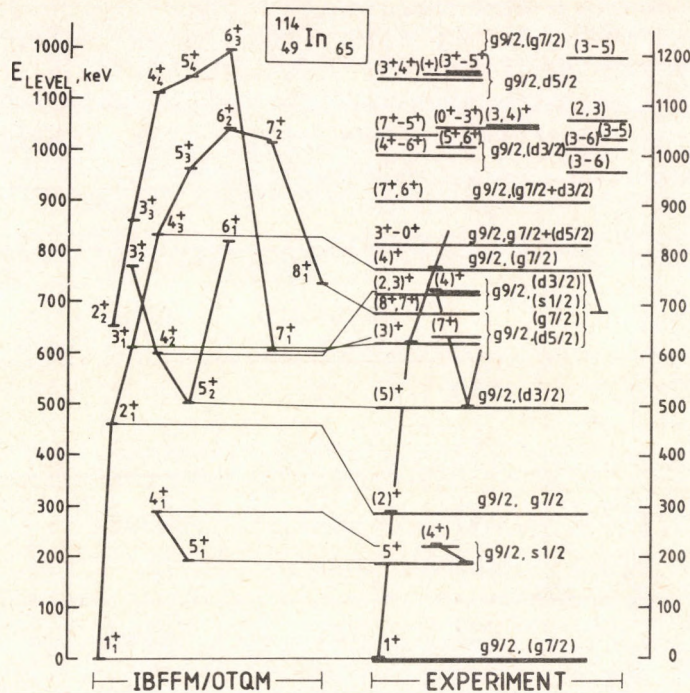


Fig. 1. The IBFFM/OTQM energy spectrum of ^{114}In in comparison with experimental data. The solid lines connect the members of a given proton-neutron multiplet

The calculated IBFFM/OTQM static moments are presented in table 1. The empirical moments were obtained from the corre-
Table 1. Magnetic dipole (μ in μ_N) and electric quadrupole (Q in eb) moments of the 1_1^+ and 5_1^+ states of ^{114}In

Electromagnetic moments	States	
	1_1^+ ground $T_{1/2} = 71.9$ s	5_1^+ $T_{1/2} = 49.51$ d
μ_{exp}	$2.815^{+0.011}$ [7]	$4.653^{+0.005}$ [6]
μ_{emp}	3.04	4.61
μ_{IBFFM}	2.87	4.55
μ_{theor} [8]	2.837	5.028
μ_{theor} [9]	2.93	4.45
Q_{exp}		0.739 ± 0.012 [6]
Q_{emp}	0.178 [7]	0.80 [6]
Q_{IBFFM}	0.153	0.738
Q_{theor} [9]	0.055	

sponding experimental moments of the neighbouring odd-even In and Sn nuclei on the basis of the additivity relation. The experimental magnetic dipole moments were reproduced by our IBFFM calculation within ~2%. The calculations show that the contributions of the collective electromagnetic operators to the magnetic moments are small and large to the electric ones.

The experimental and calculated relative γ -ray intensities are compared in table 2. As seen, the IBFFM calculation reasonably reproduces the majority of the γ -branching ratios.

Table 2. Transitions within low-lying ^{114}In states

E_i, keV	States			E_γ keV	I_γ^{Rel}		
	J_i^π	E_f, keV	J_f^π		Experimental		Theoretical
					Rabenstein, Harrach [10]	Timár et al. [1]	IBFFM/OTQM
628	$(3_1)^+$	228	$(2_1)^+$	340	100	100 M1, (E2) <2.3	100 M1+0.12% E2 4 E2
		0	1_1^+	628			
775	$(4_3)^+$	628	$(3_1)^+$	147	100	100 M1	100 M1+0.03% E2
		228	$(2_1)^+$	487	12	19	10 E2
497	$(5_2)^+$	190	5_1^+	307	100	81 M1	81 M1+0.42% E2
		221	(4_1^+)	276	60	<100	430 M1+0.45% E2
729	$(4_2)^+$	190	5_1^+	538		100	100 M1+0.03% E2
		497	$(5_2)^+$	231		12 M1	8.5 M1+0.42% E2

References

- [1] J. Timár et al., Nucl. Phys. A455 (1986) 477
- [2] T. Fényes and Zs. Dombrádi, ATOMKI Preprint 6-1988 P, Debrecen, to be published in Acta Phys. Hung.; ATOMKI Ann. Rep. 1988
- [3] T. Kibédi et al., Phys. Rev. C37 (1988) 2391
- [4] V. Paar, in In-Beam Nuclear Spectroscopy, ed. Zs. Dombrádi and T. Fényes, Akad. Kiadó, Budapest, 1984, vol. 2, p. 675
- [5] S. Brant, V. Paar, and D. Vretenar, IKP Jülich, 1985, unpublished
- [6] J. Eberz et al., Nucl. Phys. A464 (1987) 9
- [7] C. Nuytten et al., Phys. Rev. C26 (1982) 1701
- [8] J. Van Maldeghem and K. Heyde, Phys. Rev. C32 (1985) 1067
- [9] W. F. Van Gunsteren, Nucl. Phys. A265 (1976) 263
- [10] D. Rabenstein and D. Harrach, Nucl. Phys. A242 (1975) 189

NUCLEAR STRUCTURE OF ^{116}In

T. Fényes and Zs. Dombrádi

The low-lying positive parity states of ^{116}In have been described within the framework of the interacting boson-fermion-fermion / odd-odd truncated quadrupole phonon model (IBFFM/OTQM).

The Hamiltonian of the model is given by

$$H_{\text{OTQM}} = H_{\text{TQM}} + \sum_{i=p,n} H^i + \sum_{i=p,n} H_{\text{PVI}}^i + H_{\text{RES}}, \quad (1)$$

where H_{TQM} is the SU(6) quadrupole phonon Hamiltonian of the even-even core.

H^i denotes the quasiparticle Hamiltonian of the odd proton ($i=p$) and odd neutron ($i=n$) in a spherical potential.

H_{PVI}^i is the Hamiltonian of the particle-vibration interaction for proton and neutron, which consists of three terms [1]:

$$H_{\text{PVI}}^i = H_{\text{MON}}^i + H_{\text{DYN}}^i + H_{\text{EXC}}^i, \quad (2)$$

where H_{MON}^i is the Hamiltonian of the monopole interaction. H_{DYN}^i characterizes the dynamical interaction and H_{EXC}^i denotes the Hamiltonian of the exchange interaction.

H_{RES} is the residual interaction between the odd proton and neutron. We have considered only a central delta force of the form

$$H_{\text{RES}} = 4\pi\delta(r_p - r_n)[v_D + v_S \sigma_p \cdot \sigma_n], \quad (3)$$

where v_D and v_S are the parameters of the Wigner and Bartlett forces, δ is the Dirac δ symbol, r_p and r_n are the position vectors of the proton and neutron, respectively and the σ -s are the Pauli spin matrices.

The Hamiltonian (1) was diagonalized in the quasiproton-quasineutron weak coupling basis

$$|(j_p j_n) j_{pn}, NI; J\rangle, \quad (4)$$

where j_{pn} is the resulting angular momentum of the j_p and j_n states, I is the angular momentum of the N -phonon state, and J is the total angular momentum.

The computer code IBFFM/OTQM used in the calculations was written by Brant, Paar and Vretenar [2].

The shell-model space consisted of the $1g_{9/2}$ subshell for the proton quasiparticle and the $2d_{5/2}$, $1g_{7/2}$, $3s_{1/2}$, $2d_{3/2}$ subshells for the neutron quasiparticles. The parameters of the model were adjusted to the energy spectrum of ^{116}In and neighbouring nuclei.

The calculations reproduce the energy levels (fig.1) and known electromagnetic moments. γ -branching ratios have also been calculated and compared to the existing experimental data.

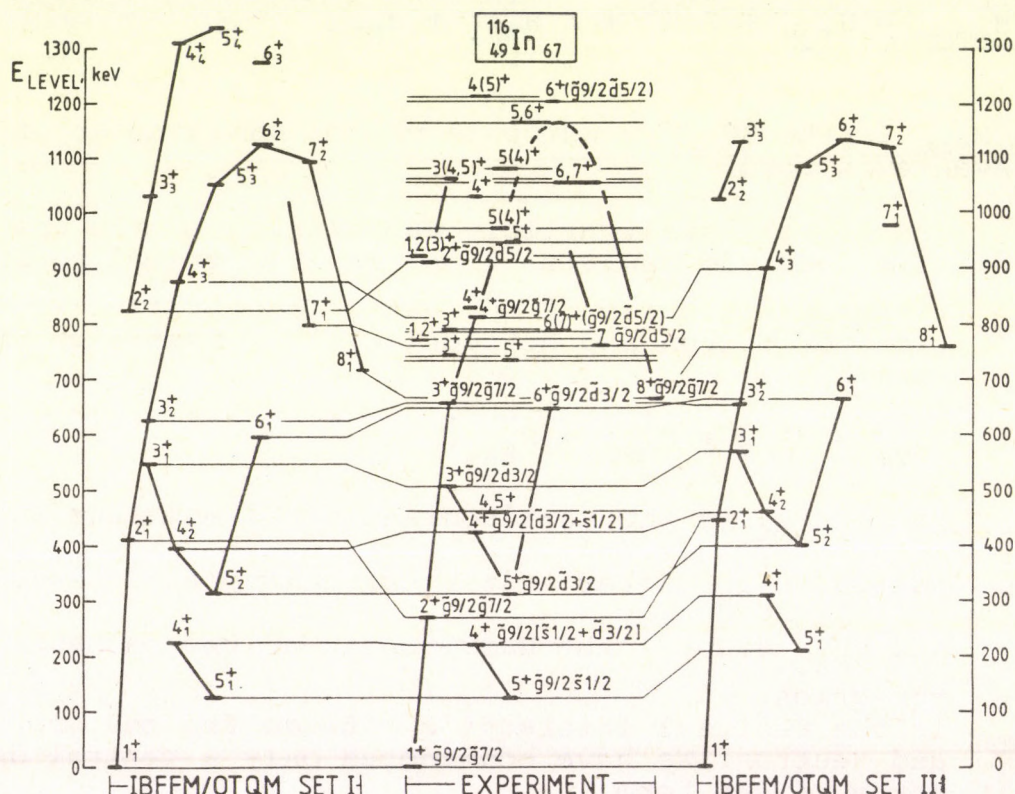


Fig. 1. Positive parity states of ^{116}In below ≈ 1300 keV. The theoretical level schemes are the results of the present IBFFM/OTQM calculations. The experimental data were taken from Alexeev et al. [3].

This work was supported partly by the National Scientific Research Foundation /OTKA/.

References

1. V. Paar, in *In-Beam Nuclear Spectroscopy*, ed. Zs. Dombrádi and T. Fényes, Akad. Kiadó Budapest, 1984, vol. 2, p. 675
2. S. Brant, V. Paar and D. Vretenar, Computer code IBFFM/OTQM, Institut für Kernphysik, KFA Jülich, 1985 /unpublished/.
3. V. L. Alexeev et al., *Nucl. Phys.* **A262** (1976) 19

Pauli effects in the six-nucleon system

K. Varga and R. G. Lovas

The norm operator \hat{A} of the resonating-group method plays a special role in the reduction of microscopic multicluster problems to ones that involve only intercluster variables [1]. It contains information on the effect of the Pauli principle. The operator can be practically treated only in terms of its spectral decomposition, so the solution of its eigenvalue problem is extremely important. The internal cluster states are usually approximated by harmonic oscillator shell-model states of the same size parameter. The eigenvalue problem is solvable analytically only in this case. In the more realistic calculations the internal states are pure harmonic oscillator configurations of unequal size or linear combinations of such [2]. Therefore, one has to apply a numerical approximation method [3].

We approximated the eigenfunctions with a linear combination of Gaussians centred around different points, thereby reducing the eigenvalue problem to that of a generator coordinate overlap matrix [4]. The analytical calculation of these kernels is simple. As an example, we investigated the eigenvalue problem of the $\alpha + d$ fragmentation of ${}^6\text{Li}$. The method appeared pretty accurate when tested against the exactly solvable case, and proved suitable for treating mixed configurations of the constituents. We then considered two improved models [4]. In one of them the cluster ground states were allowed to have different size parameters, and in the other they were chosen to be optimized mixtures of states of different size parameters. It turned out that the eigenvalue spectra and the eigenfunctions of the model of unequal size parameters considerably differ from the results belonging to the same oscillator widths, but the mixing does not imply further appreciable changes. So we came to the conclusion that calculations that use single configurations of unequal width parameters may also give acceptable accuracy for the norm operator of larger systems as well.

As an alternative to the configuration mixing, one can as well improve the description of the deuteron cluster in the cluster model by describing the ${}^6\text{Li}$ system as an $\alpha + p + n$ configuration. This model is most often implemented in a semimicroscopic form with the α particle treated as structureless and the Pauli principle approximated phenomenologically. Comparing the results for the $\alpha + d$ spectroscopic factor of the microscopic $\alpha + d$ model with those of the three-body model, one can find that the latter predicts too low values [5]. This can be understood by noting that the treatment of the Pauli principle in the three-body definition of the spectroscopic factor is wrong

[6], namely the operator $\hat{A}_{\alpha+p+n}^{1/2}$ is missing from the conventional definition. Having solved the eigenvalue problem of the $\alpha + p + n$ model, we could calculate the $\alpha + d$ spectroscopic factor of the correct definition in the three-body model. We have found [7] that inclusion of $\hat{A}_{\alpha+p+n}^{1/2}$ in the definition increased the value of the spectroscopic factor by about 1.4 in agreement with the prediction of the microscopic $\alpha + d$ model.

References

- [1] S. Saito, *Prog. Theor. Phys. Suppl.* **62** (1977) 11
- [2] R. Beck, F. Dickmann and A. T. Kruppa, *Phys. Rev.* **C30** (1984) 1044
- [3] H. Horiuchi, *Prog. Theor. Phys. Suppl.* **62** (1977) 90
- [4] K. Varga and R. G. Lovas, *Phys. Rev.* **C37** (1988) 2906
- [5] V. I. Kukulin, V. M. Krasnopol'sky, V. T. Voronchev and P. B. Sazonov, *Nucl. Phys.* **A417** (1984) 128
- [6] R. G. Lovas, A. T. Kruppa, R. Beck and F. Dickmann, *Nucl. Phys.* **A474** (1987) 451
- [7] R. G. Lovas, Contributed papers to 5th Int. Conf. on Clustering Aspects in Nuclear and Subnuclear Systems, Kyoto, 1988, ed. Y. Sakuragi, T. Wada and Y. Fujiwara (RIFP, Kyoto, 1988) p.14

SOME ASPECTS OF SUPERSYMMETRIC QUANTUM MECHANICS AND SOLVABLE POTENTIALS†

G. Lévai

Recently there has been a renewed interest in the potential problems of nonrelativistic quantum mechanics, due to the introduction of two important concepts: supersymmetric quantum mechanics (SUSYQM) [1] and shape-invariance [2]. In SUSYQM two Hamiltonians related by supersymmetry have the following form ($\hbar = 2m = 1$):

$$H_{\pm} = -\frac{d^2}{dx^2} + V_{\pm}(x) = -\frac{d^2}{dx^2} + (W^2(x) \pm \frac{dW}{dx})$$

(In fact the two Hamiltonians are the diagonal components of a supersymmetric 2×2 matrix Hamiltonian.)

In the case of unbroken supersymmetry the ground state of H_- has zero energy ($E_0^{(-)} = 0$) and the ground state wave function is related to the superpotential $W(x)$ as $W(x) = -\frac{d}{dx} \ln \Psi_0^{(-)}$. In this case the energy eigenvalues of H_+ and H_- are identical except for the ground state: $E_n^{(+)} = E_{n+1}^{(-)}$, ($n = 0, 1, \dots$). The eigenfunctions of H_- and H_+ are connected by SUSY laddering operators.

Among the numerous applications of SUSYQM we mention only one which is related to the question of deep and shallow nuclear potentials [3].

A further concept is shape-invariance. V_+ and V_- are called shape-invariant if their dependence on the coordinate is the same and they differ only in some parameters appearing in them. In this case the energy eigenvalues and eigenfunctions can be determined by elementary calculations.

These concepts turned out to be extremely useful when they were combined with traditional approaches. In particular it has been shown [4] that the known solvable potentials can be treated within the framework of SUSYQM and most of them are shape-invariant. As a by-product of such investigations new classes of solvable potentials have been found, but no general criteria for shape-invariance have been given.

In our approach we have investigated [5] a simple method [6] of finding solvable potentials from the point of view of SUSYQM. This method can be used to transform the Schrödinger equation into a linear homogeneous second

order differential equation with known special functions as solutions. Combining this method with the theory of SUSYQM we have derived criteria which have to be satisfied by these special functions in order to lead to potentials of the form $V(x) = W^2(x) - W'(x)$. (These criteria trivially exclude some potentials from our treatment, for example the Woods-Saxon potential (with $l = 0$) and any potential problem with Bessel functions as solutions.) We illustrated the above procedure with the example of orthogonal polynomials. We could get every single known shape-invariant potential and one more, which has escaped notice in other publications. Exact wave functions and energy eigenvalues have been determined in each case.

We have introduced a straightforward classification scheme of these shape-invariant potentials and have shown that they correspond to different factorisation types in terms of the factorisation method of Infeld and Hull [7]. We have compared this scheme with other classification schemes [4], [8] as well. The latter scheme by Miller is especially interesting, since it is based on the theory of Lie algebras. It would be an interesting task to investigate the relationship between the Lie algebras used by Miller and graded Lie algebras which give the mathematical framework of supersymmetry.

† This work was supported by the Oxford Visiting Graduate Student Scheme of the Soros Foundation.

- 1) E. Witten, Nucl. Phys. B 188 (1981) 513.
F. Cooper, B. Freedman, Ann. Phys. 146 (1983) 262.
A. A. Andrianov, N. V. Borisov, M. V. Ioffe, Phys. Lett. 105A (1984) 19.
- 2) L. Gendenshtein, Zh. Eksp. Teor. Pis. Red. 38 (1983) 299 (JETP Lett. 38 (1983) 356).
- 3) D. Baye, J. Phys. A:Math. Gen. 20 (1987) 5529.
- 4) F. Cooper, J. N. Ginocchio, A. Khare, Phys. Rev. D 36 (1987) 2458.
- 5) G. Lévai J. Phys. A:Math. Gen., in press.
- 6) A. Bhattacharjie, E. C. G. Sudarshan, Nuovo Cim. 25 (1962) 864.
- 7) L. Infeld, T. E. Hull, Rev. Mod. Phys. 23 (1951) 21.
- 8) W. Miller Jr., Lie Theory of Special Functions (1968 New York, Academic).

APPLICABILITY OF THE VIBRON MODEL TO NUCLEAR CLUSTER STATES

J. Cseh

The vibron model [1] is an interacting boson model of the molecule-type collective motion in which the dipole degrees of freedom play the main role. It has a $U(4)$ group structure and it has two limiting cases called dynamical symmetries characterized by the $U(3)$ and $O(4)$ groups, respectively. Applying this model to some well-known cluster bands of light nuclei in Ref 2. we concluded that the boson-boson interaction of the usual Hamiltonian which contains one and two-body terms can not account for the Pauli principle. To incorporate this effect we applied the method of the basis truncation as suggested by the Wildermuth condition [3].

Recently we have considered [4] some alternative possibilities. They are: i) the introduction of higher order terms in the Hamiltonian instead of the basis truncation, and ii) the application of Harvey's prescription [5] instead of the Wildermuth condition.

As for the introduction of higher order terms in the Hamiltonian it seems to be capable of incorporating the exclusion principle in a more refined way, namely by describing the Pauli resonances [6]. A third order term works fine in this respect. Another higher order term is required by the strong rotational-vibrational coupling of the cluster motion.

When dealing with the Pauli principle there is a crucial value for the $U(3)$ quantum number both in the basis-truncation method and in the higher order term of the Hamiltonian. If we determine that from Harvey's prescription instead of the Wildermuth condition we can take into account not only the Pauli principle, but the threshold energies of the cluster states [7] as well. This is related to the fact that Harvey's prescription is aware of the nuclear deformation while the Wildermuth condition is not.

These considerations are based on the $U(3)$ basis of the vibron model, so they are easy to apply when one uses this dynamical symmetry. When the general Hamiltonian, or the other dynamical symmetry is more appropriate one can calculate the matrix elements of the Hamiltonian between the $U(3)$ basis

states and perform a numerical diagonalization.

Fig. 1 shows an example of the application of the dynamical symmetry to some cluster bands in Ne^{20} . The $K^\pi = 0_2^+$ band is thought to contain the Pauli resonances.

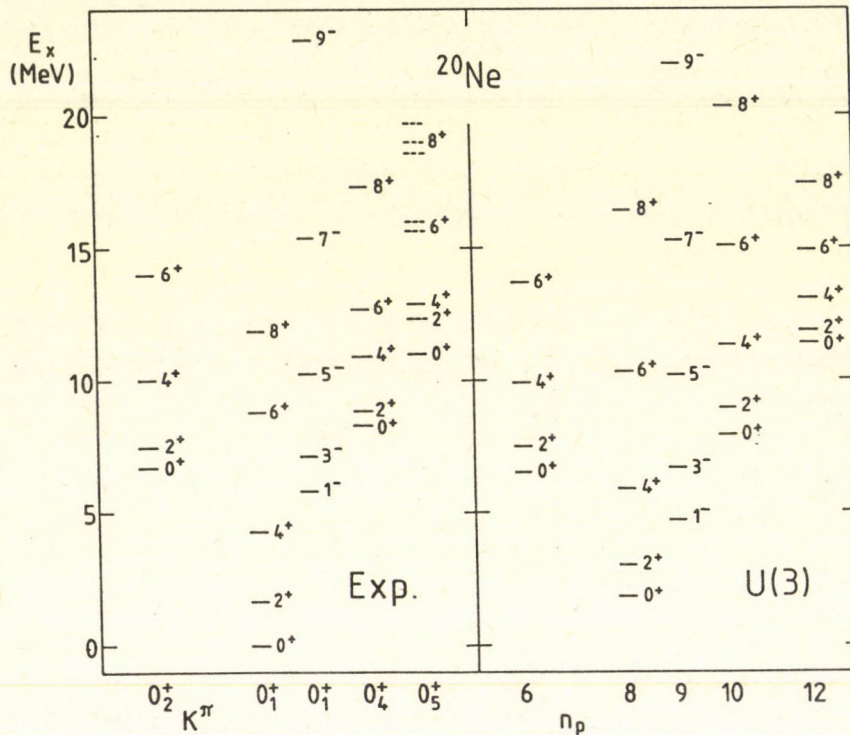


Fig.1. Energies of experimental and model states in ^{20}Ne . The dashed lines in the experimental spectrum indicate the uncertainty of the states.

- 1) F. Iachello, and R. D. Levine, J. Chem. Phys. **77**, (1982) 3046.
- 2) J. Cseh and G. Lévai, Phys. Rev. **C38**, (1988) 972.
- 3) K. Wildermuth and Th. Kanellopoulos, Nucl. Phys. **7** (1958) 150.
- 4) J. Cseh, 5th Int. Conf. on Clustering Aspects in Nuclear and Subnuclear Systems, Kyoto, 1988.
- 5) M. Harvey, Proc. 2nd Int. Conf. on Clustering Phenomena in Nuclei, (College Park, 1975) USDERA Rep. ORO-4856-26, p. 150.
- 6) H. Walliser, T. Fliessbach and Y. C. Tang, Nucl. Phys. **A437** (1985) 367.
- 7) K. Ikeda, N. Takigawa and H. Horiuchi, Suppl. Prog. Theor. Phys. Extra Number (1968) 464.

CLUSTER BANDS OF THE ^{24}Mg IN TERMS OF THE VIBRON MODEL

J. Cseh

The $^{12}\text{C} + ^{12}\text{C}$ resonances, as the best known heavy-ion resonances have been described by several models, among others by the phenomenologic algebraic dipole (vibron) [1,2] and quadrupole (IBM) [3] models. Recently we extended their treatment within the vibron model in two respects [4]. i) We took into account some internal degrees of freedom in addition to the relative motion of the two clusters. More exactly, we applied the algebraic models corresponding to the $^{16}\text{O} + \alpha + \alpha$, and the $^{12}\text{C} + ^{12}\text{C}^*$ clusterizations. ii) In addition to the $^{12}\text{C} + ^{12}\text{C}$ resonances we considered in the same descriptions the low-lying cluster bands of the ^{24}Mg as given in Ref. 5.

The $^{16}\text{O} + \alpha + \alpha$ configuration was described by the

$$U_1(4) \otimes U_2(4) \supset U_1(3) \otimes U_2(3) \supset U(3) \supset O(3) \quad (1)$$

dynamical symmetry. The Hamiltonian of this model was taken as the linear combination of the linear and quadratic Casimirs of the subgroups of (1) plus a third order term corresponding to a rotational-vibrational coupling. So it contained six parameters.

The $^{12}\text{C} + ^{12}\text{C}^*$ system was described by the $SU(3)$ limit of the nuclear vibron model [6]:

$$U(6) \otimes U(4) \supset SU_a(3) \otimes U_b(3) \supset SU_a(3) \otimes SU_b(3) \supset SU(3) \supset O(3). \quad (2)$$

We restricted the internal excitations to the lowest-lying 2^+ state of the ^{12}C . The Hamiltonian had six parameters again.

In both cases we applied the basis truncation method based on Harvey's prescription [7] to simulate the Pauli principle. The better agreement with the experimental energy spectrum was achieved by the three-cluster model, as shown in Fig. 1.

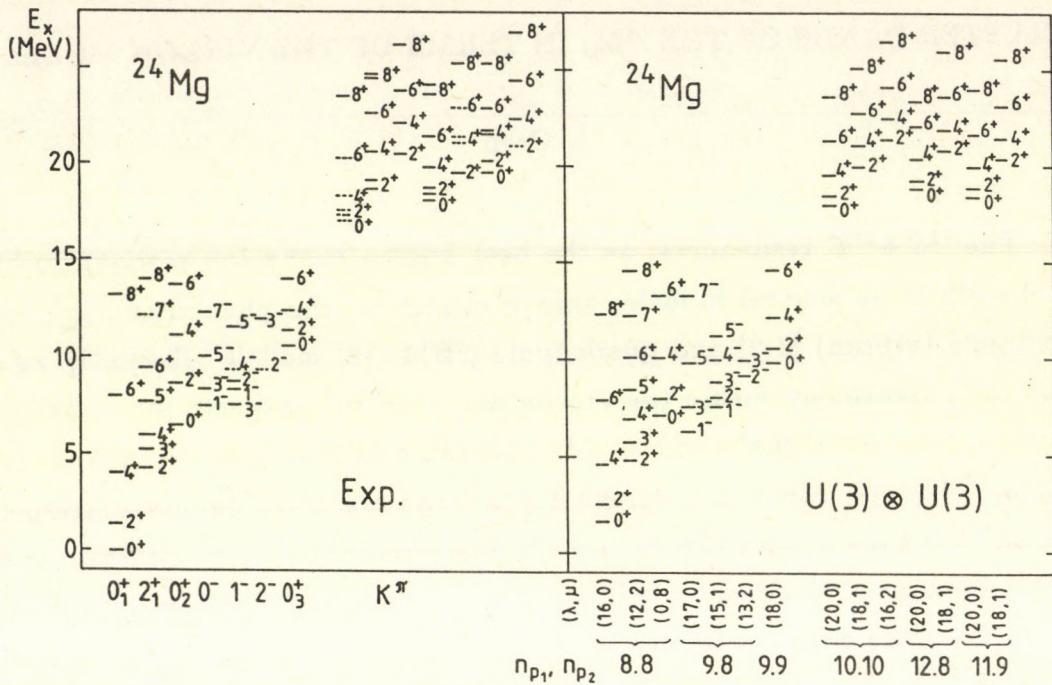


Fig. 1. Energies of experimental and model states in ^{24}Mg . The dashed lines in the experimental spectrum indicate the uncertainty of the states.

These examples are considered as favourable signs for the flexibility of the algebraic approach.

- 1) Erb, K.A. and Bromley, D.A., Phys. Rev. C**23**, 2781 (1981).
- 2) Cseh, J., Phys. Rev. C**31**, 692 (1985).
- 3) Cseh, J. and Suhonen, J., Phys. Rev. C**33**, 1553 (1986).
- 4) Cseh, J., Developments of Nuclear Cluster Dynamics, Sapporo 1988.
- 5) Descouvemont, P. and Baye, D., Nucl. Phys. A**475**, 219 (1987).
- 6) Daley, H.J. and Iachello, F., Ann. Phys. **167**, 73 (1986).
- 7) Cseh, J., 5th Int. Conf. on Clustering Aspects in Nuclear and Subnuclear Systems, Kyoto, 1988.

AN INVESTIGATION ON THE RESONANT STATE
WAVE FUNCTION OBTAINED BY COMPLEX SCALING

A. Csótó, B. Gyarmati and A.T. Kruppa

A very often used definition of a resonant state is an asymptotically purely outgoing solution of the Schrödinger equation belonging to complex energy. This solution is not a square-integrable function, but appropriate rules have been worked out to handle integrals containing it. The solution of the problem, however, with conventional bound-state techniques, e.g. expanding the wave-function on some basis set, is conceptually and practically difficult.

Under conditions which may be fulfilled in realistic cases, there exists a transformation $U(\theta)$ to be applied to the Schrödinger equation with the beautiful property of keeping the discrete eigenvalues (bound and resonant states) of the Schrödinger equation unchanged but transforming the respective wave function ψ into the square-integrable function $\psi_\theta = U(\theta)\psi$. If the transformed problem is exactly solved the inverse transformation $U(\theta)^{-1}$ gives the exact solution to the original problem, i.e. the resonant state ψ . Also the transformed problem is already accessible for the bound-state approximation methods. The basis set methods for instance yield an approximate ψ_θ^N function on a $\{\varphi_i\}$ square-integrable basis truncated to N elements.

We showed that the back-transformed wave function i.e. the approximate solution to the original problem $\psi^N = U(\theta)^{-1}\psi_\theta^N$ is extremely dependent on the choice of the basis $\{\varphi_i\}$. If the φ_i 's are the well-managable, therefore often used, harmonic oscillator wave functions ψ^N shows violent spurious oscillations where $U(\theta)\varphi_N$ is violently oscillating. The larger N the worse ψ^N is, although ψ_θ^N converges to ψ_θ .

The moral one can deduce from the above statements is that the limiting procedure $\lim_{N \rightarrow \infty} \psi_\theta^N \rightarrow \psi_\theta$ cannot be interchanged with the inverse transformation $U(\theta)^{-1}$. The practical message is that basis functions whose transforms $U(\theta)\varphi_i$'s are not or hardly oscillating should give much better approximate wave functions. Our preliminary numerical results with Gaussian basis support this conclusion.

On the role of anti-bound states in the RPA description of the giant monopole resonance

T. Vertse

Institute of Nuclear Research of the Hungarian Academy of Sciences,

H-4001 Debrecen, Pf. 51, Hungary,

P. Curutchet, R. J. Liotta

Research Institute of Physics, S-104 05 Stockholm, Sweden

and

J. Bang

The Niels Bohr Institute, University of Copenhagen, DK-2100 Copenhagen O, Denmark

The limit of the applicability of the resonant random phase approximation method is tested by calculating escape widths in the giant monopole resonance of ^{16}O and comparing them to the results of a time dependent Hartree-Fock calculation. Though the widths of the narrow s-wave component agree reasonably well, the broad p-wave component shows large disagreement, which cannot be cured by complementing the basis with anti-bound states in the RPA calculation.

**Description of the giant multipole resonances in ^{208}Pb in the framework
of the resonant RPA**

P. Curutchet*, T. Vertse and R. J. Liotta†

Considerable interest has focused recently on the decay properties of giant resonances due to the modern experimental techniques which opened a possibility for measuring the decay widths of the giant resonance into selected final states. Since giant resonances are located at high excitation energies, they often decay by particle emission, therefore the proper treatment of the coupling of the giant resonance to the continuum (the "escape width" Γ^{\dagger}) is very important. The application of the standard methods is tedious and offers very little insight into the decay process. In order to overcome these difficulties, a fast approximate method called "resonant RPA" (RRPA) has been proposed recently [1]. In the RRPA the single particle basis is composed of bound single particle states and single particle resonant (Gamow) states, and the completeness relation of Berggren [2] is used together with regularization methods for calculating the divergent integrals. The use of Gamow states takes care automatically of the possibility of the particle emission from the unbound particle states. The advantage of the RRPA method is that we deal only with discrete eigenstates of the single particle Hamiltonian therefore methods well known from nuclear structure calculations can be used. Through the resonant basis states the RRPA includes the effect of the narrow resonances in the region of the giant resonance but not the slowly varying background. The RRPA assumes that the giant resonance is based mainly on 1p-1h states where the particle is either bound or quasi-bound. In most cases this assumption is satisfied due to the effect of the Coulomb or/and centrifugal barriers. The RRPA has turned out to be especially very powerful for heavy nuclei, where the application of the other methods are extremely difficult.

In this work we applied the RRPA formalism to study giant multipole resonances in ^{208}Pb using a separable multipole-multipole interaction [3]. The parameters of the of the main components of the giant resonances for monopole ($\lambda = 0$), quadrupole ($\lambda = 2$), octupole ($\lambda = 3$) and hexadecapole ($\lambda = 4$) resonances are shown in Table 1. We found that in all cases the escape widths of giant resonances are small. This could be partially due to the fact that the smaller the transition matrix elements, the wider the states connected by the transition operator are. But it is also a manifestation of the structure of the resonances, specially those with high multiplicities. Here the main configurations of the giant resonance wavefunctions have the spins of the particle and the hole aligned with the angular momentum of the transition operator. This enhances the transition probabilities because the angular momentum recoupling coefficients acquire in this case their maximum values. Moreover, to obtain also the maximum overlap between the initial and the final radial wavefunctions in the transition matrix elements it is

* Fellow of the CONICET, Buenos Aires, Argentina and

† Research Institute of Physics, S-104 05 Stockholm, Sweden

necessary that the difference in the number of nodes of those functions is as small as possible. This is indeed the case because, for a given value of ΔN , a minimum value of Δn implies a maximum for Δl . An artificial enhancement of the proton components arises from the special choice of the relation between the isoscalar and isovector strength of the interaction and this is specially manifested in the case of the quadrupole resonance, where the importance of some non-aligned proton configurations are overestimated. Since the hole in the particle-hole giant resonance is in a bound state, the alignment mentioned above requires that the particle should move in a high angular momentum orbit. Therefore, the corresponding centrifugal barrier tends to trap this particle within the nuclear volume hindering the particle decay of the giant resonance. This also explains the success of harmonic oscillator representations to describe giant resonances.

The giant monopole resonances have completely different features as can be expected from a breathing mode but it can be observed that they are also built upon mainly bound or quasibound configurations.

The calculated escape widths agree reasonable well with available experimental data. Among the states which have not been observed so far, our calculation predicts that a candidate likely to be observed is the octupole isovector giant resonance, with 89% of its strength concentrated at about 31 MeV.

λ	T	E_n (MeV)	Γ^\dagger (keV)	S_n (%)
0	0	13.25	300	46
0	0	13.60	200	29
0	1	22.12	640	60
2	0	10.44	120	76
2	1	23.31	1020	70
3	0	18.73	20	30
3	1	30.65	1540	89
4	0	26.97	120	23

Table 1 Main component(s) of the isoscalar (T=0) and isovector (T=1) giant multipole resonances in ^{208}Pb calculated in RRPA. The value of the strength function S_n is given as % of the corresponding energy weighted sum rule.

References

1. T. Vertse, P. Curutchet, O. Civitarese, L. S. Ferreira and R. J. Liotta, Phys. Rev. C37, 876, 1988.
2. T. Berggren, Nucl. Phys. A109, 265, 1968.
3. P. Curutchet, T. Vertse and R. J. Liotta, Phys. Rev. C. to be published.

SEARCH FOR ELECTRON SCREENING OF NUCLEAR REACTIONS AT
SUB-COULOMB ENERGIES

S. Engstler*, A. Krauss*, K. Langanke*, K. Neldner*, C. Rolfs*
U. Schröder* and E. Somorjai

The reaction ${}^3\text{He}(d,p){}^4\text{He}$ has been investigated for $E=6$ to 42 keV with the use of D projectiles and ${}^3\text{He}$ atomic gas target nuclides as well as with ${}^3\text{He}$ projectiles and D_2 molecular gas target nuclides. These studies show for the first time the predicted effects of electron screening on low-energy fusion cross sections, i.e. a nearly exponential enhancement of the cross sections compared to the case of bare nuclei. The enhancement is smaller for the case $d({}^3\text{He},p){}^4\text{He}$ due to the molecular nature of the D_2 target nuclides. The reactions ${}^6\text{Li}(p,\alpha){}^3\text{He}$ and ${}^7\text{Li}(p,\alpha){}^4\text{He}$ have also been studied for $E=10$ to 65 keV with the use of solid LiF targets. The results also indicate an exponential enhancement due to the effects of electron screening. The ${}^3\text{He}(d,p){}^4\text{He}$ reaction

The results are summarized in fig.1. The data obtained with ${}^3\text{He}$ projectiles and the molecular D_2 target nuclides (fig.1b) also reveal an increase at low energies, which is however significantly smaller compared to the previous case (fig.1a) at the same energies ($U_e=66\pm 4$ eV, $\chi^2=0.39$). Since the electron cloud in the D_2 molecule is on the average about a factor 2 at larger distances compared to that in the D atom, the screening effect should be shifted to lower energies. The (p,α) reactions on ${}^6\text{Li}$ and ${}^7\text{Li}$

The results are shown in fig.2. The fitted (using eq.(2)) screening potential of $U_e=0.21$ keV in the case of ${}^7\text{Li}(p,\alpha){}^4\text{He}$ is slightly lower than the expected value quoted above, and $U_e=0.30$ keV in the case of ${}^6\text{Li}(p,\alpha){}^3\text{He}$ is somewhat higher. As both reactions should have identical screening potentials, further investigations are desirable.

Furthermore, the measurements of angular distributions in the energy range covered by the presented experiment are in progress.

References:

- /1/ C. Rolfs, H.P. Trautvetter and W.S. Rodney, Rep. Prog. Phys.50 (1987)233.
- /2/ H.J. Assenbaum, K. Langanke and C. Rolfs, Z. Phys. A327 (1987)461.
- /3/ A. Krauss, H.W. Becker, H.P. Trautvetter, C. Rolfs and K. Brand, Nucl. Phys. A465 (1987)150.

* Institut für Kernphysik, Universität Münster, FRG

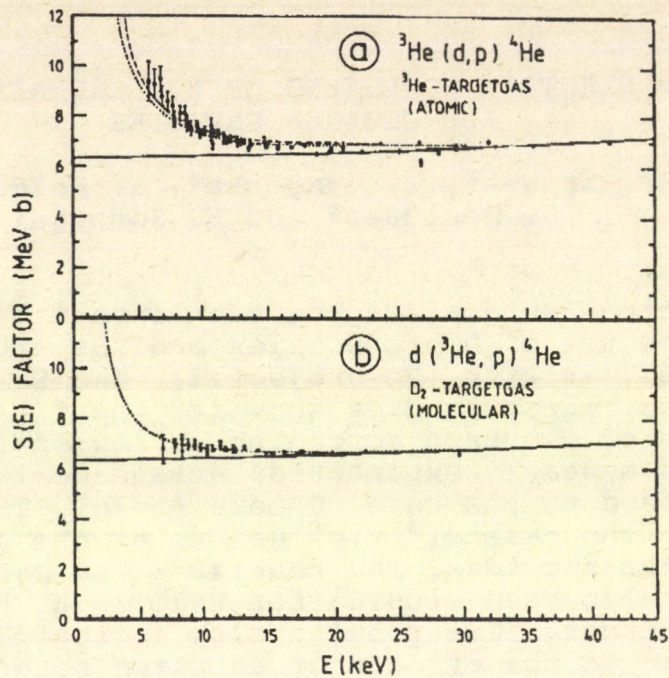


Fig. 1. $S(E)$ -factor data obtained (a) with ${}^3\text{He}$ target gas and (b) with D_2 target gas. The solid curve is obtained from a fit to high-energy data points /3/ and is assumed to represent the case of bare nuclei. The dotted curves are the calculated enhancements using eq. (2) with the fitted potentials (a) $U_e=120$ eV and (b) $U_e=66$ eV. The dashed curve in (a) is the enhancement calculated via the ratio of penetrabilities.

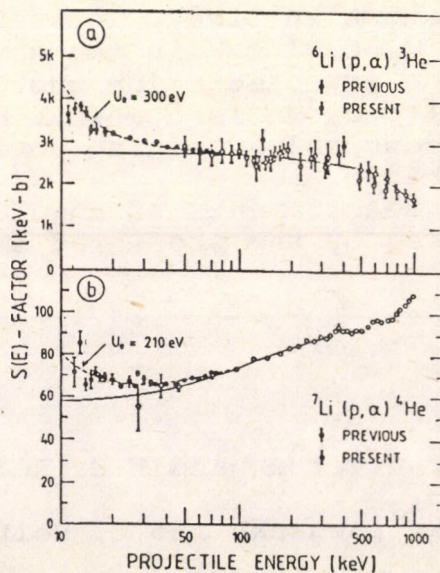


Fig. 2. $S(E)$ -factor data for (a) the ${}^6\text{Li}(p,\alpha){}^3\text{He}$ reaction and (b) the ${}^7\text{Li}(p,\alpha){}^4\text{He}$ reaction. The solid curves are obtained from a fit to the previous data at higher energies and are assumed to represent the case of bare nuclei. The dashed curves are the calculated enhancements using eq.(2) with fitted potentials.

INVESTIGATION OF ELECTRON SCREENING IN REACTIONS $H(^6\text{Li}, \alpha)^3\text{He}$,
 $H(^7\text{Li}, \alpha)^4\text{He}$ AND $D(^6\text{Li}, \alpha)^4\text{He}$.

S. Engstler*, U.Greife*, C.Rolfs*, U.Schröder* and E.Somorjai

The study of electron screening effects in nuclear reactions at sub-Coulomb energies is in progress in Münster. The enhancements in the cross sections at sub-Coulomb energies due to electron screening/1/provided screening potentials (fitted) of $U_e=0.21$ keV in the case of $^7\text{Li}(p, \alpha)^4\text{He}$ and $U_e=0.30$ keV in the case of $^6\text{Li}(p, \alpha)^3\text{He}$ /2/. As both reactions should have identical screening potentials, further investigations were desirable.

Measurements of the inverse reactions using ^6Li and ^7Li projectiles as well as H_2 and D_2 molecular gas targets, are reported here. The ^6Li and ^7Li projectiles were provided by the accelerator in Münster at energies $E_{\text{lab}}=30$ to 360 keV. A windowless gas target system of four pumping stages was used. The beam with intensity of 25 to 80 μA was stopped by a 20 W beam calorimeter. The gas pressure was measured by a capacitance manometer.

The analysis of the experimental data has not yet been completed. In this case thin targets can be used, whereby the corrections due to the infinitely thick targets are avoided.

The preliminary results are shown in fig.1. and fig.2.

References:

- /1/ H.J. Assenbaum, K. Langanke and C. Rolfs, Z. Phys. A327 (1987) 461.
- /2/ U. Schröder, S. Engstler, A. Krauss, K. Neldner, C. Rolfs, E. Somorjai and K. Langanke, Nucl. Instr. and Meth. (in press)

* Institut für Kernphysik, Universität Münster, FRG

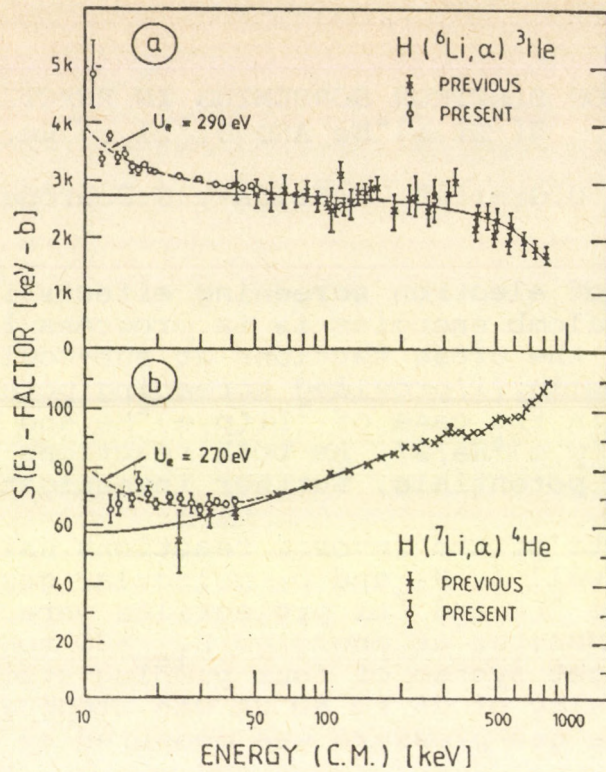


Fig. 1. $S(E)$ -factor data obtained with H_2 gas target bombarded by (a) ^6Li and (b) ^7Li projectiles. The solid curves are obtained from a fit to the previous data at higher energies and are assumed to represent the case of bare nuclei. The dashed curves are the calculated enhancements with fitted potentials.

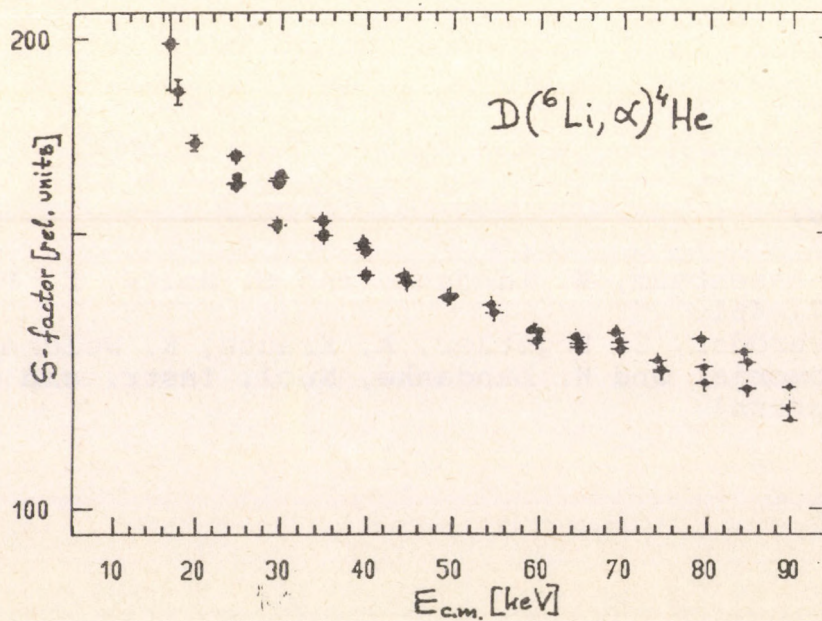


Fig. 2. $S(E)$ -factor data obtained for the reaction $D(^6\text{Li}, \alpha)^4\text{He}$ using D_2 gas target.

ATOMIC PHYSICS

SOME BASIC INFORMATION ON THE COLLISION MECHANISM AND ON THE IONIC TRANSITIONS IN FAST HEAVY ION - ATOM COLLISIONS

I.Kádár, S.Ricz, B.Sulik, D.Varga, J.Végh and D.Berényi

Institute of Nuclear Research of the Hung. Acad. Sci.,
Debrecen, Hungary

A research program was carried out in Dubna for years on the experimental study of the Ne K Auger spectra in fast heavy ion (5.5 MeV/u) - Ne collisions (see e.g. in [1,2]). Out of the whole body of measuring data the series of spectra measured with high resolution (FWHM ≤ 1 eV) at Ne³⁺, Ne¹⁰⁺, Ar⁶⁺, Ar¹⁶⁺ impact were analyzed together with the corresponding spectrum at H⁺ (5.5 MeV/u) taken at the ATOMKI cyclotron in Debrecen [3].

A characteristic partial result of the evaluation is shown in Fig. 1 where the relative intensity of the different "spectrum components" is shown after summing up the intensity of the lines pertaining to the satellite-group concerned. The evaluation of these whole series of spectra is nearly ready and will be published soon [3]. Here some of the most important conclusions will be given.

1. Although the first order perturbation theories fail to describe the average quantities for multiple ionization (e.g. $p_L(0)$), an IPM based geometrical model developed by us [4,5] seems to give fairly good results in this respect.

2. The evidence obtained for PCI at the velocity concerned [6] shows that the production of the multiply ionized state and its decay cannot be regarded as completely separated, even in the present high velocity region.

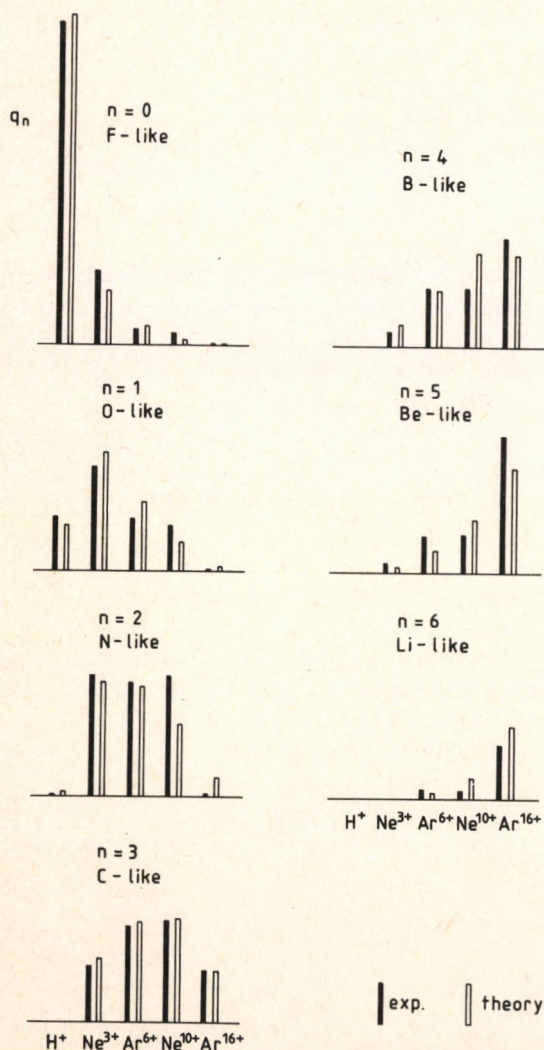


Fig.1. Relative intensity of the different satellite-components of the Ne K Auger spectra (q_n) depending on the projectile in comparison with the theory [4].

3. Finding a definite A_4 asymmetry parameter in fitting the Auger electron angular distribution for the 720.8 eV $1s^1 2s^2 2p^4 \ ^2D - 1s^2 2s^0 2p^4 \ ^1D$ transition ($A_2 = 0.05 \pm 0.03$; $A_4 = -0.17 \pm 0.05$) proves the presence of correlation among the electrons of the target in the ionization process which shows the limit of IPM-based description of the multiple ionization.

4. Also from our Auger electron angular distribution measurements, the presence of configuration interaction i.e. electron correlation in the Auger decay of multiply ionized atoms was shown. Namely, in $Ne^{3+} - Ne$ collision for the decay of the $1s^1 2s^2 2p^5 \ ^1P$ state to $1s^2 2s^2 2p^3 \ ^2P$ and to $1s^2 2s^2 2p^3 \ ^2D$ an $A_2(^1P - ^2P) = 0.08 \pm 0.06$ and $A_2(^1P - ^2D) = -0.18 \pm 0.03$, respectively were determined. The non-zero value of A_2 in the first case proves the above statement.

References

1. I.Kádár, S.Ricz, V.A.Shchegolev, B.Sulik, D.Varga, J.Végh, D.Berényi and G.Hock, Journal of Physics B: At. Mol. Phys. 18 (1985) 275-287.
2. S.Ricz, I.Kádár, V.A.Shchegolev, D.Varga, J.Végh, D.Berényi, G.Hock, B.Sulik, J. Phys. B: At. Mol. Phys. 19 (1986) L411-L416.
3. I.Kádár, S.Ricz, B.Sulik, D.Varga, J.Végh and D.Berényi, 'High Resolution Target Auger Spectroscopy at the Impact of Energetic Heavy Ions on Ne', 10th Conference on the Application of Accelerators in Research and Industry, Nov 7-9, 1988, NTSU, Denton, Texas, USA; ATOMKI Preprint 21-1988 P; in course of publication in Nucl. Instr. Meth. B.
4. B.Sulik, I.Kádár, S.Ricz, D.Varga, J.Végh, G.Hock and D.Berényi, Nucl. Instr. Meth. B28 (1987) 509.
5. B.Sulik, G.Hock and D.Berényi, Journal of Physics B: At. Mol. Phys. 17 (1984) 3239.
6. S.Ricz, I.Kádár and J.Végh, 'Post collision interaction observed at high-energy ion-atom collisions', 10th Conference on the Application of Accelerators in Research and Industry, Nov 7-9, 1988, NTSU, Denton, Texas, USA; ATOMKI Preprint 4-1988 P; Nucl. Inst. Meth. B, in press

ON THE M2/E1 MIXING IN L₃ X-RAY TRANSITIONS

T. Papp, J. Pálinkás and L. Sarkadi

Institute of Nuclear Research of the Hungarian Academy
of Sciences(ATOMKI), Debrecen, Pf. 51., H-4001, Hungary

The determination of the multipole mixing ratios in x-ray transitions gives a unique possibility for testing the components of the multipole expansion. When the electric dipole transition (E1) is allowed, the magnetic quadrupole (M2) term is the second largest in the multipole expansion. The ratio of the M2 and E1 amplitudes (the M2/E1 mixing ratio) can be determined experimentally from the angular distribution of an x-ray transition, if the charge distribution of the initial and final states are known.

The charge distribution in a given electronic state can be characterised by the alignment parameter (A_2), which is a combination of the relative population of the different magnetic substates. If the final state of the x-ray transition is anisotropically populated by a specific process (e.g. x-ray cascades or charged particle impact ionisation) and the initial state is statistically populated, the angular distribution of the x-ray transition can be expressed as

$$I(\theta) = I_0 [1 + \beta P_2(\cos\theta)],$$

where I_0 is the total intensity, $P_2(\cos\theta)$ is the second order Legendre polynomial. The β anisotropy parameter is related to the A_2 alignment parameter of the final state through $\beta = \alpha A_2$, where α depends on the angular momentum of the initial and final states of the electromagnetic transition and on the M2/E1 mixing ratio [1]. In the L x-ray spectra the $L_{\alpha 2}$ line (M4-L₃ transition) does not have magnetic terms, one can determine the alignment parameter of the L₃ subshell from the measured angular distribution of the $L_{\alpha 2}$ line. Using this alignment parameter, the α -s and the M2/E1 mixing ratios can be determined for the other transitions from the measured anisotropy parameters.

Thin uranium and thorium targets were bombarded by 1.5 MeV protons, obtained from the VdG accelerator of the ATOMKI. The x-rays were detected by a Si(Li) detector at 10 different angles. From the angular distribution we determined the anisotropy parameters for the L₁, L_{α1,2}, L_{β6}, L_{β2,15} x-rays of Th and U, and for the $L_{\alpha 2}$ of U. In the case of U the separation of the $L_{\alpha 2}$ from the $L_{\alpha 1}$ was achieved by using a bromine absorber, with its absorption edge falling between the $L_{\alpha 2}$ and $L_{\alpha 1}$ lines. Using appropriate absorber thickness, the measured intensity of the $L_{\alpha 1}$ line can be kept

below one per cent of the $L_{\alpha 2}$ intensity. Following the way proposed in [1] we obtained the mixing ratios for the $L_{\alpha 1}$, $L_{\alpha 2}$ and $L_{\beta 3}$ transitions of uranium. It was found, that the $L_{\beta 3}$ transition has quite large M2 components.

In figure 1. the β anisotropy parameter ratios of the $L_{\alpha 1}$ and $L_{\alpha 1,2}$ transitions are displayed for gold (open circle, from ref. [2]), thorium and uranium (full circle, present data). The obtained experimental data deviate significantly from the pure E1 transition assumption (full line) and from the theoretical results, displayed by dashed curve [3]. The measured data do not follow the tendency of the theoretical prediction.

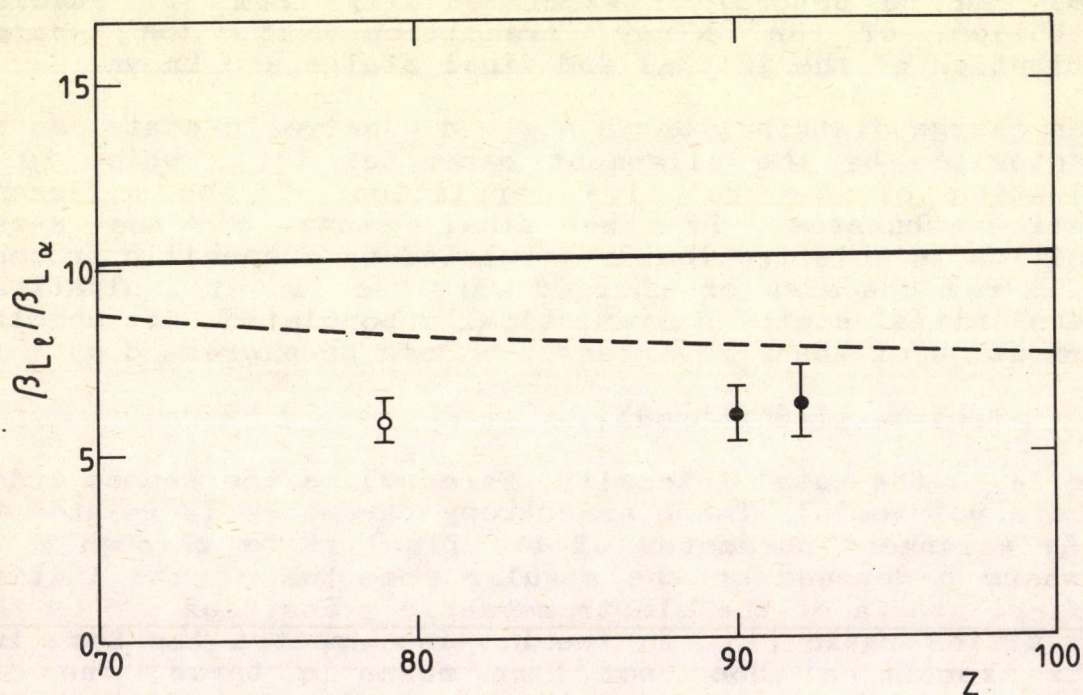


Figure 1. The ratios of the anisotropy parameters of the $L_{\alpha 1}$ and $L_{\alpha 1,2}$ transitions (see text).

References:

- [1] T. Papp, Proc. of 3rd Int Seminar on High Energy Ion-Atom Coll. Debrecen, Aug. 2-5, 1987., in Lecture Notes in Physics 294, Eds. D. Berényi and G. Hock (Springer-Verlag Berlin Heidelberg 1988) p. 204
- [2] T. Papp and J. Pálinkás, Phys. Rev. A38 (1988) 2686.
- [3] J.H. Scofield, Phys. Rev. 179, 9 (1969).

EXPERIMENTAL STUDY OF THE L₃-SUBSHELL ALIGNMENT OF MULTIPLY IONIZED ATOMS

T Papp*, J Pálincás*, L Sarkadi*, C Neelmeijer†, K Brankoff†,
D Grambole, C Heiser†, F Herrmann†, W Rudolph† and L Kocbach*

* Inst. of Nucl. Res. of the H.A.S. (ATOMKI), Debrecen, Hungary

† Zentralinstitut für Kernforschung, Rossendorf, GDR

• Department of Physics, University of Bergen, Norway

In the inner shell ionization studies of heavy target atoms ionized by heavy projectiles the multiple ionization may play important role [1]. The semiconductor x-ray detectors cannot resolve the different satellite lines in energy. In inner shell alignment studies the alignment parameters are usually determined from the angular distribution of the L₁ line. The measured intensity is the sum of the intensity of the diagram (single ionization) and satellite (multiple ionization) lines. At the same time the theoretical alignment parameters are calculated for the single ionized atoms [2,3] except for a recent study where calculation was made for double ionized atoms [4].

To study the effect of the multiple ionization on the L₃ subshell alignment a measurement was designed, where part of the satellite lines were absorbed by an absorber material, whose absorption edge falls above the diagram line. For the absorber the transmission of the diagram and satellite lines was planned to differ significantly. Here some preliminary results for Tl target and Cu absorber are presented. The K absorption edge of Cu absorber are above the L₁ diagram line of Tl by 23 eV. The energies of the L₃M satellites are larger than the energy of the absorption edge. The absorber thickness was 17 mgcm⁻², which resulted in a value of 150 for the transmission ratio before and after the absorption edge. 2.5 MeV proton and 1 MeV/nucl. N, Si and Cl ion beams of the heavy-ion tandem accelerator of the Zentralinstitut für Kernforschung (Rossendorf, GDR) were used as projectiles.

The spectra measured with Si(Li) detector at 55° without and with Cu absorber are presented in fig. 1. Measuring without absorber the L₁/L_α intensity ratios are the same for the different projectiles. Measuring with absorber the satellite intensities are greatly reduced. The evaluated L₁/L_α ratios normalised to the ratio of the proton impact case are shown in fig. 2. It can be seen that the multiple ionization is a dominating process for heavy projectiles. The angular distribution was also measured with and without the absorber. The evaluation of the data is in progress.

References.

- [1] W Jitschin, R Hippler, R Shanker, H Kleinpoppen, R Schuch and H O Lutz, J. Phys. B.: At. Mol. Phys. 16 (1983) 1417.
- [2] F Rösler, D Trautmann and G Baur, Z. Phys. A304 (1982) 75.
- [3] L. Sarkadi, J. Phys. B: Atom. Molec. Phys, 19 (1986) 2519.
- [4] T Papp and L Kocbach, J. de Physique C9 (1987) 245.

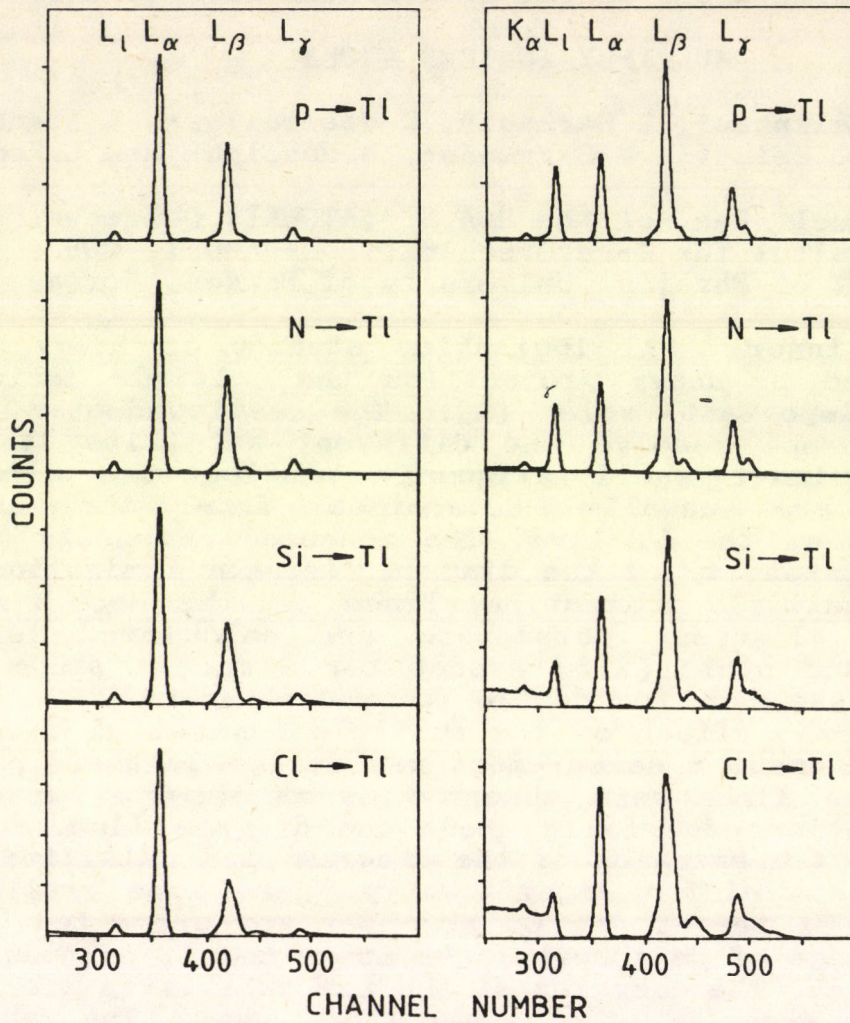


Fig. 1. L X-ray spectra of Tl induced by 2.5 MeV proton and 1 MeV/amu N, Si and Cl ion impact, recorded with a Si(Li) detector (left side), and using 17 mg/cm² Cu absorber in front of the Si(Li) detector (right side).

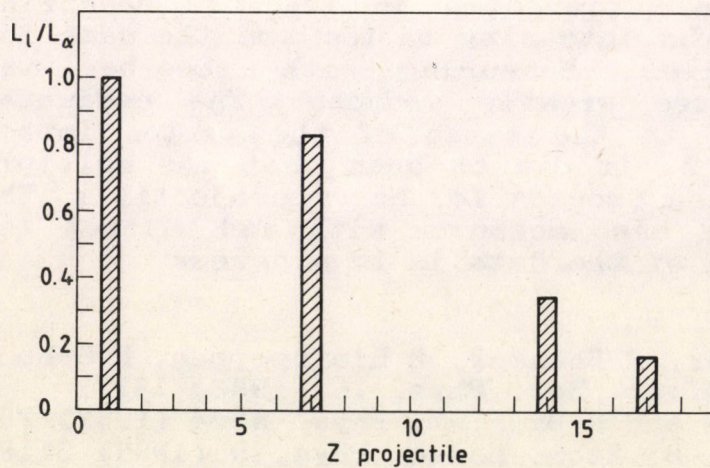


Fig. 2. The intensity ratio of the L₁ and L_α lines of Tl, recorded using 17 mg/cm² Cu absorber in front of the Si(Li) detector. The target was ionized by 2.5 MeV proton and 1 MeV/amu N, Si and Cl ion impact.

MEASUREMENTS WITH A SOLLER-TYPE X-RAY CRYSTAL SPECTROMETER

I. Török

Our Soller-type X-ray crystal spectrometer working on ion beams became operational in 1986 [1,2]. Three main themes, mentioned in the last Annual Report and at the X'87 conference in Paris[3], were investigated further in a more detailed manner.

A/ The $K\alpha$ X-ray lines of the following elements were measured: Mg, Al, Si, Ca, Ti. P_L values obtained from our relative satellite intensity data were compared with the predictions of a simple geometrical model [4]. The calculations show agreement within 25%. Sample spectra are shown in Fig. 1., which also reveals chemical effects.

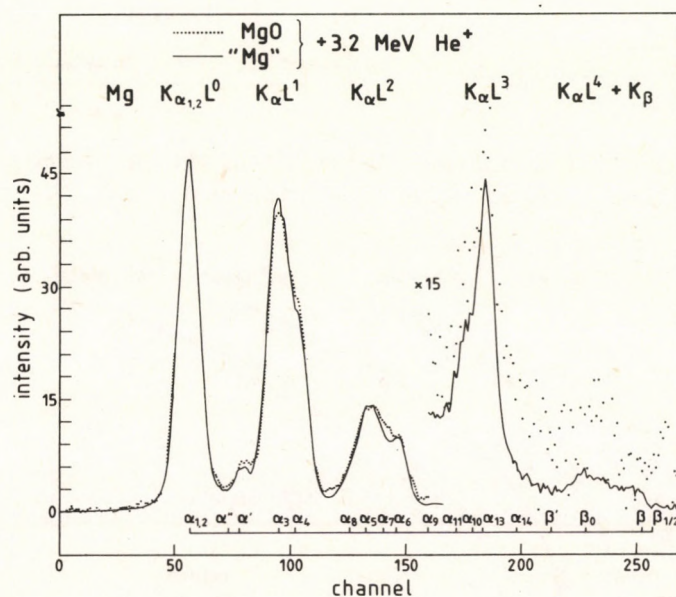


Fig. 1. $K\alpha$ X-ray lines of Mg obtained bombarding 0.5 mm thick metal targets with 3.2 MeV He^+ ions. Solid line: spectrum from a target etched in acetic acid, dotted line: spectrum from a target oxidized in air for many years. Note the α_3 and α_4 amplitudes. Satellite labels and energies are from ref.[5].

B/ The Mg/Ca ratio determination in limestones, using the third order reflection of Ca $K\alpha$ and first order reflection of Mg $K\alpha$ lines with ADP crystal, was helped by measurements of known $CaCO_3+MgCO_3$ mixtures and the creation of a calibration curve for 2 MeV protons. Effects of detector window material and window thickness, the X-ray production cross section vs. bombarding energy dependence (see Fig. 2.), and other technical factors have been investigated to determine how they could be used in optimizing the measurements.

C/ The Ta $M\alpha$ and $M\beta$ satellites also were measured at several bombarding energies with proton and He^+ projectiles, and by X-ray excitation for comparison. The experimental results compared with the preliminary values from a geometrical model [4] show agreement within about 30 %.

For the above measurements ca. 3 weeks of accelerator beam time was used at the 5 MV Van de Graaff generator of our institute.

The experimental energy resolution values obtained in the different measurements were compared with the energy resolutions calculated from the 0.3 degree angular divergence of the Soller-slits, see Fig. 3.

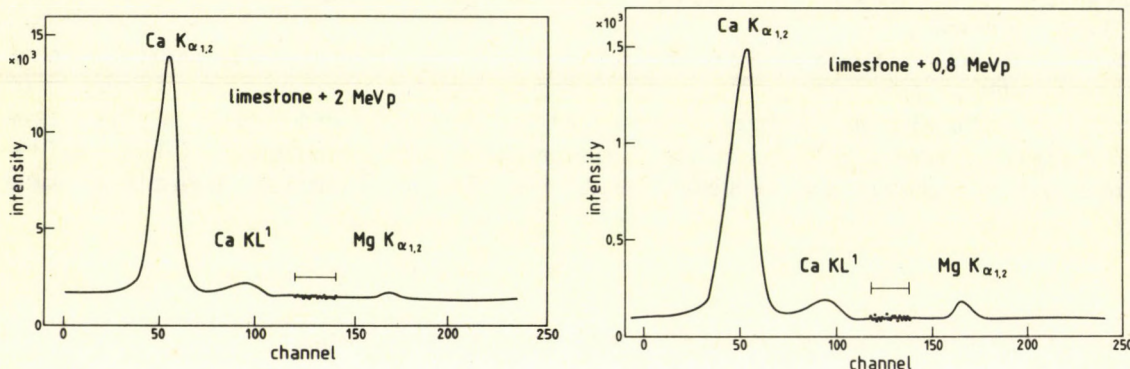


Fig. 2. Ca and Mg K_{α} lines from limestone bombarded by 2.0 and 0.8 MeV protons. Note the enhancement of Mg peak at 0.8 MeV.

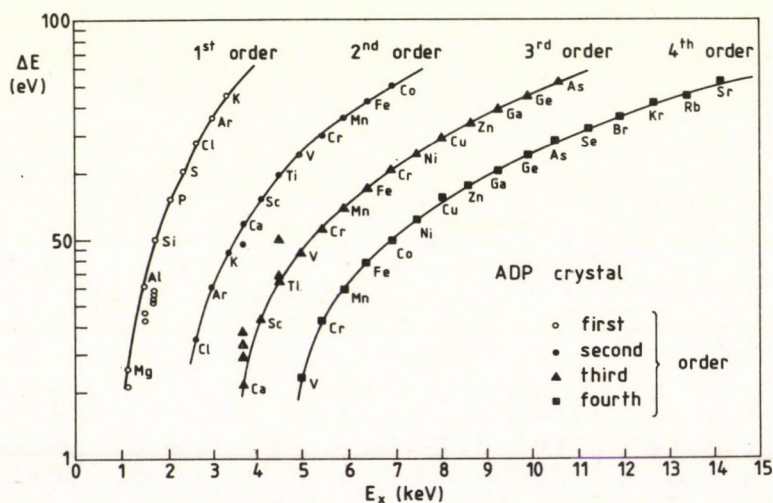


Fig. 3. Predicted and experimental energy resolution of our X-ray crystal spectrometer using ADP crystal.

References

- [1] I. Török, B. Tóth, ATOMKI Ann. Rep. 1986, p.60.
- [2] I. Török, B. Tóth, ATOMKI Ann. Rep. 1987, p.66.
- [3] I. Török, B. Tóth, J. Physique, C9 suppl. no.12. 48(1987)C9-79.
- [4] B. Sulik, I. Kádár, S. Ricz, D. Varga, J. Végh, G. Hock, D. Berényi, Nucl. Instrum. Meth. B28(1987)509.
- [5] M. D. Krause, J. G. Ferreira, J. Phys. B: At. Mol. Phys. 8(1975)12, 2007.

AN EXPERIMENTAL METHOD FOR THE DETERMINATION OF ABSOLUTE X-RAY WIDTHS BY THE HELP OF COMBINED ICES AND XPS MEASUREMENTS

L. Kóvër

In the quantitative applications of different electron spectroscopic methods, as e.g. the X-ray photoelectron spectroscopy (XPS) or the internal conversion electron spectroscopy (ICES), the accurate knowledge of the respective contributions of the X-ray excitation or the finite analyzer resolution to the measured spectra are of basic importance. It is difficult, however, to find experimental methods for determining these contributions separately. Data on X-ray line shapes e.g. were obtained earlier (by photoelectron spectroscopy) assuming known instrumental functions [1,2]. A short description of an experimental method, applicable for the absolute measurement of the X-ray contribution to the width of the $AlK\alpha$ excited photoelectron spectra (without assumptions on the instrumental function) and based on independent and subsequent ICES and XPS measurements of Tc 3d electron peaks, is presented in the followings.

The $3d_{5/2}$ core level in the Tc atom has a considerably low (~ 0.1 eV [3,4]) natural width and the internal conversion of the Tc $3d_{5/2}$ electrons from the Tc 99m isomer state has a rather high probability. The corresponding transition energy is 2.17 keV and the multipolarity is $E3$ [5].

As a first step of the method proposed, the Tc 99m M $_{4,5}$ conversion electron spectrum should be measured by an electrostatic electron spectrometer in Fixed Analyzer Transmission (FAT) working mode, selecting an analyzer pass energy belonging to good resolution. In FAT mode, the analyzer determines the resolution of the spectrometer, independently of the kinetic energy of the electrons emitted from the sample. Secondly, the 3d XPS spectrum of the same sample should be measured by using FAT mode at the same analyzer electron pass energy. While in the case of the ICES measurements the main contributions to the width of the M $_{5}$ electron peak are due to the respective natural level width and the analyzer resolution, the $3d_{5/2}$ XPS spectrum measured in the way given above will differ from the ICES spectrum essentially only in a broadening caused by the X-ray (e.g. $AlK\alpha$) excitation. If the shape of the X-ray line is assumed to be a Lorentzian one, an optimum fit of the XPS spectrum by the corresponding ICES spectrum convoluted by Lorentzians having various widths, will provide the experimentally determined value for the absolute natural width of the exciting X-ray line.

The main assumptions made in this procedure are:

- 1., the resolution function of the spectrometer is determined by the analyzer in FAT mode
- 2., inelastic electron scattering events have negligible effects on the electron line widths (ICES and XPS peaks are sampling different depths inside of the specimen surface region).

For determining the $AlK\alpha$ natural width, NH_4TcO_4 samples are proposed since the respective Tc 3d lines from this compound proved to be fairly symmetric [6].

The described method is applicable for determining the natural widths of the several keV single X-ray lines, however, the increasing role of the inelastic electron scattering at higher energies should be taken into account.

Experiments for the determination of the natural width of the $AlK\alpha_{1,2}$ X-ray line by using the method described here are in progress, in cooperation with the electron spectroscopic group of the Nuclear Physics Institute, Prague.

References

- [1] M.O. Krause, J.G. Ferreira, J. Phys. B: Atom. Molec. Phys. 8 (1975) 2007
- [2] N. Beatham, A.F. Orchard, J. Electron Spectrosc. and Rel. Phenom. 9 (1976) 129
- [3] L. Kövër, J. Tóth, I. Cserny, M. Fišer, Poverhnost N^o10 (1987) p.17
- [4] I. Cserny, L. Kövër, J. Tóth, M. Fišer, J. de Physique C9 Suppl. N^o12 48 (1987) C9-1017
- [5] O. Dragoun, Advances in Electronics and Electron Phys. 60 (1983) 1
- [6] O. Dragoun, M. Fišer, V. Brabec, A. Kovalik, A. Kuklik, P. Mikušik, Phys. Lett. 99 (1983) 187

COINCIDENCE STUDIES OF THE FORWARD ELECTRON CUSP

Á. Kövér, L. Sarkadi, J. Pálinkás, L. Gulyás, Gy.
Szabó, T. Vajnai⁺, D. Berényi, O. Heil*, K. O.
Groeneveld*, J. Gibbons^{\$} and I. A. Sellin^{\$}

The motivation of the present work was the discrepancy found between the experiment and theory in our former study [1] of the forward ejected "cusp" electrons in He^+ - He collisions. For structured projectiles (like He^+) the two main processes producing cusp electrons are: (i) the loss of an electron from the projectile into its continuum states (ELC), (ii) the capture of an electron from the target into the continuum states of the projectile (ECC). Until our present work it was believed that for collisions involving structured projectiles the dominant process is ELC. The failure of the ELC theories in description of our measured single differential cross section values of the cusp production in He^+ - He collision [1], however, indicated an increasing contribution from ECC with decreasing collision velocity. Recently Heil et al. [2] showed experimentally (for 0.2 - 0.33 MeV/amu $^3\text{He}^+$ - He collisions) that the discrepancy is indeed due to the presence of the ECC process.

In the present study we extended the measurement of Heil et al. [2] to lower projectile velocities providing further, more convincing experimental verification of the growing contribution of the ECC process. The experimental method was based on the coincident detection of the cusp electrons with the charge-state selected outgoing projectiles. The ECC events are correlated with unchanged charge state, the ELC process leads to an increase of the projectile charge by one. The experiments were performed for He^+ - He and He^+ - Ar collision systems in the energy range 0.05 - 0.15 MeV/amu. The He^+ beam was obtained from the 1.5 MeV Van de Graaff accelerator of ATOMKI. The electrons were analyzed by a double stage cylindrical mirror electron spectrometer (ESA-13). The ions were detected by a fast particle detector based on collection and amplification of secondary electrons emitted from a metallic surface hit by the particles. Coincidences between the electrons and the outgoing projectiles with specific charge states were established using standard fast electronic circuits.

Fig. 1 shows the obtained relative contributions to the cusp electron production. The figure includes also the results obtained for a two-electron process, namely for transfer ionization (TI). This process consists of simultaneous capture of two electrons (one into a bound state and one into a continuum state of the projectile). The figure demonstrates the dominance of ECC over ELC at low projectile velocities.

As a continuation of our studies of the cusp produced by structured particles we made further coincidence measurements applying neutral atoms (H^0 , He^0) as projectiles. At 0.075 MeV/amu bombarding energy we observed a substantial contribution from the ECC channel. This observation proves that the ECC proc-

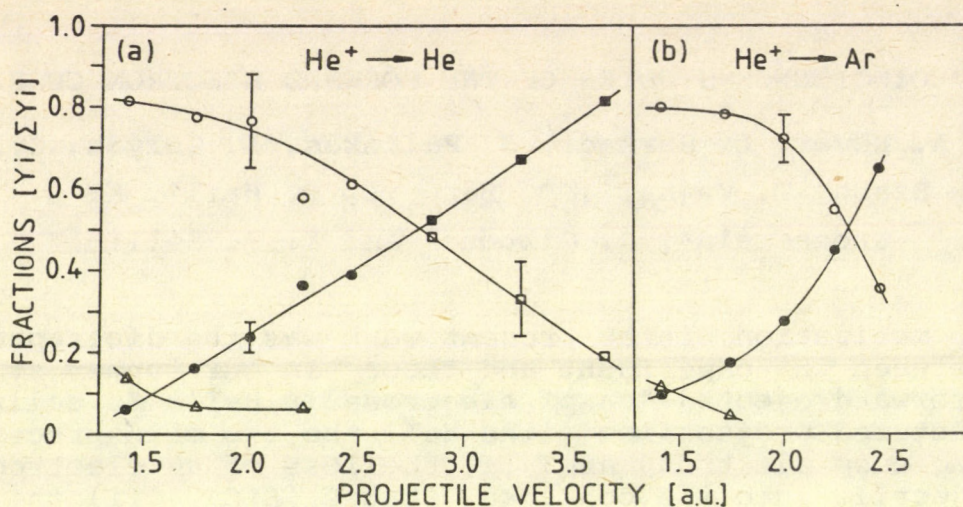


Fig. 1. Relative cusp yields as a function of the projectile velocity. Present results: •, ELC; o, ECC; Δ, TI. The data of Heil et al. [2]: ■, ELC; □, ECC.

ess exists also for projectiles with completely screened Coulomb potential. It is interesting to note that the ECC for neutral atom impact is characterized by a considerably smaller width of the cusp than for ion impact.

Concerning the shape of the cusps measured in the present work, the data are not accurate enough to perform a quantitative analysis. A qualitative comparison of the spectra shows that the shape sensitively depends on the process (ELC, ECC), on the target, as well as on the charge state of the incoming particle. In spite of the large statistical errors, the ELC spectra for He^+ impact have been fitted with the series expansion method. The definitely positive values obtained for the β_2 parameter at low collision velocities indicate the existence of cusp inversion in the ELC process [3] (appearance of a dip at the maximum of the peak).

References

- [1] Á. Kövér, Gy. Szabó, D. Berényi, L. Gulyás, I. Cserny, K. O. Groeneveld, D. Hofmann, P. Koschar and M. Burkhard, *J. Phys. B: At. Mol. Phys.* **19** (1986) 1187.
- [2] O. Heil, J. Kemmler, K. Kroneberger, Á. Kövér, Gy. Szabó, L. Gulyás, R. DeSerio, S. Lencinas, N. Keller, D. Hofmann, H. Rothard, D. Berényi and K. O. Groeneveld, *Z. Phys. D - At. Mol. and Clusters* **9** (1988) 229.
- [3] J. Burgdörfer, M. Breinig, S. B. Elston and I. A. Sellin, *Phys. Rev. A* **28** (1983) 3277.

⁺ On leave from Technical University for Heavy Industry, Miskolc, Hungary

* Institute for Nuclear Physics of J. W. Goethe University, Frankfurt am Main, Germany

\$ University of Tennessee and Oak Ridge National Laboratory, Oak Ridge, Tennessee, USA

**CUSP-SHAPE STUDIES BY MEANS OF CONTOUR LINES AND BY MULTIPOLE
SERIES EXPANSION OF THE ELECTRON DISTRIBUTION AS A FUNCTION OF
THE ELECTRON ENERGY AND EMISSION ANGLE**

L.Gulyás, Gy.Szabó, A.Kövér and D.Berényi

Institute of Nuclear Research of the Hung. Acad. Sci.,
Debrecen, Hungary

O.Heil and K.O.Groeneveld

Institute of Nuclear Physics of J.W. Goethe University,
Frankfurt/M, FRG

The cusp in the ejected electron spectrum was studied at H^0 , He^+ , He^{2+} (0.2 MeV/u) - Ne, Ar, Kr collisions to obtain information on the shape of it in a three-dimensional presentation and to compare the experimental data with the theoretical calculations. The energy spectra were taken at different emission angles from 0° to 4° and so the analysis of the cusp was made in a three-dimensional approach (contour lines, fitting of the three-dimensional data set to obtain the coefficient of the multipole series expansion). Such a study is the more justified because the number of experimentally determined coefficients are very few and they are missing for light ions with accompanying electrons. At the same time these values are important to check the theoretical predictions.

Fig. 1 shows two typical examples for the contour lines in the case of He^+ -Kr and H^0 -Kr in comparison with the corresponding theoretical patterns (see details in [1]). In general, the agreement between the theory and experiment is better for He^+ than for H^0 . The pattern for H^0 is more similar to that obtained for He^{2+} than for He^+ .

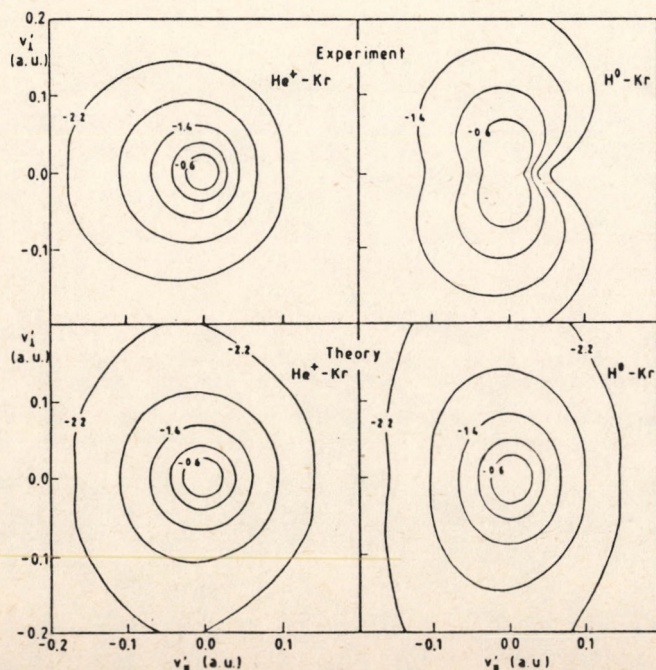


Fig.1. A comparison of the deconvoluted experimental and theoretical contour lines. The numbers at the contour lines represent the logarithmic ratio of the concerned and the top level. The abscissa and the ordinate are the components of the electron velocity [1].

The values β_1 and β_2 are defined as $\beta_k = B_{0k}/B_{00}$. β_1 characterizing the asymmetric velocity distribution of the cusp along the direction of the projectile was found to be negative and finite for all the three projectiles. The non-zero value of this parameter for H^0 and He^+ (projectiles with accompanying electron) is in contradiction with the theoretical predictions [2,3].

As regards β_2 , it was found to be negative in the present experiment, and it is higher for H^0 than He^+ (for He^{2+} similar to that of H^0). The high negative value (i.e. close to -1, which is the maximum value of β_2) means a strong symmetric transverse velocity distribution along the projectile velocity (the contour lines show a "finger-biscuit" pattern). At H^0 and He^{2+} , however, this symmetric "finger-biscuit" form is "distorted" by the "influence" of β_1 parameter which results in a contour lines with the "infolding" (see the figure).

The giant monopole resonances have completely different features as can be expected from a breathing mode but it can be observed that they are also built upon mainly bound or quasibound configurations.

The calculated escape widths agree reasonable well with available experimental data. Among the states which have not been observed so far, our calculation predicts that will be likely to be observed

is the octupole isovector giant resonance, with 89% of its strength concentrated at about 31 MeV.

1. L.Gulyás, Gy.Szabó, A.Kövér, D.Berényi, O.Heil, K.O.Groeneveld; accepted for publication in Phys. Rev. A., 1988
2. I.Burgdörfer, M.Breinig, S.B.Elston and I.A.Sellin, Phys. Rev. A28, 3277 (1983)
3. M.H.Day, I. Phys. B 13 L65 (1980)

λ	T	E_n (MeV)	Γ (keV)	S_n (%)
0	0	13.80	200	100
2	0	15.41	120	72
2	1	26.31	1040	73
3	0	16.73	50	35
3	1	30.65	1540	65
4	0	26.87	120	23

Table 1. Main components of the β_1 and β_2 parameters calculated with the present method. The escape widths Γ are given in keV and the strength S_n in %.

References

1. T. Yano, P. Chuganov, G. H. Heise, L. S. Petricola and R. E. Olson, Phys. Rev. A 38, 1000 (1988)
2. F. Burgdörfer, Nucl. Phys. A190, 265, 1988
3. P. Chuganov, T. Yano and R. E. Olson, Phys. Rev. C 38, 1000 (1988)

**On the dependence of recoil-ion velocity on the screening
effect of the target electrons**

B. Sulik and L. Végh

The measurement of multiple-ionization cross sections as a function of the recoil-ion velocity provides a deeper insight into the collision mechanism than the measurement of the total cross sections. The dependence of the multiple ionization cross section on the energy of the recoil ion provides information about the interplay of the interactions acting between the projectile and the target nucleus, between the projectile and the target electrons, the nucleus and electrons of the target, and between the different electrons of the target.

The repulsive projectile-target nucleus Coulomb interaction pushes away the target nucleus and at the same time the projectile attracts the electrons of the target. The interplay of the repulsive and attractive interactions results that, for elastic scattering, the relative motion of the projectile and the target can be described by a screened projectile-atom interaction. For a collision, where the target atom is ionized, the description of the motion of the target ion by the use of a screened Coulomb interaction is not well established. Due to the electron-electron interactions, the electrons remained attached to the target ion have possibility to interact with the ejected electrons. Furthermore, the final state interaction between the ejected electrons and the target nucleus may lead to a screening-like effect. Therefore the recoil energy depends on the intensity of the ejected-electron target-electron and ejected-electron target-nucleus interactions.

Ullrich et al.[1] have measured the multiple ionization cross-sections for the $U^{32+} - Ne$ collision system as a function of the recoil-ion momentum component transverse to the beam axis. The recoil-ion energy has a negligible dependence on the Q -value of this reaction and can be taken to be equal with the recoil energy of the fully elastic collision. In ref. [1] the differential cross sections are given for the production of recoil ions with charge states $q = 1...8$.

Analysing the data [1] using the independent electron approximation we have obtained the surprising result that the agreement between the experimental data and the

theoretical curves seems to be the best in the case of the unscreened projectile-target nucleus Coulomb interaction [2]. The agreement is better for small values of q which corresponds to larger impact parameters. For smaller impact parameters our calculated cross sections are larger than the measured ones.

The results suggest that already in the case when only one target electron is ejected, the screening effect of the target electrons, related to the motion of the target ion, is negligible. The screened Coulomb interaction, which is a suitable tool for calculation of the elastic ion-atom scattering cross-sections, fails to describe the motion of the recoil ion produced during the ionization process. This effect suggests that the momentum, given to the electrons of the target atom by the projectile, is transferred to the ionized electrons by some electron-electron correlation effects. At the same time, the validity of the independent electron approximation requires that this correlation effect should be a final state interaction. The screening-like effect at high values of q may be explained by the ejected-electron target-nucleus collisions which deaccelerate the target nucleus.

This picture involves that with the decrease of q the mean energy of the ejected electrons, compared to the ionization potentials, increases. Furthermore, the sum of the transverse momenta of the ejected electrons is about the same as the transverse momentum of the recoil ion. Our assumption is supported by the results of the classical-trajectory Monte-Carlo calculations [3] for the projectile energy-loss and ejected electron energy and angular spectra. Moreover the increase of the asymmetry of angular distribution of the ejected electrons with the decrease of the recoil-ion charge-state can be predicted.

REFERENCES

- [1] Ullrich, J., Horbatsch, M., Dangendorf, V., Kelbch, S., Schmidt-Böcking, H. : *J. Phys.* **B21**, 611 (1988).
- [2] Végh, L. and Sulik, B to be published in *Proc. of Conf. SCFEI, Bucharest, 29 August-2 September 1988*.
- [3] Olson, R. E., Ullrich, J., Schmidt-Böcking, H. : *J.Phys.* **B20**, L809 (1987).

Scattering Correlation in Multiple Ionization

L. Végh

Institute of Nuclear Research of the Hungarian Academy of Sciences, Debrecen, Hungary

T. Watanabe

The Atomic Processes Laboratory, The Institute of Physical and Chemical Research, Wako-shi, Japan

There is an increasing interest in the study of the scattering correlation effects using electron, proton, antiproton and multicharged ion impacts. Since the cross section of the Rutherford scattering does not depend on the sign of the projectile charge, the dependence of the measured cross sections on the sign of the charge should be attributed to the interplay of the interactions between the projectile and electrons and those between the electrons.

Using atomic targets, the single-ionization cross section obtained with fast proton and antiproton projectiles are found to be the same. As for the double ionization processes, a marked projectile-charge-sign dependence of the cross section has been found [1]. The ratios $R_2 = \sigma^{++}(p^-)/\sigma^{++}(p^+)$ and $\sigma^{++}(e^-)/\sigma^{++}(p^+)$ have values about 2 at different targets for fast projectiles. The experimental data [1] shows that for the triple ionization of the Ne target there is a larger difference between the cross sections of antiprotons and protons than it is for the double ionization. The ratio $R_3 = \sigma^{+++}(p^-)/\sigma^{+++}(p^+)$ can have the value of 4. This result suggests that the larger is the number of the ejected electrons, the more striking is the dependence on the sign of the projectile charge. This means that the multiple ionization cross section should have a strong dependence on the scattering electron-electron correlations which manifest themselves during the collision processes.

At the same time the independent electron approximation is thought to be an excellent method to describe the multiple ionization processes [2]. How can we reconcile this success with the importance of the electron-electron correlations which should involve the failure of the independent electron approximation?

The majority of the study of the multiple ionization probabilities has been confined to the investigation of the KL^n vacancy configurations produced by heavy ion impact. The electron-electron correlation effects, which are significant in the study of the total ionization cross sections with singly charged projectiles are probably unimportant in close-collision processes induced by multiply charged ions.

Now we propose a simple picture which may elucidate the difference between the correlation effects occurring in the calculation of the total ionization cross section and

that of the ionization probabilities at small impact parameters. In the independent electron approximation the potential energies of the two electrons with positions \vec{r}_1 and \vec{r}_2 depend only on the absolute values r_1 and r_2 and does not depend on the angle θ where $\cos\theta = \vec{r}_1\vec{r}_2/r_1r_2$. Taking into account the electron-electron interaction, the potential energy of the two electron system has a minimum at $\theta = 0$. Increasing θ the interaction energy is increased compared to the noncorrelated case. Now we assume that during the process of multiple ionization induced by the direct Coulomb interaction with the fast projectile the ejected electrons leave the target volume at the same time interval. This results in an increase of the potential energies of each ejected electrons. The effect may approximately be described by an effective increase of the potential of the projectile. For the potential of a positively charged projectile this involves an effective decrease of its strength, that is the interaction will be weakened. For a negatively charged projectile this effect increases the strength of the projectile-electron interaction that is the interaction will be enhanced [3].

In the ionization process the plane defined by the line of the projectile path and the position of the target nucleus has a distinguished role namely the orbits of the ejected electrons are close to this plane. The higher is the impact parameter, the closer are the ejected electron orbits to this plane and the more intensive are the correlation effects. This picture suggests that the multielectron correlation effects are more pronounced for higher impact parameters. At the region of zero impact parameter the ejection of electrons does not depend on the azimuth angle ϕ that is the correlation effects are decreased.

The correlation effects should decrease with the increase of the projectile charge. For higher projectile charge the weight of the correlation interaction is smaller at a given impact parameter. Therefore in the small impact-parameter heavy-ion induced multiionization processes the correlation effects are of less importance.

REFERENCES

- [1] L. H. Andersen, P. Hvelplund, H. Knudsen, S. P. Moller, A. H. Sorensen, K. Elsener, K.-G. Rensfelt, and E. Uggerhoj, Phys. Rev. **A36** (1987) 3612
- [2] R. L. Becker, A. L. Ford, and J. F. Reading, Phys. Rev. **A29** (1984) 3111
- [3] T. Watanabe and L. Végh to be published in Nucl. Instrum. Meth. B

Critical Angle in Double Ionization

L. Végh

The production of singly- and doubly-charged He ions in proton-helium collision has been measured as a function of the projectile scattering angle θ in the region $\theta = 0.25 - 4.1\text{mrad}$ at incident energies $E_p = 300 - 1000\text{keV}$ by Giese and Horsdal (1988). The fraction of the doubly-charged ions $F_2 = \sigma^{++}/(\sigma^+ + \sigma^{++})$, where σ^{++} and σ^+ are the cross sections for double and single ionisation, respectively, exhibits a distinct peak at $\theta \sim 0.9\text{mrad}$. The maximum scattering angle for a proton off a free electron at rest is $\theta_{max} = m/M = 0.545\text{mrad}$, where m and M are the masses of the electron and the proton, respectively. Therefore the large scattering angle of the projectile is related to the deflection in the Coulomb field of the target nucleus. There is no reason to expect a peak for this mechanism at all.

We suggest that the distinct peak at scattering angle 0.9mrad can be explained by the kinematics of a multiple scattering mechanism which is similar to that of given by Thomas (1927) for electron capture. Following a violent projectile - electron collision, the scattered electron knocks out the second electron and there is a third collision, the second projectile-electron scattering, see the figure. As large deflection angles correspond to large-angle electron-proton scatterings, we restrict ourselves to the study of the process where the second projectile-electron collision is a head-on scattering, see the paper of Végh (1988).

Neglecting the target-electron motion and the binding effects, the velocity of the knocked electron after the first proton-electron collision is

$$v_1 = 2vcos\alpha \quad (1)$$

where v is the velocity of the incident proton and α is the angle of the electron motion, see the figure. Let the angle between the projectile velocity \vec{v} and the electron velocity \vec{v}_2 be β . The velocities after the electron-electron binary collision have the values

$$v_2 = v_1 cos(\alpha + \beta), v_3 = v_1 sin(\alpha + \beta) \quad (2)$$

To ensure the head-on collision between the projectile and the electron in the second projectile-electron scattering we obtain that $\beta = 90^\circ - 2\alpha$ and the sum of the two deflection angles of the proton is given as

$$\theta = \theta_1 + \theta_2 \approx \frac{m}{M}(\sin 2\alpha + \sin 4\alpha) \quad (3)$$

that is, the deflection angle θ can be expressed by the angle α of the first proton-electron collision.

The cross section of the first scattering with electron velocity v_1 into a cone of semi-angle between α and $\alpha + d\alpha$ is

$$\sigma_1 = 2\pi\sigma_{pe}(\alpha, v_1)\sin\alpha d\alpha \quad (4)$$

where $\sigma_{pe}(\alpha, v_1)$ is the appropriate proton-electron Coulomb scattering cross section in the laboratory system. The electron-electron collision should have an impact parameter in the interval $b + db$ and an azimuth angle in the interval $\phi + d\phi$. Here b corresponds to the scattering angle $\alpha + \beta = 90^\circ - \alpha$ and $\phi + d\phi$ is the azimuth angle region of the first projectile-electron collision. The probability p that the electron-electron collision is characterized by these intervals is given by the ratio

$$p = \frac{b db d\phi}{\pi r_0^2} \quad (5)$$

where r_0 denotes the radius of the He atom. Using the relation

$$\sigma_{ee}(90^\circ - \alpha, v_2) = 2\pi b db \quad (6)$$

where $\sigma_{ee}(90^\circ - \alpha, v_2)$ is the corresponding electron-electron scattering cross-section in the laboratory system and taking into account Eqs.(4-6), for the calculation of the double-ionization cross section at deflection angle θ we obtain the following equation

$$\sigma(\theta, \phi) \sin\theta d\theta d\phi = \sigma_{pe}(\alpha, v_1) \sigma_{ee}(90^\circ - \alpha, v_2) \frac{\sin\alpha d\alpha d\phi}{\pi r_0^2} \quad (7)$$

The final expression can be calculated by using Eq. (3):

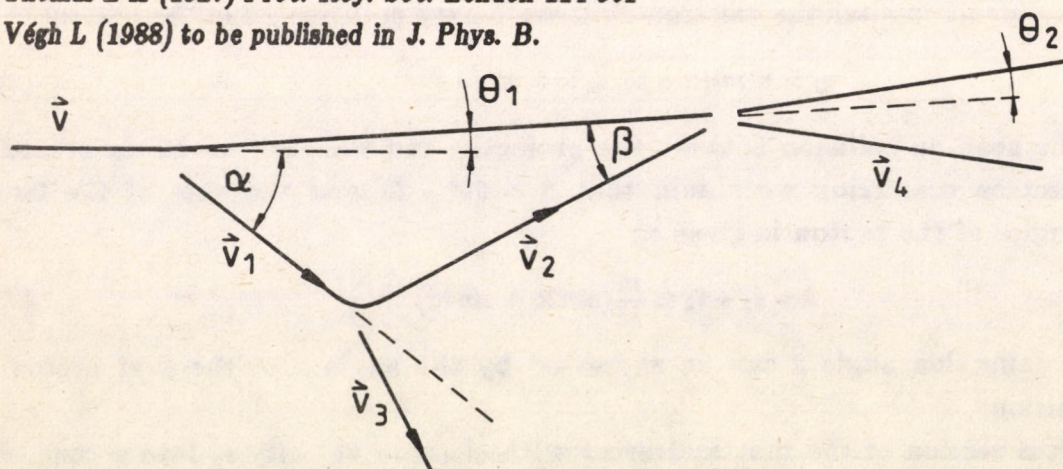
$$\sigma(\theta, \phi) = \frac{M^2}{m^2} \frac{\sin\alpha}{2(\cos 2\alpha + 2\cos 4\alpha)(\sin 2\alpha + \sin 4\alpha)} \frac{\sigma_{pe}(\alpha, v_1) \sigma_{ee}(90^\circ - \alpha, v_2)}{\pi r_0^2} \quad (8)$$

This cross section formula is singular at angle $\alpha = 26.81^\circ$. The correspondent scattering angle is $\theta_0 = 0.96 \text{ mrad}$. The position of the 0.96 mrad singularity does not depend on the proton velocity. The kinematical origin of the effect involves the presence of the 0.9 mrad peak for other targets.

Giese J P and Horsdal E (1988) *Phys. Rev. Lett.* 60 2018

Thomas L H (1927) *Proc. Roy. Soc. London* 114 561

Végh L (1988) to be published in *J. Phys. B.*



The mechanism of the double ionization and projectile deflection

INTERPRETATION OF NON-SEPARABILITY BY MEANS OF CONNECTIVE STRINGS

E. Vatai

Experimental confirmation of the theory-independent existence of non-separability [1] and of its two distinct levels [2] indicates that theory-independent explanation of non-separability (or non-locality) may exist also. Available descriptions [3] do not explain the existence of two levels of non-locality and the contradiction with relativity, according to which the speed of energy propagation is limited by the speed of the light c .

The explanation, free of the above difficulties, is based on the following assumption: (a) Elementary particles (quarks, leptons and photons) create around themselves massless and spinless fields of particle-antiparticle pairs, and of photons with opposite spins by polarization of the vacuum. (b) Particle fields form connected subspace, i.e., they have string structure. (c) Strings can be broken by vacuum fluctuations. The correctness of assumption (a) for photon field is proved in quantum field theory [4]. Assumption (b) follows from the production mechanism of low mass neutral particles [5], while (c) is trivial.

Wave propagation along classical string is $v = \sqrt{T_0 / \rho}$, where T_0 is the tension (energy/unit length) and ρ is the linear density. Evidently, when $\rho \rightarrow 0$ then $v \rightarrow \infty$, so any disturbance may propagate with such speed. This does not allow non-local energy transfer, because $\rho \sim 0$. An additional condition should be fulfilled: The latent energy-momentum, i.e., compensated by that of other components of the vacuum, of the particle in the particle-antiparticle field should be constant throughout the connected subspace. The non-local transfer of an elementary particle in such connected space can be described as splitting and shifting of the compensating string by one unit, so that it compensates the particle at the first location x and the compensation disappears, i.e., the particle appears, at location y . It is noteworthy that nothing is changed or transferred between x and y : This model makes possible non-local particle transfer without superluminal energy propagation, so relativity is not violated. Such transfer causes non-local development of the first kind of a quantum system, i.e., such development is not described by the time dependent Schrödinger equation (see e.g., the movement of the electron in the atom).

Non-locality of the second kind, which is characteristic for quantum systems with normal time development, is caused by non-local transfer of virtual photons or π -mesons. Such non-locality is possible for systems of elementary particles (e.g., nucleons), and for elementary particles connected by photon field. Both quark-antiquark strings, or spin up and down strings of photons are to be splitted and shifted in this case.

The present model suggests a new interpretation of the

atomic wave functions as well: The density distribution, $\rho = \Psi\Psi^+$, is proportional to the relative number of fluctuations above a threshold, which is required to split the e^+e^- double string.

References

1. A. Aspect, J. Delibard and G. Roger, Phys. Lett. 49 (1982) 1804; E. Vatai, J. Phys. B20 (1987) L731
2. E. Vatai, Phys. Rev. A38 (1988) 3777
3. D. Bohm, Phys. Rev. 85 (1952) 166, 180; Y. Ne'eman, in Symposium Found. Mod. Phys., ed. P. Lahti and P. Mittelstaedt (World Scientific, Singapore, 1985)
4. W. Heitler, The Quantum Theory of Radiation (Clarendon, Oxford, 1954)
5. E. Vatai, see in this issue

IDENTIFICATION OF THE NEW NEUTRAL PARTICLES AS OSCILLATING STRINGS

E. Vatai

The difficulties encountered by the identification of the neutral particles found in high energy ion-atom collisions [1] are caused by the following puzzling properties: (a) The particles are created at rest in the center of mass system, therefore the available phase-space is small or zero, which contradict to their high production rate. (b) Dependence of the production cross-section on the united nuclear charge is the same ($\delta_{exp} \sim Z_u^{2 \pm 2}$) as predicted for the e^+e^- pair production mechanism in the case of four particles found at masses 1.53, 1.69, 1.81 [1] and probably 1.92 (± 0.01) MeV/c², while the fifth, which was found at 1.73 MeV/e² in the coincidence spectrum only, in measurements at angles differing from that used in single measurements, does not exhibit the above property [2].

The masses in the first group were found [3] to correspond to the energy spectrum of an oscillating string, $m_n^2 = 1/\alpha' \times \sum_n n a_{un} a_n^\dagger$, where $1/\alpha' = 0.47 \pm 0.02$ (MeV)² is the Regge parameter, n the number of oscillations' mode and a_{un} are operators in Fock space. The experimental m_n^2/α' yield integer numbers, which allows one to assume that $m_0 \sim 0$, i.e., the mass of the basic particle (the non-oscillating string) is nearly zero. The mass spectrum obtained fits the experimental data and yields additional extrapolated masses and is given in Table 1.

Table 1.

n	0	1	2	3	4	5	6	7	8	9	10
M	0.0	0.68	0.97	1.18	1.37	1.53	1.70	1.81	1.94	2.06	2.17
M ²	0.0	0.47	0.93	1.40	1.87	2.35	2.88	3.29	3.37	4.24	4.71

Such string structure is similar to that exhibited by hadrons, therefore it is straightforward to assume that these particles are light (or lepto-) analogues of mesons. I shall show in a forthcoming paper [5] that similar conclusion can be reached by starting from the explanation of the ball lightnings' properties: It requires the existence of lepto-nucleons with weak electric charge, $e_w \sim 10^{-5}e$. Decay of hadrons into light particles is forbidden, because particles with electric charge $e' = e - e_w$ do not exist.

Dependence of the production probability on the united charge ($\sim Z_u^{2 \pm 2}$) is then explained as follows: It has been shown [5], that the proton (or nucleus) creates a massless string-field, which makes possible non-local transfer of electrons by the double-string mechanism. If the e^+e^- pair is created in this string, then the electron can be captured into the bound state of the united atom, while the positron annihilates with the original 1s electron by producing a quark-antiquark pair

$(\pi_W^0 = q_W \bar{q}_W)$ with weak electric charge ($e_W/3$ or $2e_W/3$), and exciting it into higher oscillation mode.

This production mechanism explains why these particles are produced at rest in the center of mass system. It is an internal process, which occurs at resonance energies only, and cannot give linear momentum to the particles.

References

1. W. Koenig, F. Bosch, P. Kienle et al. Z. Phys. A128 (1987) 129
2. E. Berdermann et al. GSI-88-35 preprint and P. Kienle private communication.
3. E. Vatai, to be published
4. J. Scherk, Rev. Mod. Phys. 47(1975) 123
5. E. Vatai, to be published. See also this issue.

BALL-LIGHTNING AS OBSERVATIONAL EVIDENCE OF THE EXISTENCE OF LEPTO-NUCLEONS AND THEIR CLUSTERS

E. Vatai

The existence of lepto-analogues of π^0 -mesons [1] indicates that lepto-analogues of the nucleons (lepto-nucleons) may exist also. Assuming that the ball-lightning is composed of lepto-nucleons, one can determine the main parameter (mass, interaction) of lepto-nucleons from ball-lightning observations. This makes possible to give a coherent explanation of the puzzling properties of the ball-lightning, which is impossible otherwise [2]. The class of explained properties is much broader than that used for the determination of lepto-nucleons' properties, which proves the correctness of the assumptions.

Below, the logical scheme of the investigations is given only, the details will be published elsewhere [3]. Observations, primary, secondary and tertiary implications are denoted by Arabic and Roman numbers, Roman and Greek letters, respectively.

1. The ball-lightning emits separate lines of visible light.
 - (i) Attractive potential exists between electrons and lepto-nucleons. (ii) The potential well is of atomic dimensions.
 - (a) Lepto-nucleus (and/or atom) exists. (α) A binding potential exists between lepto-nucleons and their mass is expected to be in the keV region. (β) A repulsive potential exists between lepto-nucleons, which limits the dimension of lepto-nuclei. (γ) The range of the attractive potential is shorter than that of the repulsive one, otherwise the dimension of lepto-nuclei cannot be limited.
2. The light emission of the ball-lightning is stationary.
 - (i) The lowest (1s) bound state of the electron in the lepto-nucleus (or atom) is deeper than that of the atomic or molecular valence electrons. (a) Ionic crystal bond between ions and lepto-atoms is possible. (b) Adhesion to solid bodies is possible.
3. Creation of ball-lightnings by streak or bead lightnings.
 - (i) Existence of atmospheric lepto-nucleons. (a) Absence of thermal escape from the Earth's gravitational field, i.e., the lepto-nucleons are bound. (ii) Atmospheric lepto-nucleons are bound in deeper energy state than lepto-nucleons in lepto-nuclei and in the ball-lightning. (a) Atmospheric lepto-nucleons are in bound state (cf. 3.i.a). (b) Repulsive medium or long range interaction exists between lepto-nucleons, which is growing with the particle density (cf. 1.ii.a. β). (c) The attractive interaction is of shorter range, than the repulsive one (cf. 1.ii.a. γ).
4. The density of the ball-lightning created by a bead-lightning is only slightly higher than that of the air.
 - (i) The number of lepto-nucleons in the lepto-nucleus is $\sim 10^5$. (ii) The interaction with electrons is $g_1 \sim 10^{-5}e$ (e-electron charge).

5. The movement of the ball-lightning is independent from the wind.
(i) Existence of a background lattice, the lepto-net, to which the ball-lightning is anchored and on which it is moving (cf. 2.i.a).
6. Absorbtion of normal matter (window handle, etc.,).
(i) Confirmation of the ionic crystal model (2.i.a).
7. Stone in the ball-lightning. The lifting power of the ball-lightning cannot be explained by differences in the densities. The movement of the ball-lightning is independent from the presence of the stone in it.
(i) Confirmation of 2.i by using 2.i.b and of 5.i.
8. The ball-lightning shape changes independently from the movement of the air.
(i) Confirmation of 5.i.
9. Sudden appearance of the ball-lightning in clear weather. Observation of ball-lightnings with extremely high energy densities.
(i) Non-local energy supply of the ball-lightning is possible.

The existence of lepto-nucleons can solve the problem of barion number asymmetry of the Universe: Quarks and lepto-quarks are shown to be different charge excitations of some basic particle-antiparcicle pair [4], so creation of neutron and lepto-neutron pairs does not violate conservation laws and is, therefore, possible.

References

1. W. Koenig, F. Bosch, P. Kienle et al. Z. Phys. A128 (1987) 129. E. Vatai, present issue
2. W. N. Charman, Phys. Rep. 54 (1979) 261; Gy. Egely, KFKI Preprint 1987-10/D; B.H. Smitnov, Phys. Rep. 152 (1987) 177
3. E. Vatai, Nuovo Cim., submitted
4. E. Vatai, to be published

**MATERIALS SCIENCE
AND ANALYSIS**

EXPERIMENTAL STUDY OF ELECTRIC CURRENT TRANSPORT IN HIGH T_c SUPERCONDUCTORS

S. Mészáros, K. Vad, G. Halász and F. J. Kedves*

Since the discovery of high T_c superconductors an intensive study of their macroscopic superconductive properties has been performed in many laboratories. The goals are twofold: firstly, to understand the mechanism of superconductivity in these materials, secondly, to clear up the perspectives of applications.

In order to measure macroscopic superconductive properties of these materials an equipment was constructed with the following main features: temperature range 4.2+250 K, magnetic field range 0+6 T, sample access hole diameter 18 mm. A computer controlled electronics and data acquisition system was used to collect and handle the data.

With the help of this equipment the current conduction properties of high T_c materials were investigated. The following measurements were performed on YBaCuO ceramics and BiSrCaCuO screen printed films:

1. Measurement of temperature dependence of electrical resistance with external magnetic field and transport current as parameters.
2. Measurement of current-voltage characteristics and their magnetic field and temperature dependence to elucidate the current conduction and electric power dissipation mechanisms.
3. A contactless method was developed to measure transport critical currents of ring-shaped samples and used to study their temperature and magnetic field dependence.

Conclusions of the experimental results drawn from our measurements are the followings:

- High T_c ceramics and printed films are granular superconductors. The current conduction properties are strongly influenced by the intergrain weak superconducting couplings, which are much more sensitive to preparation technology than the superconducting phase inside the crystallites.
- The observed characteristics indicate the presence of a bulk superconducting phase with very high H_{c2} and a network of weak superconducting connections containing a large number of Josephson junctions.
- The coupling strength of the network is much higher in the Bi-based materials than in the Y-based ones.

Two illustrative examples of the measured characteristics are given in Figs. 1 and 2.

* Department of Solid State Physics, Kossuth University, H-4010 Debrecen, P.O.Box 2, Hungary

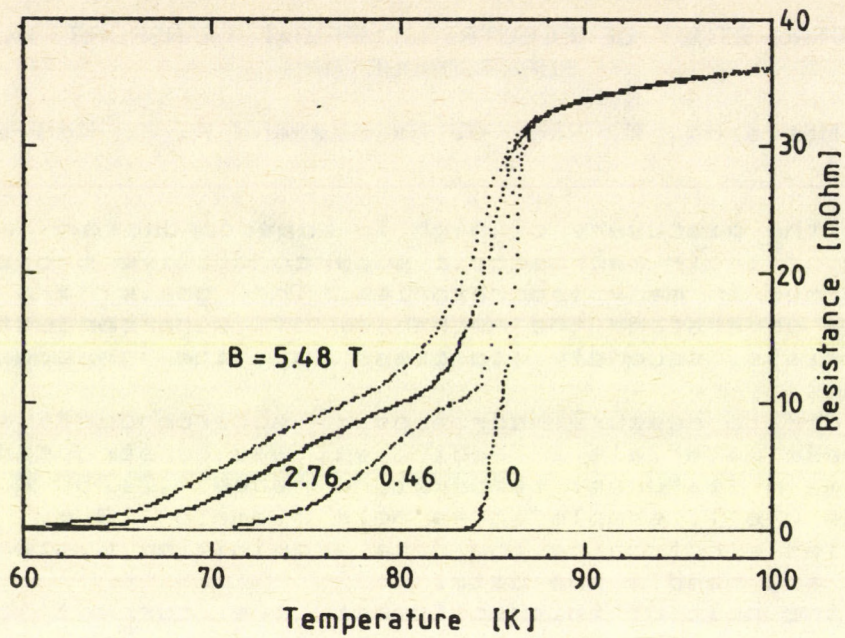


Fig. 1. Resistance-temperature characteristics of an YBaCuO ceramic sample in different magnetic fields

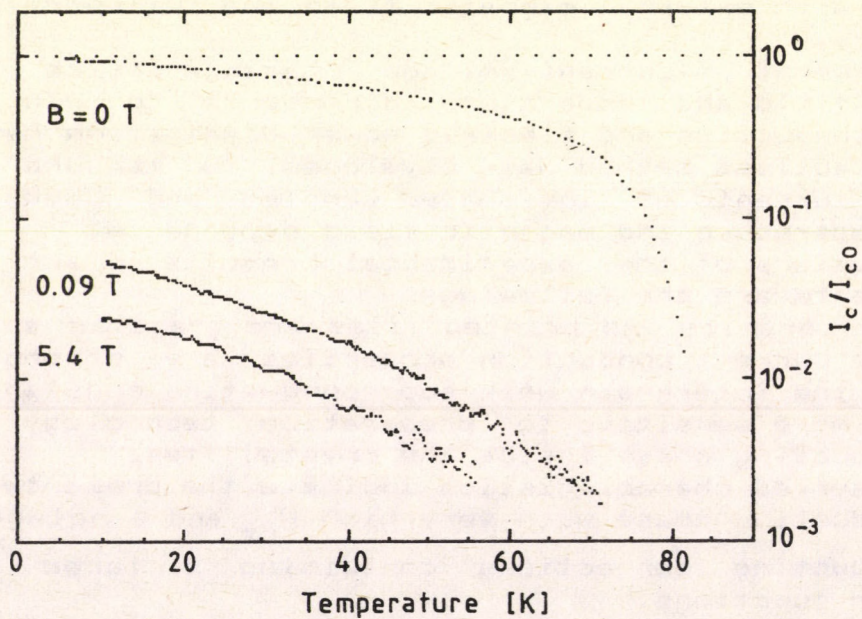


Fig.2. Temperature and magnetic field dependence of the critical current of an YBaCuO ring, $I_{c0} = I_c (B=0, T=0)$

REFERENCES

- [1] S. Mészáros, G. Halász, K. Vad, F.J. Kedves and Sz. Bala-nyai, Physica C 153-155 (1988) 1529.
- [2] S. Mészáros, G. Halász, K. Vad, F.J. Kedves and Sz. Bala-nyai, Physica C, to be published.

Laboratory for Materials Science and Application

I. Mahunka, I. Dombi, S. Takács, F. Ditrói

The demands of high technology makes it necessary to use nuclear methods in different fields of materials science. Taking into consideration the requirements for the application of nuclear analytical methods and thin layer activation technic a small laboratory has been established, connected to the cyclotron laboratory. The new laboratory consists of two parts.

a., sample preparation and handling room. Equipments (chemical box, laminary box, lead shielded manipulation table,...) and instruments (vacuum evaporator, metal microscope, thickness and hardness measuring instrument, ultrasonic cleaner, polishing machine,...) placed here could be used for the chemical and mechanical treatment of samples before and after the irradiation at the cyclotron beams.

b., low background measuring room. Semiconductor (HpGe, Ge(Li)) and scintillation detectors have been placed here for single gamma and gamma-gamma coincidence spectra measurements. To decrease the background a lead-cadmium-copper shielding could be used at the detectors. The electronic modules of the detector systems are connected to a Canberra S35-Plus portable multichannel analyzer which has connection to a minicomputer [1]. For off-site measurement we have a portable and computer controlled gamma-spectrometer too.

The arrangement and instrumentation of the laboratory give good possibilities to continue our investigations in the field of trace element analysis of high purity materials [2,3] and to use the thin layer activation technic in the areas of wear, corrosion and erosion [4]. The establishment of this laboratory was partially supported by the National Technical Development Committee (OMFB).

[1.] F. Ditrói, S. Takács, submitted to Nucl.Instr.Meth.

[2.] S. Takács, F. Ditrói, I. Mahunka, Nucl.Instr.Meth. B10/11 (1985) 1051

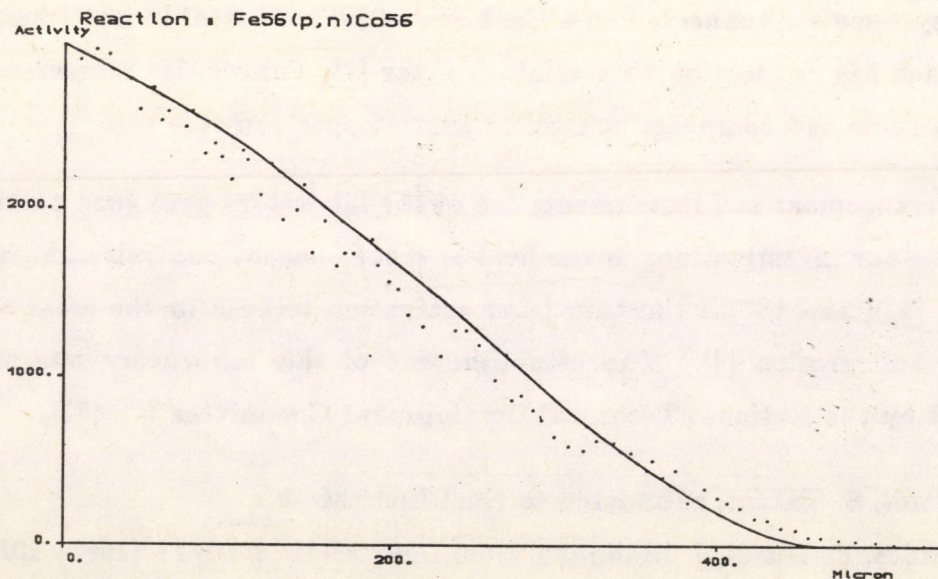
[3.] F. Ditrói, I. Mahunka, S. Takács, S. Seif El-Nasr to be published
in J. Radioanal. Nucl. Chem.

[4.] F. Ditrói, S. Takács, I. Mahunka, Advanced Technologies, 88/4, 23

Determination of Wear by Thin Layer Activation in Iron

S. Takács, F. Ditrói, I. Mahunka

Thin Layer Activation (TLA) method is one of the most powerful possibilities to trace the wear, corrosion or erosion of materials. A common feature of these measurements is the doping of thin surface layers with trace quantities of radioactive species. From the change of the activity of the sample the material loss of the surface can be determined. The TLA has a great importance in areas such as steel-industry, railways, car, oil and electricity generating [1]. Using TLA method for wear, corrosion and erosion study one has to know the produced activity distribution under the surface. To study this phenomenon we made a set of experiments on steel material. The samples were irradiated with different particles accelerated by our MGC-20 cyclotron at different energies. Then the activated surface of the sample was polished away step-by-step, while the thickness of the remained layers and the change of the activity were measured in order to determine the activity-depth relation. The Figure shows the result coming from $E_p=15.7$ MeV proton irradiation (dots) the solid curve shows the result of the theoretical calculation.



[1.] T.W. Conlon, ATOM 287(1980)233

Determination of Bulk Oxygen Concentration in Aluminium Made by Powder Metallurgy

S. Takács, F. Ditrói

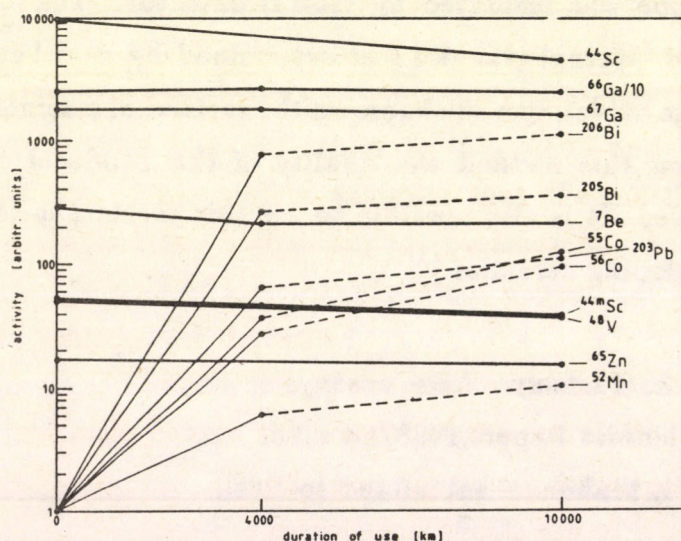
The recent developments in powder metallurgy require the quality control of its products. Samples from aluminium industry were measured by CPAA method. The aim of the investigation was to determine the thickness of the surface oxide-layer of internal aluminium granules. These granules were supposed to be spheres with an average diameter of 50 μm . The samples were irradiated by $^3\text{He}^{++}$ beams at 13 MeV particle energy, and the $^{16}\text{O}(^3\text{He},p)^{18}\text{F}$ and $^{16}\text{O}(^3\text{He},n)^{18}\text{Ne} \rightarrow ^{18}\text{F}$ reactions were used for oxygen determination [1]. The 511 keV annihilation radiation of the ^{18}F isotope was measured by Ge(Li) detector. The oxide-layer thickness on the surface of internal granules was determined by model calculation [2]. The calculated average oxide-layer thickness on the surface of internal granules was $8.5 \pm 3\text{nm}$. By using this method the quality of the products of powder metallurgy can be improved. It is also possible to use this method in the case of other metals [3] and developing ceramics [4].

- [1.] S. Takács, F. Ditrói, F. Tárkányi, F. Szelecsényi,
The Ábo Akademi Biennial Report, 1983/84 p.95.
- [2.] S. Takács, F. Ditrói, I. Mahunka, submitted to Nucl.
Instr. Meth.
- [3.] P. Debeve et al, J. Radioanal. Nucl. Chem., 64(1-2), (1981), 213
- [4.] A. Niiler, 10th Conf. on the Application of Accelerators
in Research and Industry

Investigation of the micro-elemental composition of motor-oil after different duration of use

I. Mahunka, F. Ditrói, S. Takács, S. Seif El-Nasr

Normal motor-oil was investigated by CPAA method on external proton beam. The bombarding energy was 18 MeV. The oil samples were taken from the oil carter of a car after different duration of use [1]. One of the samples was unused oil. The beam was extracted to the air through a 11 μm thick Duratherm-type foil. The oil samples were filled into an aluminium cup and were covered by 13 μm thick aluminium foil to avoid evaporation. The change of the relative concentration of the trace elements is shown in the Figure.



To avoid contaminations from the container, the irradiations were repeated using plastic test tubes. The elements found in the samples were sorted according to their possible origins (engine-wall, piston-ring, factory-added, air pollution). This method is capable for testing the wear of engine parts and for comparing the different types of lubricants also.

[1.] F. Ditrói, I. Mahunka, S. Takács, S. Seif El-Nasr
to be published in J. Radioanal. Nucl. Chem.

* Faculty of Basic Education (girls), Kuwait

Microelemental Investigation of Different Types of Glasses by Using Cyclotron Beams

*F. Ditrói, S. Takács, I. Mahunka, Z. Gémesi**

A great problem of the glass production is the large variety of types of structural disorders. These disorders can cause the unexpected break of the glass product, and some types of them are visible and are not aesthetic. The aim of this work was to determine the elemental constitution of different types of structural disorders in different sorts of glasses, and the normal (good) quality part of the glass samples. From the comparison of the elemental constitution a conclusion could be made for the possible cause of disorder. More than 10 samples from different Hungarian glass factories were investigated with different nuclear analytical methods (CPAA, NAA) and the causes of the different types of disorders were concluded [1]. As an example the table shows the disorder/normal concentration ratio in two samples from the same glass-factory, which contain stone-like closure. The large amount of Zr in the vicinity of the disorder comes from the furnace wall.

elements	sample No. 2 disorder/normal	sample No. 7 disorder/normal
Na	1.12	0.78
Al	1.31	0.73
Ca	1.02	0.69
Fe	1.13	0.59
Zr	112.80	77.40

- [1.] S.Takács, F.Ditrói, I.Mahunka, Investigation of disorders in glasses,
Report to the Scientific-Technical Park of Debrecen, 1988 November,
unpublished

* SZIKKTI, Budapest

RADIOISOTOPE PRODUCTION AT THE MGC CYCLOTRON

I. Mahunka, F. Szelecsényi, L. Andó

One of the main tasks of the Debrecen cyclotron is the production of radioisotopes for medical application. The MGC-20 machine is capable for producing the most important radioisotopes used in nuclear medicine [1].

During the last year we started the routine production of ^{67}Ga , ^{111}In and ^{123}I non-positron emitter isotopes. The irradiations took place at the vertical beam-line of the cyclotron [2] [3]. The irradiated targets were elaborated in our radiochemical laboratory to get intermediers and the labelling procedures were carried out in the Isotope Institute, Budapest [4]. The radiopharmaceuticals were distributed for medical use in Hungary.

Table 1 summarises some production parameters of radioactive isotopes for off-site use in 1988. The greatest demand was for ^{67}Ga which was made nightly and which is used in the detection of inflammatory diseases and in the practice of Oncology for detecting the presence of malignancy [5] [6].

Table 1. Production of radioisotopes for off-site use in 1988

Isotope	Target material	Reaction	Bombarding energy (MeV)	Target thickness (g/cm ²)	Yield (mCi/μAh)
^{67}Ga	^{67}Zn (91%)	$^{67}\text{Zn}(p,n)^{67}\text{Ga}$	14	0,25	1,3
^{111}In	^{111}Cd (95%)	$^{111}\text{Cd}(p,n)^{111}\text{In}$	15	0,35	1,5
^{123}I	^{123}Te (71%)	$^{123}\text{Te}(p,n)^{123}\text{I}$	15	0,25	2,0

To meet the future demand of our medical partners, several new radioisotop production method were (and are) elaborated in the cyclotron laboratory during this period.

We started the preliminary experiments to get ^{201}Tl using mercury gas target and two short-lived positron emitter radioisotopes (^{11}C , ^{18}F). The experiments for producing the PET isotopes are carried out in collaboration with the Biomedical Cyclotron Lab., Med.Univ.School of Debrecen and the Central Institute of Nucl.Res.Rossendorf, GDR.

REFERENCES

- [1] I. Mahunka, I. Uray, ATOMKI Közlemények 24(1982)63
- [2] L. Andó et al., Lectures and Symposia 14th Int.Cancer Congr. Budapest, vol.8.p.145. Karger, Basel/Akadémia Kiadó, Budapest 1987.
- [3] I. Mahunka et al., Medical Application of Cyclotrons IV., Ann.Univ.Turkuensis, D:27 1988 p.137
- [4] Z. Kovács, P. Mikecz, I. Szabó, Nucl.Med. 26(1987)197
- [5] P.B. Hoffer, Int.J.Nucl.Med.Biol. 8(1981)243
- [6] G.S. Johnson, Int.J.Nucl.Med.Biol. 8(1981)249

VACUUM EFFECT ON ETCH INDUCTION TIME AND REGISTRATION SENSITIVITY OF POLYMER TRACK DETECTORS

I. Csige, I. Hunyadi, G. Somogyi and M. Fujii*

* Institute of Space and Astronautical Science
3-1-1 Yoshinodai, Sagamihara, 229 Japan

The vacuum effect on the etch induction time and track etch rate ratio of plastic track detectors were studied systematically with Cf-252 alpha particles of different energies. The growth of alpha track diameter vs. etching time was studied. The etch induction time was determined from the intersection of the etching time axis with the line of the best linear fit to the measured diameters. The etch rate ratio was determined from the slope of this line.

The results of that work were published in two papers [1,2] and are summarized here.

1) If the irradiation of samples was performed in normal air, neither pre- nor post-irradiation storage time in vacuum could make a change in sensitivity.

2) The track etch rate ratio decreased drastically when the detectors were irradiated and kept in vacuum for a few hours before and for a few minutes after the irradiation.

Fig. 1 shows how the etch-pit diameter of 6.1 MeV alphas grows vs. etching time for different outgassing times before irradiation. It seems that in the first two hours the etch rate ratio remained practically the same and only the induction time increased. Then both changed drastically and after three hours outgassing the effect went into saturation.

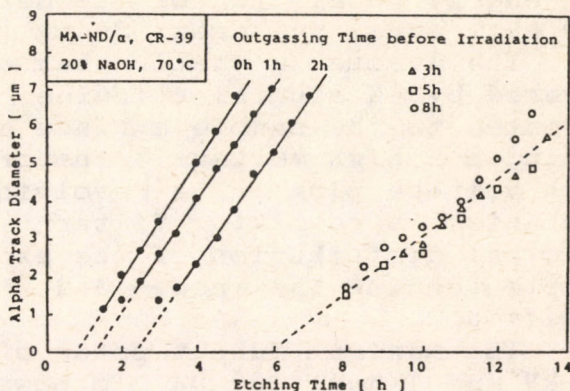


Fig. 1. Alpha diameter vs. etching time.

3) It seems that the ratio of (Etch Rate Ratio-1 in vacuum / Etch Rate Ratio-1 in air) and the ratio (Etch Ind. Time in vacuum / Etch Ind. Time in air) do not depend on alpha particle energy.

4) After a few hours pre-irradiation outgassing and irradiation in vacuum, original registration sensitivity could be recovered by an immediate supply of air after the particle incidence.

5) If the post-irradiation vacuum time was longer than a few minutes the decreased sensitivity could not be recovered even in a pure oxygen atmosphere of high pressure.

6) Practically no change in response is observable if the pre-irradiation storage time in vacuum is not longer than a few minutes. This is important in those experiment, where calibration must be made in vacuum, but we need to know the response in air.

REFERENCES

[1] Fujii M., Csige I. and Somogyi G. (1987), Proc. 20th Int. Conf. on Cosmic Rays, 2, 414-417.
[2] I. Csige, I. Hunyadi, G. Somogyi and M. Fujii. (1988), Proc. 14th Int. Conf. on SSNTDs, to be published.

DEVELOPMENT OF A LOW POWER X-RAY TUBE EXCITATION
SYSTEM FOR XRF ANALYSIS

M.Kis-Varga, G.Kalinka, P.Kovacs, G.Pinter

A flexible tube excitation-detection system has been developed for energy dispersive X-ray fluorescence analysis. The excitation is based on a low power X-ray tube type BH-1 having five changeable transmission anodes: Fe, Cu, Ge, Mo and Ag. After building a tube stand for BH-1 and performing the optimization measurements (1), the arrangement shown in Fig.1. was constructed.

In order to achieve close detector-sample geometry a detector cryostat with 20 mm diameter end cap (Be window thickness: 25 μm) tilted at an angle of 45° was manufactured. The energy resolution of the detector for the Mn K α line is 160 eV (sensitive area: 30 mm², thickness: 4 mm).

The evacuable sample chamber is made of stainless steel covered by 4N aluminium inside. The X-ray tube stand is oriented to the sample surface also at 45°. The tube stand includes a high voltage transformer, a protecting resistor, a high voltage plug-in, a revolving magnetic anode positioning mechanism, a revolving filter- and collimator plate. The spectral distribution of the excitation beam can be altered by simple turning the anode- and filter plates to the required position.

The maximum output power of the tube is 5 Watts: U(max)= 50 kV and I(max)=200 μA . To power the tube a small size X-ray generator was constructed. The high voltage can be regulated from 0 to 50 kV in 5 kV steps and continually, and the setting range for tube current is 0 to 200 μA .

Experiments show that this tube excitation system gives lower detection limits for elements Z<30 than the radioisotope (Fe-55, I-125 and Am-241) excitation does. As an example the pure element yields of Si, S and Ti are shown in Fig.2. for Fe-55 isotope- and Fe anode tube excitation measured in atmosphere and in vacuum. The superiority of tube excitation is obvious in this energy region.

To improve the sensitivity below Z=15 the 25 μm Be window of the detector will be replaced with a thinner one.

Reference

- (1) M.Kis-Varga, Isotopenpraxis 24, 11/12 (1988) 435.

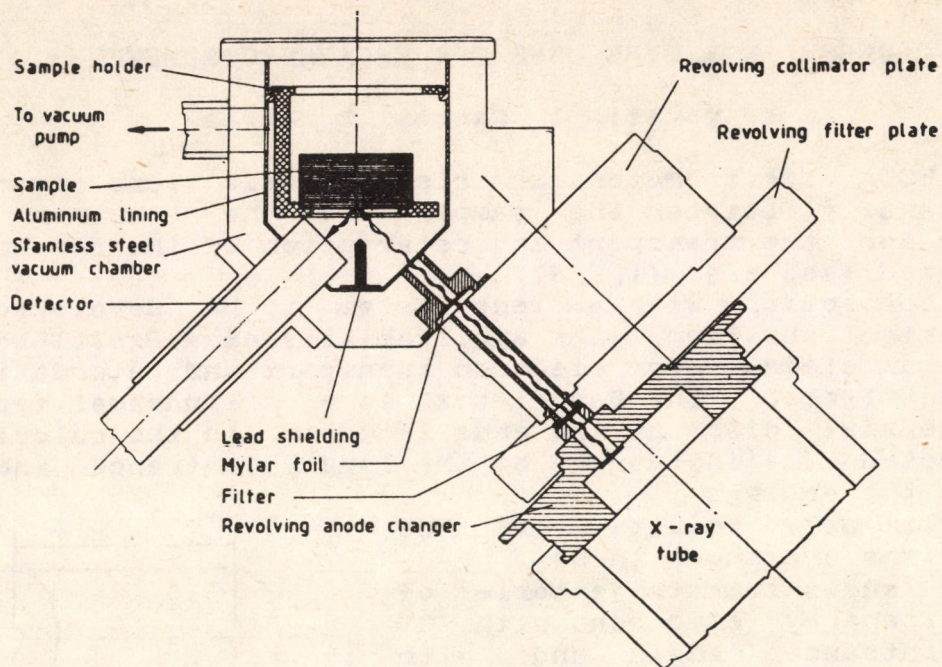


Fig. 1. The scheme of the excitation-detection arrangement.

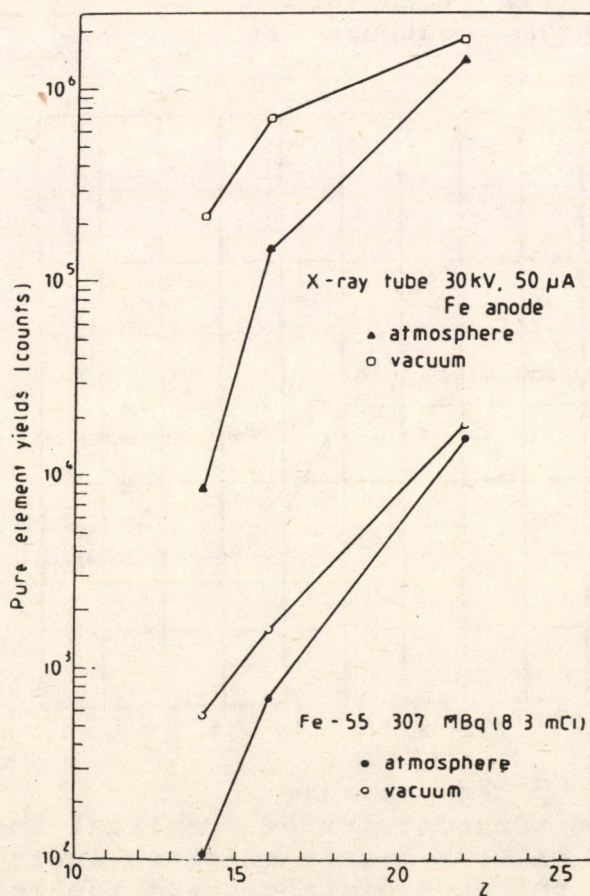


Fig. 2. Pure element yields of Fe-55 isotope and Fe-anode tube excitation.

BESSEL-BOX TYPE LENS FOR ESCA SPECTROMETER

K. Tökösi, I. Cserny, D. Varga

In ESCA spectrometers an electrostatic lens system is placed usually between the sample and the electron energy analyzer for the transport and retardation of the electrons to be analyzed (see e.g. [1, 2, 3])

In connection with a lens system to be developed for a hemispherical analyzer, the applicability of a Bessel-box type lens as an element for electron transport and retardation has been investigated. The Bessel-box is a cylindrical type lens having coaxial discs at the ends (Fig. 1). In the calculations we neglected the influence of the small (entrance and exit) holes at the endings.

Preliminary results of the calculations are shown in Figs. 2-3. Figure 2 shows some trajectories of identical energy electrons with 0° degree entrance angle and with different distance from the lens axis, in the case of the transport lens ($V_3/V_1=1$). It can be seen that at small distances ($r/R < 0.1$) a parallel beam input is transformed to a parallel beam output, if $V_2/V_1=0.01172$.

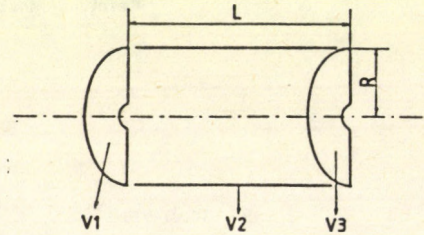


Fig. 1 Schematic diagram of the Bessel-box type lens

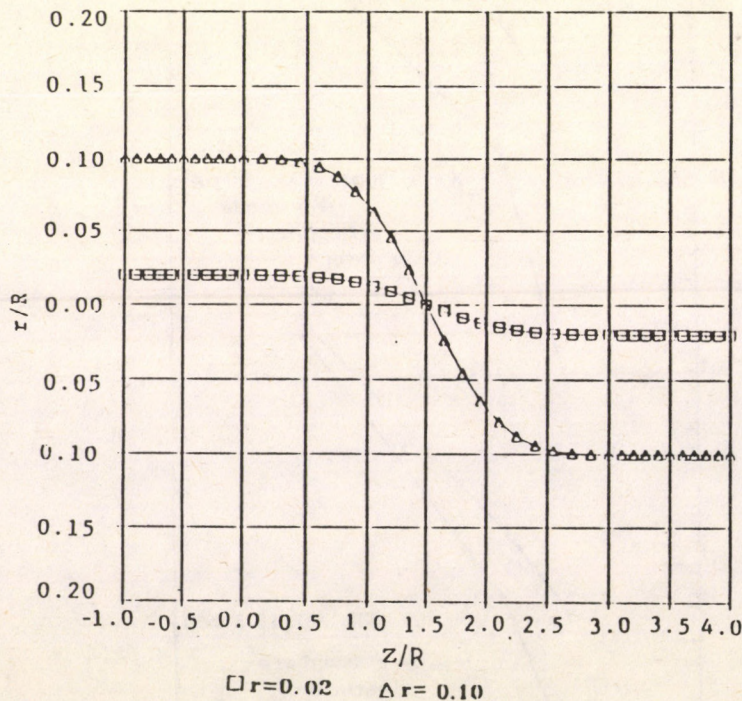


Fig. 2 Calculated trajectories of identical energy electrons with 0° degree entrance angle and with different entrance distance from the lens axis ($V_3/V_1=1$, $V_2/V_1=0.01172$, $L/R=3$).

Using a Bessel-box as retarding lens and (e.g. for $r/R=0.1$) requiring the case of a parallel beam input, the electrons should be focused in a point being at a given distance from the end of lens, the focusing voltage (V_2) will be dependent on the retardation, as it is shown in Fig. 3.

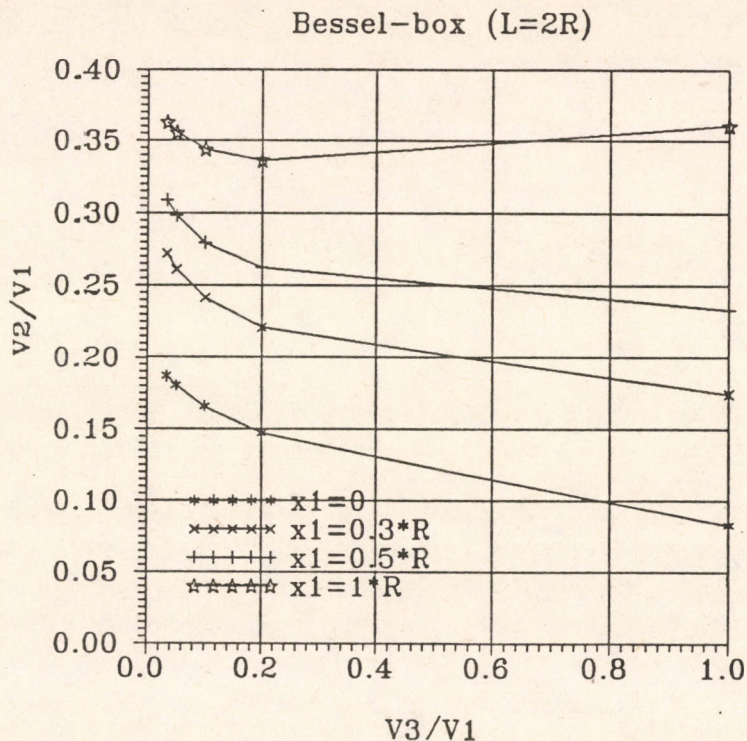


Fig 3 Calculated functions describing the dependence of the V_2/V_1 potential ratio on V_3/V_1 , when the focal point is at a given position from the end of the lens (x_1) in the case of a parallel electron beam input

References

1. U. Gelius, H. Fellner-Feldegg, B. Wannberg, A. G. Nilsson, E. Basilier and K. Siegbahn, UUIP-855 Uppsala University, 1974 April
2. B. Wannberg and A. Skölleremo, J. Electron Spectrosc. Relat. Phenom. 10(1977)45-78
3. U. Gelius, L. Asplund, E. Basilier, S. Hedman, K. Helenelund and K. Siegbahn, Nuclear Instrum. Meth. B1(1984)85-117

**EARTH AND COSMIC SCIENCES,
ENVIRONMENTAL RESEARCH**

Rb-Sr DATING OF ALPINE EFFECTS IN THE SOPRON CRYSTALLINE

A. Kovách and E. Svingor

The polymetamorphic crystalline complex of the Sopron Mountains represents the easternmost occurrence of the Austroalpine crystalline basement at the surface. Its main mass consists of various acidic orthogneisses including leucocratic varieties of probably volcanoclastic origin as well as biotitic metagranites on the one hand, and high grade metapelitic rocks on the other [1] [2]. Both suites bear signs of a typical polymetamorphic development including effects both of Herzynian and Alpine character in general. Based on petrographical studies, a multistage metamorphic development scheme has been compiled [1], the exact timing of the individual metamorphic events, however, still remained indeterminate.

Earlier whole-rock Rb-Sr dating work carried out by the present authors [3] pointed to the presence of a Late Herzynian effect at about 290 Ma in both the parametamorphic and orthometamorphic parts of the complex. This result having been obtained on small samples of hand specimen size could be interpreted essentially as a cooling age, i.e. as an age marking the thermal decline of the (andalusite-sillimanite grade) Late Herzynian metamorphic event. In order to check the validity of this interpretation, as well as to obtain information on the timing of further metamorphic events of Alpine age in general, new mineral age determinations have been carried out on different micas (muscovites and biotites) from two localities in the orthometamorphic suite, representing the type localities of the fine-grained leucocratic gneisses (Sopronbánfalva quarry) and biotitic metagranites (Várisi quarry) respectively.

Petrographical studies [1][2] pointed to the presence of at least two generations of white micas in the orthometamorphic suite, differing markedly in their grain sizes. In the course of the present measurements, three determinations have been carried out on fine-grained phengitic micas (80-160 μm), nine mineral samples represented the coarse fraction of the white mica separates (315-630 μm grain size). From the crystallographic point of view no difference could be ascertained, all samples belonged to the $2M_1$ polytype.

The model ages of the coarse grained samples scatter between the limiting values of 205 ± 7 Ma and 281 ± 7 Ma respectively, and clearly point to the "mixed age" character of the individual age values. The coincidence, however, of the upper age limit with the total rock isochron ages of the orthometamorphic suite makes it highly probable, that this model age represents the true cooling age of the Herzynian component of the composite muscovite assemblage, and supports the previous interpretation of the total rock isochron ages determined in a previous work.

The three fine-grained samples yielded model ages of 90 ± 4 ; 93 ± 4 and 98 ± 5 Ma respectively, with a weighted average of 93 ± 3 Ma. The reality of this model age as a true age is supported by

the fact, that in one of the cases a well-defined mineral isochron age of 92 ± 4 Ma was obtained by using a feldspar separate (consisting mainly of newly formed albite) besides the respective total rock sample in defining the isochrone. Based on this correspondence, we feel justified to interpret this age as defining the age of the Early Alpine metamorphic event during which the young generation of muscovitic micas has been developed.

The five biotite samples taken from the Várisi quarry yielded model ages (referred to the respective total rock samples) of 44 ± 3 ; 41 ± 2 ; 41 ± 2 ; 46 ± 3 and 55 ± 4 Ma respectively, in good accordance with the biotite ages of 46 ± 2 and 49 ± 2 Ma determined in a previous work [3]. The scatter of the model ages exceeding the analytical errors might be connected with the regeneration of previously existing dark micas in the individual samples, in spite of this slight scatter, however, the results point to the fact, that the regional emergence of the crystalline mass occurred during the Eocene. This conclusion is in accordance with the fact, that during the Ottnangian the crystalline served already as an erosional surface.

References

- [1] Lelkes-Felvári, Gy., Sassi, F.P., Visona, D.: Rend.Soc. Ital. Mineral. Petrol., 39 (1984) 593.
- [2] Kisházi, P., Ivancsics, J.: Acta Geol. Acad. Sci. Hung., 28 (1985) 191.
- [3] Kovách, A., Svingor, É.: Proc. Reports of the 13th Congr. of CBGA, Cracow, 1985. p. 383.

GEOCHRONOLOGICAL STUDIES WITH THE K/Ar METHOD

K. Balogh, E. Árva-Sós, Z. Pécskay

In 1988 a number of publications dealing with chronological problems of magmatic rocks from different regions appeared; these are based on results obtained in previous years.

A summarizing paper appeared on the chronology of post-Sarmatian basaltic volcanism in Hungary [1], this is a joint work with the Hungarian Geological Institute, Budapest. K/Ar dating of Pliocene basalts has been used for unveiling the evolution history of the Tapolca-basin [2] (Cooperation: Kossuth Univ., Debrecen). In the course of dating Mesozoic magmatism results on gabbros from the Bódva-valley and Bükk Mts. (N. Hungary) and on magmatic rocks of different chemical composition and related partly to iron ore mineralization have been published [3] (Coop.: Hung. Geol. Inst., Budapest). Results of extensive studies on Miocene volcanic activity in the Tokaj Mts. [4] (Coop.: Kossuth Univ., Debrecen) and in the Great Hungarian Plain [5] (Coop.: Kossuth Univ., Debrecen) have been appeared too. In a cooperation with the Institute of Geology and Geophysics, Bucharest, the age of volcanic rocks in the Harghita Mts. (Romania) has been determined [6].

In 1988 we continued the study of Miocene volcanic areas, namely the Great Hungarian Plain (Coop.: Hydrocarbon Exploring Company, Szolnok; Kossuth Univ., Debrecen) and around the town of Várpalota (Coop.: Hung. Geol. Inst., Budapest). Mesozoic rocks have been dated from the territory of the Transdanubian Middle Mts. (Coop.: Eötvös Univ., Budapest), from boreholes among the rivers Danube and Tisza (Coop.: József Univ., Szeged) and from the southern foreground of the Mecsek Mts. (Coop.: Hung. Geol. Inst., Budapest). Clay minerals have been dated from the basement of the Little Plain and Dráva-basin and demonstrated that $<2\mu\text{m}$ clay minerals are suitable for dating secondary effects and to locate areas free of secondary effects (Coop.: Geochem. Res. Lab. of Hung. Acad. Sci., Budapest). Work continued on dating the manganese ore mineralization at Urkut (Coop.: József Univ., Szeged).

In cooperation with Hungarian geological expeditions working abroad, dating continued on Mesozoic rocks from Cuba and the reliability of 8-11 Ma ages of basalts from Vietnam, which are related to the bauxitization, has been proved.

In the frame of international cooperation results on Miocene-Pliocene basalts from Austria (Burgenland) have been submitted for publication (Coop.: Univ. Wien; Geol. Bundesanstalt, Wien; Hung. Geol. Inst., Budapest), continued dating of Pliocene-Pleistocene basalt lavas from Armenia (Coop.: Geochron. Lab. Arm. Acad. Sci., Jerevan) and experimental-theoretical studies started for checking the reliability of K/Ar ages obtained on young basalt samples (Coop.: Geol. Ust. D. Stura, Bratislava; Hung. Geol. Inst., Budapest).

References

- [1] K. Balogh, E. Árva-Sós, Z. Pécskay, L. Ravasz-Baranyai. Acta Miner. Petrogr., Szeged. 28 (1986) p. 75.
- [2] Z. Borsy, K. Balogh, M. Kozák, Z. Pécskay. Acta Geogr. Debrecina, 23 (1984) p. 79.
- [3] E. Árva-Sós, K. Balogh, L. Ravasz-Baranyai, Cs. Ravasz. Ann. Rep. Hung. Geol. Inst. of 1985. (1987) p. 295.
- [4] Z. Pécskay, K. Balogh, V. Széky-Fux, P. Gyarmati. Földt. Közl. 117 (1987) p. 237.
- [5] V. Széky Fux, Z. Pécskay, K. Balogh. Földt. Közl. 117 (1987) p. 223.
- [6] S. Peltz. E. Vajdea, K. Balogh, Z. Pécskay. D. S. Inst. Geol. Geofiz., Bucharest, 72-73 (1987) p. 323.

COMPUTER CONTROLLED $\text{H}_2^{18}\text{O}-\text{C}^{16}\text{O}_2$ EXCHANGE SET-UP FOR $\delta^{18}\text{O}$
ASSAY OF NATURAL WATERS

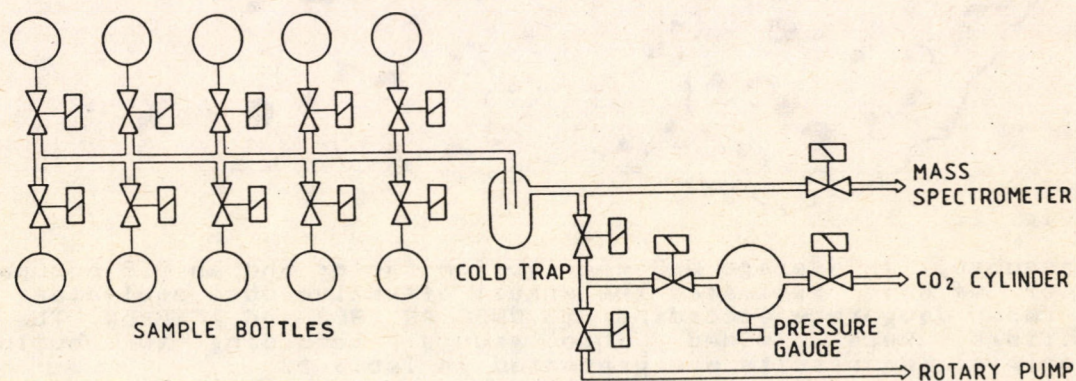
E. Hertelendi, S. Fekete, M. Győrffi, S. Mészáros, J. Kiss

An equipment for computer controlled $\delta^{18}\text{O}$ analysis of water samples is described. It is based on a common principle of equilibrating the water samples with CO_2 gas [1] the isotopic composition of which is then analysed in the mass spectrometer. The handling time is reduced to about 10 min/sample by operating several samples in parallel and by pumping the air from the equilibration vessels through capillary tubes [2] without freezing down the water samples. The capillaries control the loss of water vapour and pneumatically actuated soft-sealed valves prevent mixing between the samples. The vessels are shaken during pumping and equilibration.

The set-up is air thermostated at 25 °C. Water vapour is freed out in a specially designed variable temperature cooling trap. Pressure is controlled by a solid state pressure transducer.

The whole preparation procedure (performed on 9+1 samples) needs about 4 hours.

The standard reproducibility of sample preparation is about 0.1‰ and the process is not very sensitive to precision of preparation work and reaction conditions except temperature.



Block diagram of $\text{H}_2^{18}\text{O}-\text{C}^{16}\text{O}_2$ equilibration system

REFERENCES

- [1] S. Epstein, T. Mayeda, *Geochim. Cosmochim. Acta* 4 (1953) 213
- [2] W. Roether, *Int. J. Appl. Rad. Isotop.* 31 (1970) 379

RADON SURVEY IN DWELLINGS IN HUNGARY

G. Somogyi, I. Nikl*, I. Csige and I. Hunyadi

* "Frederic Joliot-Curie" National Research Institute for
Radiobiology and Radiohygiene, Budapest

We have carried out a country wide radon+daughters survey in Hungary during the period 1985 Feb.-1987 Jul. 122 dwellings were investigated, each at a meteorological station. In each dwellings 10 measurements were carried out, the exposure time was a quarter of a year.

The radon activity concentration was measured with Kodak-Pathe LR-115-II type solid state nuclear track detector. We have used the cup technique with an internal detector foil and with a 50 μm thick polyethylene covering foil on the cup to keep out the thoron from the internal detector. An external detector foil was also used to estimate the activity concentration of daughters. The measuring device was calibrated experimentally in a well defined radon+daughters field.

The Fig. 1. shows the indoor radon activity concentrations measured in the houses of 122 meteorological stations (2.5 year average).

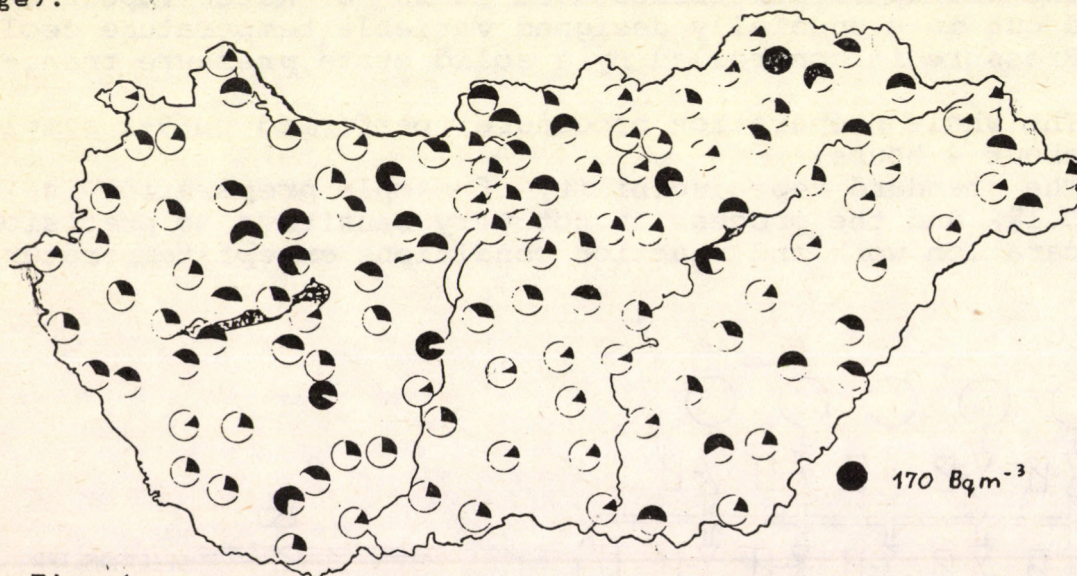


Fig. 1.

Assuming an average 0.5 equilibrium factor and an 0.8 occupancy factor we have estimated the annual effective dose equivalent due to radon+daughters according to UNSCEAR 1982 and ICRP-50. The 122 dwellings were divided into groups according to building materials. The results are presented in Table 1.

BUILDING MATERIALS	mSv/year/person	
	UNSCEAR (1982)	ICRP-50
ALL THE 122 HOUSES	1.3	2.2
ADOBE HOUSES	2.1	3.5
ALL THE BRICK HOUSES	1.1	1.8
BRICK HOUSES	1.2	2.0
GROUND FLOOR	0.7	1.2
FIRST FLOOR		

Table I. The annual effective dose equivalent

RADON PROFILE IN A 270 M DEEP WELL : TRANSPORT VELOCITY MEASUREMENTS

J. Hakl, L. Lenart* and G. Somogyi

Technical University for Heavy Industry, H-3515, Miskolc

Recently the use of plastic track detectors within a defined air volume has become the most reliable procedure for time integrated, long term measurement of radon activity concentrations under different environmental conditions. For a better understanding of the role of external factors, which can significantly influence the transport of radon in water, we have been investigating, for three years, the change of radon content in a deep well.

The well is located at the University Campus of Miskolc in a limestone area. It was completed with an iron tube casing 270 m length and 30 cm in diameter and screened only at the bottom. The water in the well is stagnant.

Assuming that under steady-state conditions a radon concentration gradient exist only in the vertical direction, the transport inside the water column, neglecting local radon production and diffusion, is governed by the differential equation:

$$\frac{d}{dz}(v(z)c_w(z)) - \lambda c_w(z) = 0 \quad (1)$$

where $c_w(z)$ is the radon concentration in water at depth z , $v(z)$ is the upward transport velocity and λ is the decay constant of radon. (1) yields for the track density:

$$\ln(F(z) \cdot \frac{\rho(z)}{\rho(0)}) = \int_0^z \frac{1}{v(z)} (\lambda - \frac{dv(z)}{dz}) dz \quad (2)$$

where in $F(z)$ are included all the correction factors for registration efficiency and radon partition for water-air phases, $\rho(z)$ is the measured track density at depth z .

For the period of observation the shapes of radon distributions obtained were similar to the curve shown in Fig.1. After performing the transformation (2) it is clearly seen that the radon content gradually decreases with increasing distance from the bottom of the well. Data can be well fitted with a power type function $f = a \cdot z^b$.

Fig.2. shows the result of such a calculation. V_c is an integration constant, the value of which can be determined from the boundary condition at the top of the well. In our case it was estimated from the upper three points and the obtained values are in the range 0.05-0.25 m/h.

The observed high transport velocities can be interpreted by thermal gradient induced convective mixing of water.

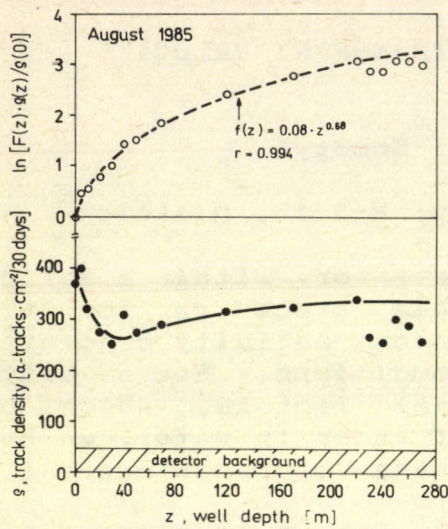


Fig. 1. A typical radon profile and the corresponding transformed curve

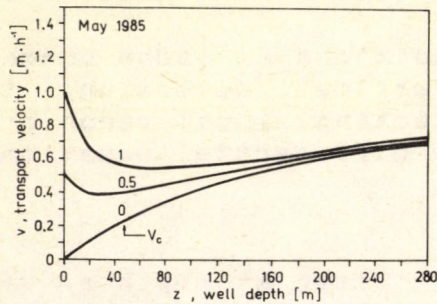


Fig. 2. Upward velocity vs. depth calculated for different v_c values.

References:

G. Somogyi and L. Lenart: Time-integrated radon measurements in springs and well waters by track technique. Nucl. Tracks, 12, 1986, 731-734

J. Haki, L. Lenart and G. Somogyi: The radon profile in a 270 m deep drilled well, Proc. of the 1st. Yug. Conf. on SSNTDs, Beograd, Sept. 28-30, 1988 (to be published)

AN XPS STUDY OF THE SURFACE COMPOSITION OF URBAN AEROSOLS FRACTIONIZED BY THEIR SIZES BY THE HELP OF CASCADE IMPACTORS

J. Tóth, L. Kóvér

During 1988 the XPS investigations of size fractionized ($0.5-1\mu$, $1-2\mu$, $2-4\mu$, $4-8\mu$, $8-18\mu$) aerosol particles' surfaces were continued to increase the selectivity of our sampling method [1]. This year there was an important step in monitoring only the particles' surfaces without the adsorption of gas pollutants on the surface of the sampler. For this aim teflon proved to be a useful material because of the low level of surface contamination and chemical interactions between the sampler and aerosol particles' surfaces. The photoelectron lines of teflon do not overlap the most important lines of S, N, C, which are interesting from the point of view of this study giving an other advantage of teflon sampler.

Not only teflon, but metallic Cu was used for sampling as well. As different sampling speed impactors were used, it was possible to see whether was any difference between the compounds developed on Cu surfaces exposed to high (10^3 l/min) or low (10 l/min) air flux [2]. The sampling time was the same in both cases. The coverage of the surfaces of the samplers by aerosol particles was negligible, because in the case of the high speed sampling the particles were reflected by the hard surface of the sampler, while in the case of low speed sampling at the $4-8\mu$ and $8-18\mu$ size particle fractions the number of particles were very small.

To show correlation between the nitrogen and the carbon content of surface layers of aerosol particles, the N 1s and C 1s photoelectron spectra have been measured. It is easier by the help of teflon samplers than with metal samplers, because the binding energy of C 1s peak, which is coming from the carbon content of soot particles, is different from the C 1s of teflon. In the case of metallic samplers, the C 1s peaks coming from CO_2 (or CO) and hydrocarbons adsorbed, for example, on the surface of metallic Cu overlap very strongly. The separation of them from the peaks originating from the soot particles, even with decomposition of peaks, is very questionable not using monochromatic X-ray excitation for the XPS measurements.

From the XPS data there are some interesting results [2] depending on the particles sizes and seasonal changes, which show that on the surface of airborne soot particles the sulfur is in the form of sulfate and the nitrogen is in the form of so called N_x (binding energy about 400 eV).

Presently, from the point of view of the selectivity of monitoring sulfur compounds, a new series of measurements is in progress. By the help of metallic Cu and Ni samplers

difference can be made between the chemisorption of H_2S and SO_2 assuming that the modifications caused by other sulfur compounds in the energy regions of sulfur peaks of the XPS spectrum are negligible. In the new measurements the teflon samplers are going to be used.

The motivation of using XPS is strong enough because this is almost the only method to show directly the chemical compounds of aerosols surface. This way information about "dry" acidic deposition can be obtained without using wet methods in studying the acidity of aerosols.

By the help of cascade impactors you can collect samples in a few hours, so you can get time versus information. If you choose the time region representatively as a function of the part of the day, you can make difference between the local environmental pollution and the global one, this way you can get information about the origin of the pollution.

References:

- [1] See in this issue amongst the CONFERENCE CONTRIBUTIONS
- [2] To be published in SIA (Surf. and Interface Anal.)

BIOLOGICAL
AND
MEDICAL RESEARCH

STUDY OF TOXIC HEAVY METAL CONCENTRATIONS IN HUMAN HAIR
AND TISSUES*.

J. Bacsó, B. Dezső¹, G. Lusztig², I. Szigeti², I. Uzonyi

¹ Inst. of Pathology, Med. High School, Debrecen, Hungary

² Inst. of Pathology, County Council Hospital Hollós
József, Kecskemét, Hungary

Motor traffic, burning of fossil fuel, use of chemicals in agriculture and housekeeping, discharges from metallurgical plants, etc are causing strong environmental pollution, contaminating soil, water, air and, in biosphere itself, the human body, too. The toxic heavy metals infiltrate into hair and tissues. The figures of hair analyses according to their clinical usefulness are inconsistent. Therefore it is important to investigate whether the toxic metal concentration measured in hair could monitor intrinsic body burdens. For this purpose a Co-ordinated Research Programme was organized by the International Atomic Energy Agency.

Hair, brain, lung, liver, kidney and bone samples were collected from forty to sixty years old deceased men at autopsy. The selection of population to be included, the method and handling of samples are prescribed by a PROTOCOL FOR AUTOPSY STUDIES.

Samples were collected from 56 men, and prepared for measurement: dried, ground, homogenized and pressed into pellets. The elemental concentrations were determined by XRF technique. The concentration of P, S, Cl, K, Ca, Mn, Fe, Br, Rb, Sr was determined beside that of As, Cd, Cu, Hg, Se and Zn done at the request of IAEA

Investigating the plot of elemental concentration in tissues, as a function of elemental concentration in hair for the same element, (see Fig.1) made it possible to study the probable form of concentration distribution in tissues, depending on taking place of the sampling time to duration of exposition (see Fig.2) [1].

References:

[1] Bacsó J. Dezső B. Lusztig G. Szigeti I. Uzonyi I:
Belsőszövetben és hajban mért ásványi elem koncentrációk
közötti kapcsolat vizsgálata. ATOMKI Riport X/35 (1987)
pp 157-169.

* The measurement was carried out with support of IAEA
in frame of a Co-ordinated Research Programme.
Contr.No.: 3668

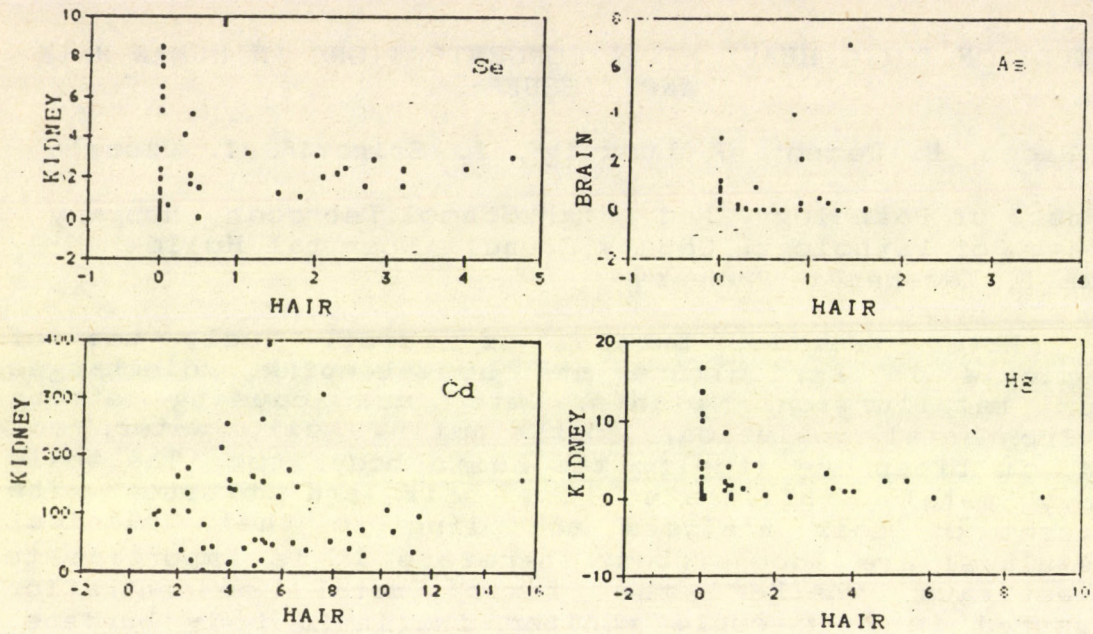


Fig. 1. Plots of elemental concentration in tissue as a function of concentration in hair.

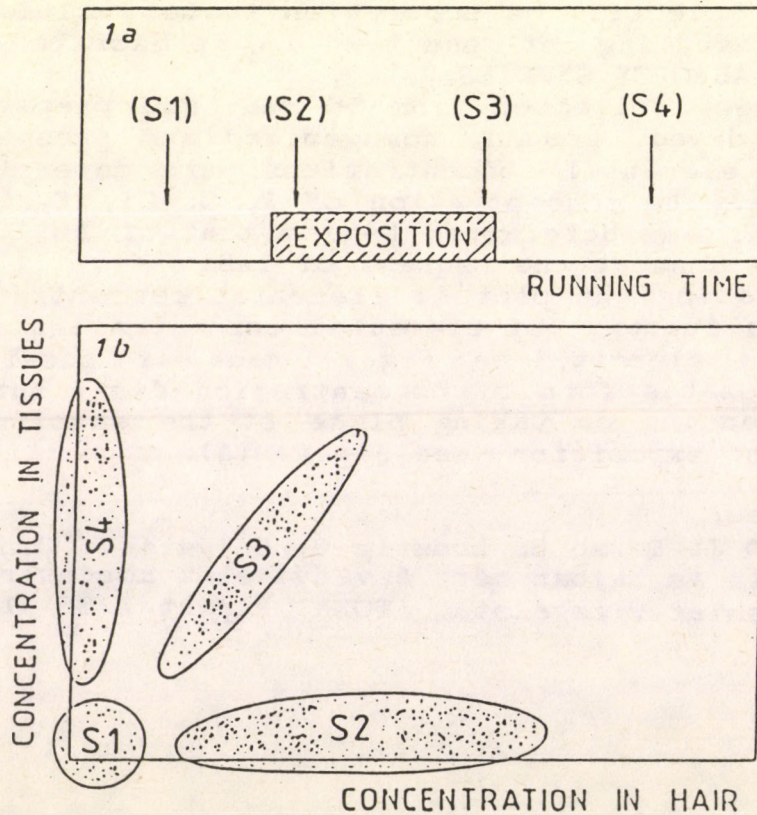


Fig. 2. The expected distributions of toxic heavy metal concentration measured in tissues and hair depending on sampling compared to exposition time.

INVESTIGATION OF MINERAL CONCENTRATIONS, MECHANICAL AND
BIO-CHEMICAL PARAMETERS IN RAT HAIR AND BONE, AND
CORRELATIONS BETWEEN THEM.

J. Bacsó¹, I. Uzonyi¹, A. V. Bakulin², A. S. Rachmanov² and
V. S. Oganov²

¹Inst. of Nucl. Res. of the Hung. Acad. of Sci. (ATOMKI)
Debrecen, HUNGARY,

²Institute of Biomedical Problems (IBMP), Moscow, USSR.

Ischaemic heart disease, cerebral haemorrhage, osteoporosis in postmenopausal women, etc. are thought to be in connection with Ca imbalance. The bone loss (demineralization of bone) of astronauts in micro gravity is also believed to be brought on by Ca metabolic disorders caused by inactivity (weightlessness). The diagnosis of Ca imbalance before manifestation of its aftermath, and the prevention of diseases, if it is possible, is important according to health state of society and long period space flight, respectively.

Experiment was conducted in different groups: (hypodynamia=H); and (vivarium contr.=V) of white Wistar rats for different times. Investigation of drug treatment of animals was carried out with ipriflavon (I) and placebo (P). 7-10 animals in every group were decapitated at the end of experiment. The sign of groups are: basic control (BC); hypodynamia 40 days ipriflavon treatment (H40I), etc. the second number in sign marks the readaptation period. The hair samples were cut from the backside of animals near to skin. Proximal metaphysis of tibia was separated for determination of mineral content in bone. The samples were pressed into pellets for determination of concentration of elements: P, S, Cl, K, Ca, Fe, Cu, Zn, Br, and Pb by XRF method. Regression between the elements in different tissues was investigated(1). Regressions for hair-Ca (H-Ca) and bone-Ca (B-Ca) and (B-Ca)-(B-P) are shown in Fig.1.

Some biochemical parameters in bone and blood, and mechanical parameters in bone were determined in IBMP. The mechanical parameters were determined by compression method(2). The stress-strain curves observed, were used for calculating elastic strength (σ_1), ultimate strength (σ_2), relative strain $\sigma_1/\sigma_2 = \epsilon$, Young's modulus (E) and specific work of elastic strain (a). Fig. 2 shows the mechanical parameters of bone in function of H-Ca and B-Ca.

Our results demonstrate that the Ca metabolic rate of bone in rats can be investigated (characterized) by measurement of Ca in hair.

References:

[1] Presented at the Meeting of Working Groups of Socialistic Countries on Cosmic Biology and Medicine (INTERCOSMOS), Baranow-Sandomersky, Poland, 6-10. 6. 1988.

[2] Stupakov G.P. et al.: In: Effect of flight dynamic factors on the animal body. Moscow, Nauka, 1979, pp: 174-178.

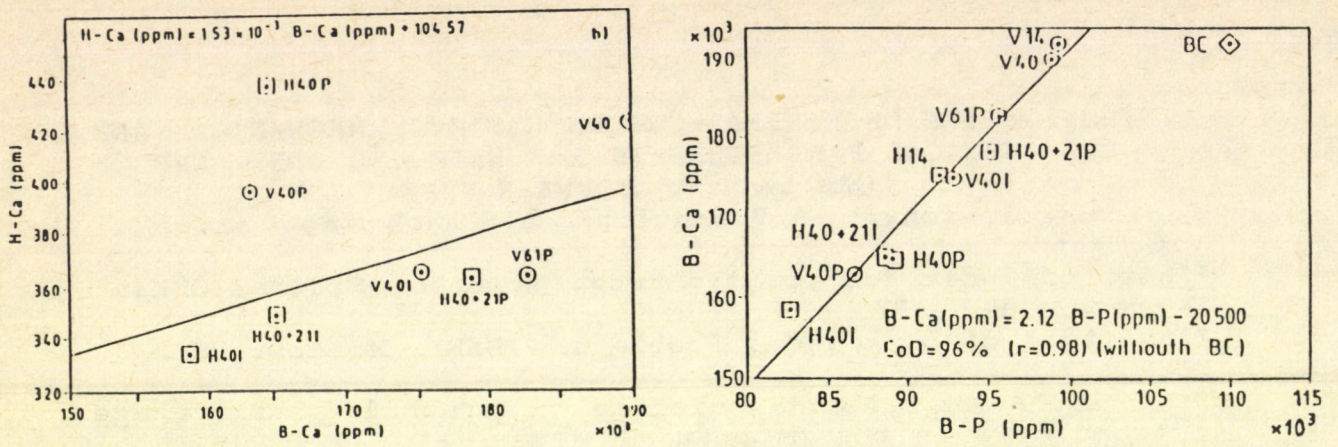


Fig. 1.: Regression line for Ca concentration in hair and bone, as well as for Ca and P in bone.

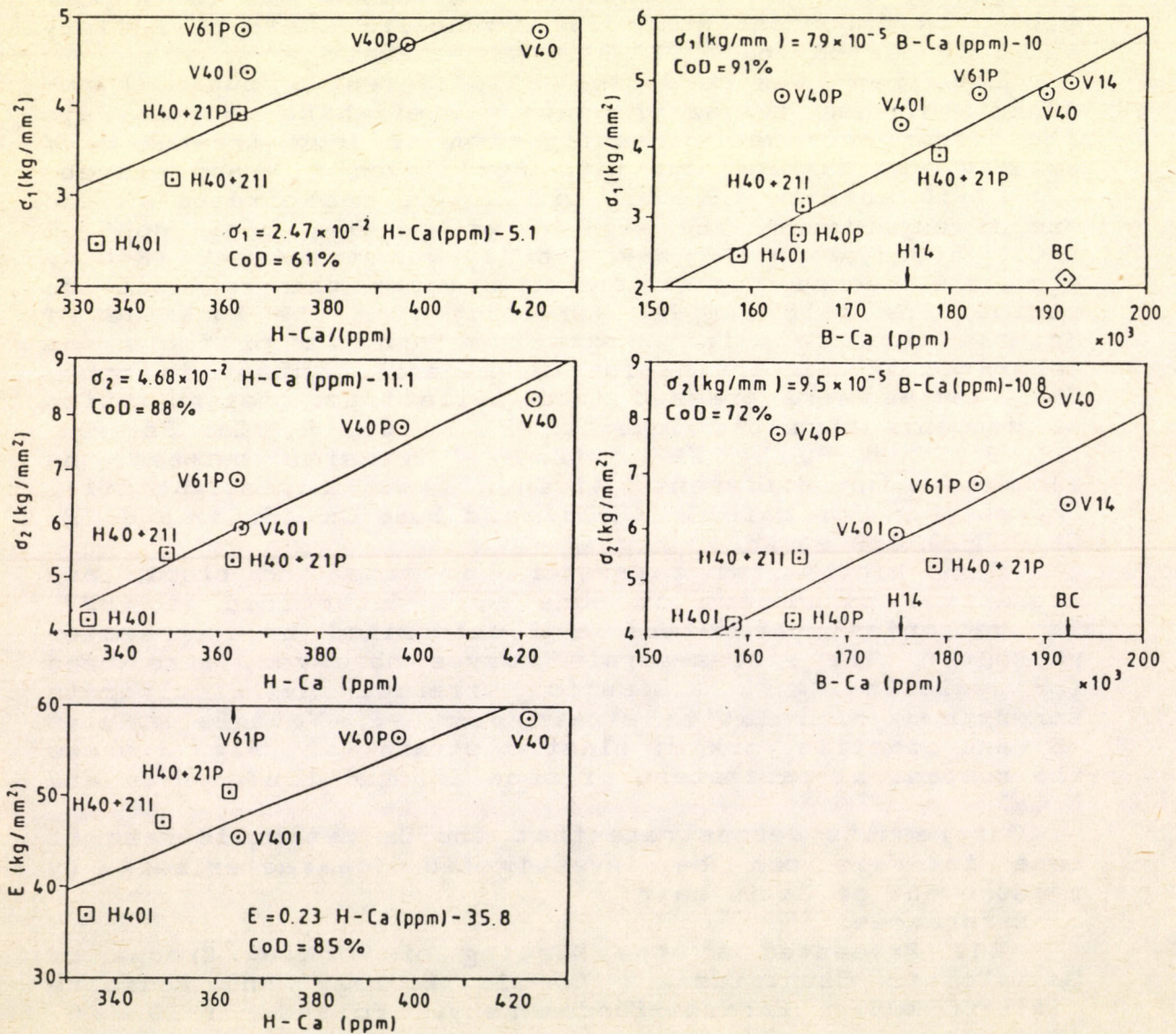


Fig. 2.: Mechanical parameters as a function of Ca concentration in hair and bone.

APPLICATIONS OF FAST NEUTRON SOURCES BASED ON THE MGC-20 CYCLOTRON

A. Fenyvesi, T. Molnár⁺, I. Mahunka

One of the projects at the MGC-20 cyclotron is the development and application of intense fast neutron sources for interdisciplinary and practical purposes. Based upon our $p(18 \text{ MeV})+\text{Be}$ and $d(10 \text{ MeV})+\text{Be}$ intense fast neutron sources [1], the following programs have been in progress in our laboratory:

a) production of carrier-free ^{24}Na isotope by the $^{27}\text{Al}(n,\alpha)^{24}\text{Na}$ reaction for investigation of water-transport in healthy and diseased oak (*quercus peraea*) trees for ecological [2] and, in the case of tomato plants, for agricultural purposes [3]

b) irradiations of grains of onions and capsicums for stimulation and mutation breeding purposes [3]

c) irradiations of cultures of mammalian cells and tissues for basic radiobiological studies and to establish the techniques of biological dosimetry of mixed $n-\gamma$ fields at our cyclotron neutron sources [4]

d) elaboration and adaptation of methods capable of determination of fast neutron spectra and dose-rates at the irradiation positions and in the samples.

The necessary information on spectral distributions of fast neutrons above $E_n=1 \text{ MeV}$ was gained by multifoil activation and a spectrum unfolding technique [5]. One of the unfolded spectra is shown in Fig. 1.

The separate neutron and gamma dose-rates and their spatial distributions were measured mainly by the usual twin ionization chamber method. A TE-TE (tissue equivalent chamber flowed by tissue equivalent gas) and a Mg-Ar chamber were used in the biomedical investigations. A pair of CH-equivalent CH-C₂H₂ and Mg-Ar chambers recommended by the IAEA was used for agrobiological irradiations. Profiles and depth dose distributions of collimated beams were measured in water phantom also by solid state nuclear track detectors (SSNTD-s) [6].

⁺Biomed. Cycl. Lab., Med. Univ. School of Debrecen,
Nagyerdei krt. 98., Debrecen, Hungary, H-4012

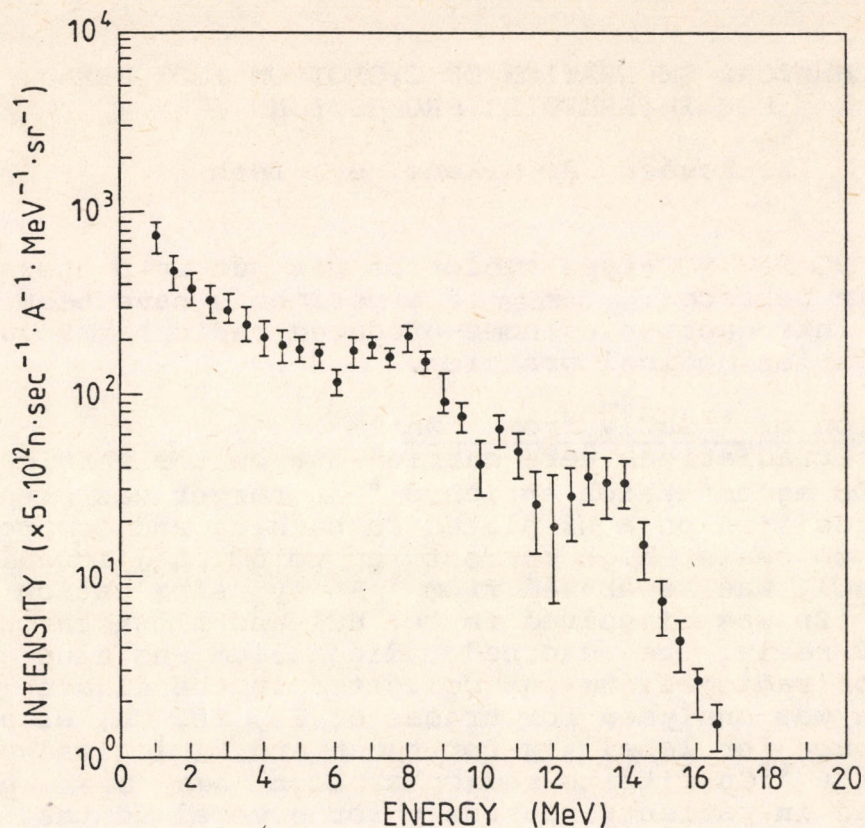


Fig.1. Unfolded zero degree spectral distribution of neutrons from the $^9\text{Be}+p(18 \text{ MeV})$ reactions at a distance of 23 cm from the target.

References:

- [1] L. Andó et al., Lectures and Symposia, 14th Int.Cancer Congr. Budapest 1986, vol.8, pp.145-152, eds. K. Lapis and S. Eckhardt, Karger, Basel/Akadémiai Kiadó, Budapest 1988
- [2] A. Fenyvesi et al., Bul. of the Am. Phys. Soc., vol.33, No. 8(1988), p. 1737
- [3] I. Mahunka et al., Annual Rep. on Supported Research, unpublished
- [4] A. Csejtey, Diploma Thesis, Faculty of Sci., Lajos Kossuth Univ., Debrecen, 1988
- [5] S. Sudár, LSQUNF: a Fortran IV-PLUS Unfolding Code, private communication
- [6] L. Medveczky et al., Proc. of. the 1st Yugoslavian Symp. on Solid State Nucl. Track Detectors, Beograd, 28-30 September 1988, to be published

RADIOCHEMICAL SEPARATION OF CYCLOTRON ISOTOPES
FOR INTERMEDIER PRODUCTION

Z. Kovács, P. Mikecz, Gy. Tóth⁺

A 20 MeV MGC-type cyclotron was put into operation 3 years ago in Debrecen. A series of experiments have been carried out for introduction of home-produced radiopharmaceuticals into the Hungarian medical practice.

Production of $^{67}\text{GaCl}_3$ from ^{67}Zn

All the irradiations were carried out on the vertical beam-line [1]. 300 mg/cm² thick enriched ^{67}Zn target was prepared by electrodeposition on a Ni plated Cu backing and compressed with 750 MPa to resist high current (up to 50 μA) irradiation.

The $^{67}\text{GaCl}_3$ was separated from ^{67}Zn by using cation exchange. The ^{67}Zn was dissolved in cc. HCl and flown through a DOWEX 50 WX 2 resin. The adsorbed radiogallium was eluted with 4M HCl. 90% of radiogallium was collected in the eluate (Fig.1.). This solution was analysed for traces of Fe, Zn, Cu, Ni and found to be pure for labelling for human and biological application [2]. The ^{67}Ga -citrate radiopharmakon has been produced and used in patients routinely for several months.

Production of Na ^{123}I from $^{123}\text{TeO}_2$

400 mg/cm² thick target was prepared by melting $^{123}\text{TeO}_2$ onto a platinum plate. The separation of radioiodine was carried out by dry distillation in a directly heated quartz oven. The target was gradually heated up to 850 °C to melt the $^{123}\text{TeO}_2$ and after 30 seconds was allowed to cool down (Fig.2.). The evaporated radioiodine was carried by air stream into a trap containing 0,002M NaOH solution. The separation yield was over 85% and the loss of enriched target material was less than 3 mg/run.

The chemical form of radioiodine was 95% I which is suitable for radiopharmaceutical requirements. The product is used with the Iodobell kits [3] as o-Iodo-Hippuric Acid for kidney imaging and ^{123}I Heptadecanoic Acid for myocardial imaging.

Production of $^{111}\text{InCl}_3$ from ^{111}Cd

350 mg/cm² thick target was prepared by electrodeposition on a Ni plated Cu backing and compressed with 50 MPa to get better thermal conductivity. After irradiation the ^{111}Cd was dissolved from the backing in 6M HBr. From this solution the In isotopes were extracted by isopropyl-ether. The organic phase was washed three times by 6M HBr saturated with isopropyl-ether for removing the traces of ^{111}Cd and interfering radioisotopes.

⁺ Biomed. Cycl. Lab., Med. Univ. School of Debrecen,
Nagyerdei krt. 98, Debrecen, Hungary, H-4012

The radioindium was reextracted into injection water. After evaporation the dry residue was picked up in 0,05 M HCl which is ready for labelling after sterile filtration.

Production of other radioisotopes

The cyclotron is suitable for production of positron emitters, like ^{18}F , ^{11}C , ^{13}N and ^{15}O . Technological development has been begun for production of these isotopes. For example, experiments have been done for production of $\text{KH}^{11}\text{CO}_3$ in order to investigate the carboxylation process of propionyl-Co-A in the methylmalonyl-Co-A synthesis. Several experiments for the synthesis of ^{18}F FDG production have also been carried out.

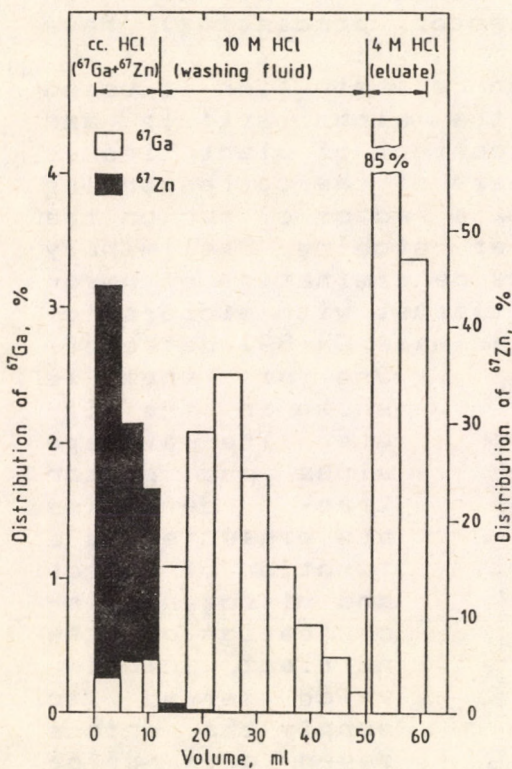


Fig.1. Separation of $^{67}\text{GaCl}_3$ from enriched ^{67}Zn target.

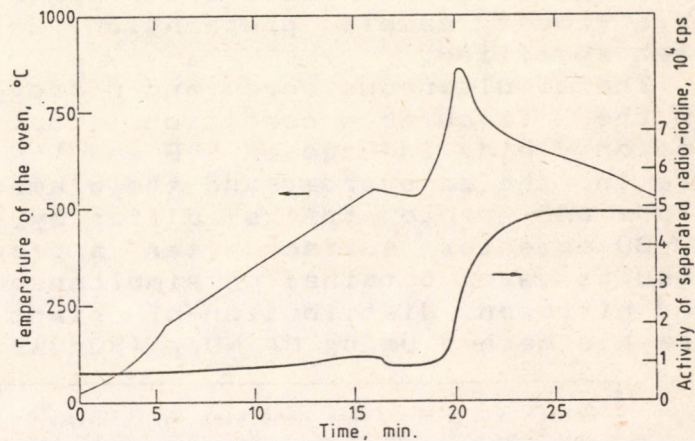


Fig.2. Temperature and time dependence of evaporation of radioiodine from $^{123}\text{TeO}_2$

References

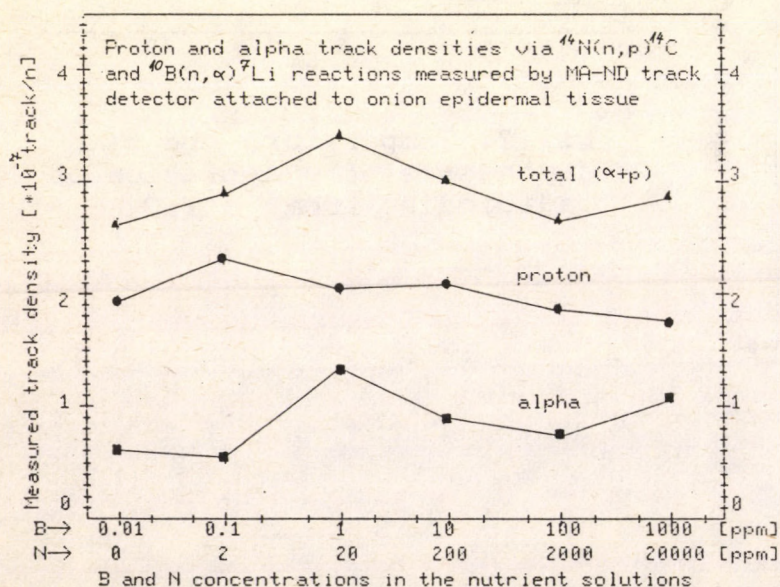
- [1] L. Andó et al., Lectures and Symposia 14th Int. Cancer Congr. Budapest 1986, vol.8.p.145, eds. K. Lapis and S. Eckhardt, Karger, Basel/Akadémia Kiadó, Budapest, 1988.
- [2] J. Környei et al., Radioanal. Nucl. Chem. Letters, 1989, in press
- [3] J. Környei et al., Izotóptechnika, 31, 57, 1988.

BORON AND NITROGEN SIMULTANEOUS DETERMINATION IN PLANT TISSUES BY NUCLEAR TRACK TECHNIQUE

I. Hunyadi, G. Somogyi, F. Körösi*, L. András**

Nuclear track technique for boron determination via $^{10}\text{B}(n,\alpha)^7\text{Li}$ thermal neutron induced nuclear reaction has been elaborated in the early 80s in the ATOMKI using polycarbonate as an alpha detector and it has been successfully applied to study passive boron transport processes in plant tissues [1]. When the proton sensitive CR-39 has become available we have made efforts to overcome serious methodical difficulties in nitrogen determination by using the $^{14}\text{N}(n,p)^{14}\text{C}$ reaction at thermal energies. Having revealed the source of disturbing background tracks induced in the bulk of detector by neutrons [2], the most favourable experimental conditions (irradiation arrangement, sample preparation, detector processing) have been specified.

The simultaneous boron and nitrogen determination is based on the favourable condition, that the alpha particle and proton yields induced on ^{10}B and ^{14}N content of plant tissues are in the same order and the diameters of the corresponding alpha and proton tracks differ by \approx a factor of two on the CR-39 detector surface after a proper etching. Preliminary results were obtained on simultaneous determination of boron and nitrogen distribution of plant tissues with microradiographic method using MA-ND/p (Hungarian made CR-39) detector.



One of them is shown in the figure. The average alpha and proton track densities are presented as a function of boron and nitrogen concentration of the nutrient solution which served to supply the onions seven days prior to the tissue preparation. The irradiation was performed in the thermal neutron channel of the nuclear reactor in Budapest.

References

- [1] Varro I., Somogyi G., Najžer M., Mádi I.: *Isotopenpraxis*, 18, (1982) 418
- [2] Somogyi G., Varga Zs., Hunyadi I., Freyer K., Treutler H.C. *Nuclear Tracks*, Vol. 12, Nos 1-6, pp. 949-952, 1986.

* Agricultural University of Godollo, Hungary

** Central Research Institute for Physics, Budapest, Hungary

THE ANALITICAL APPLICATION OF CHARGED PARTICLE INDUCED X-RAY EMISSION METHOD

I. Borbély-Kiss, E. Koltay, Gy. Szabó

Aerosol research

Regular sampling has been continued in collaboration with Central Institute of Atmospheric Physics. Samples of atmospheric aerosol particles collected in rural sites of Hungary were analysed, up to 21 elements, by PIXE method. Selenium and vanadium related concentration data for selected trace elements sometimes used as elemental tracers in characterising regional aerosols were deduced and compared with data from literature. Conclusions were drawn from these elemental ratios on the character and effect of regional aerosols [1], [2].

Food industry

The ultrafiltered lactalbumin concentrate as additive is widely used by the food industrial technologies in order to increase the protein content of foodstuffs. The aim of these investigations was to measure the composition of concentrated lactalbumin powder without and with Fe^{2+} by PIXE method and the effect of gamma radiation on these samples by ESR, thermo- and chemoluminescence methods and by electrical and dielectrical measurements [3].

Biomedical research

PIXE analysis (with different bombarding proton energies) has been performed on biomedical samples in order to find optimum excitation conditions for improved sensitivity limits for some trace element. Among others the case of selenium has been carefully studied due to an increased interest in the role of selenium in biomedical processes.

The determination of elemental concentration in erythrocyte and plasma samples from patients treated with telecobalt therapy revealed the effect of irradiation on the iron level in blood plasma. Such an effect predicted in the literature was found to be insignificant in the case of the irradiation of small bone marrow portions in one of our earlier papers. For the case of a combined irradiation of costal, spinal and coxal marrow portions in a patient suffering in non-Hodgkin lymphoma (Fig.1.), measured iron concentrations are shown in plasma and erythrocyte samples together with haemoglobin, haematocrit and mean corpuscular haemoglobin concentration data, as a function of total tumor dose and actual biological effect. Vertical dashed line indicates the end of irradiation period. Full and empty arrows correspond to normal iron concentration values in plasma and erythrocytes, respectively. Prompt and prolonged effects are clearly observable in plasma iron level [4].

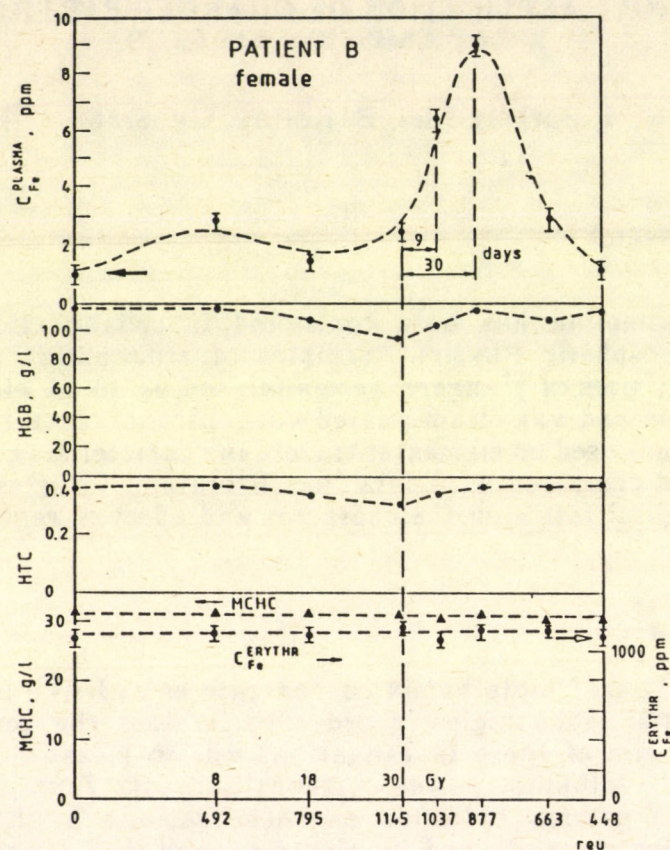


Fig.1.

References

- [1] I.Borbély-Kiss, E.Koltay, E.Mészáros, Gy.Szabó: in Eds. Paul E.Wagner, G.Vali: Atmospheric Aerosols and Nucleation. Lecture Notes in Physics Vol. 309. Springer-Verlag. Berlin, p. 279.
- [2] I.Borbély-Kiss, E.Koltay, E.Mészáros, Gy.Szabó: Submitted to the journal IDŐJÁRÁS.
- [3] J.Kispéter, J.Beczner, I.Borbély-Kiss, L.Horváth, L.Kiss and Z.Rózsa: ESNA XIXth Annual Meeting, Aug. 29.-Sept.2. 1988. Vienna. Book of Abstracts p.116.
- [4] É.Pintye, E.Groska, I.Borbély-Kiss, E.Koltay, Gy.Szabó, A.Kiss, in preparation.

C ACTIVITY AND DISTRIBUTION IN GASEOUS EFFLUENTS FROM PAKS PRESSURIZED WATER REACTORS[†]

E. Hertelendi*, Gy. Uchrin** and P. Ormai***

We present results of airborne ^{14}C emission measurements from the Paks PWR nuclear power plant. Long-term release of ^{14}C in the form of carbon dioxide or carbon monoxide and hydrocarbons were simultaneously measured. The results of internal gas-proportional and liquid scintillation counting agree well with theoretical assessments of ^{14}C releases from pressurized water reactors. The mean value of the ^{14}C concentration in discharged air is $130\text{Bq}\cdot\text{m}^{-3}$ and the normalized release is equal to $740\text{GBq}/\text{GW}_e\cdot\text{yr}$. More than 95% of ^{14}C released is in the form of hydrocarbons, ca. 4% is apportioned to carbon dioxide and <1% to carbon monoxide (Fig.1.). Tree-ring measurements were also made and indicated a minute increase of ^{14}C content in the vicinity of the nuclear power plant (Fig.2.).

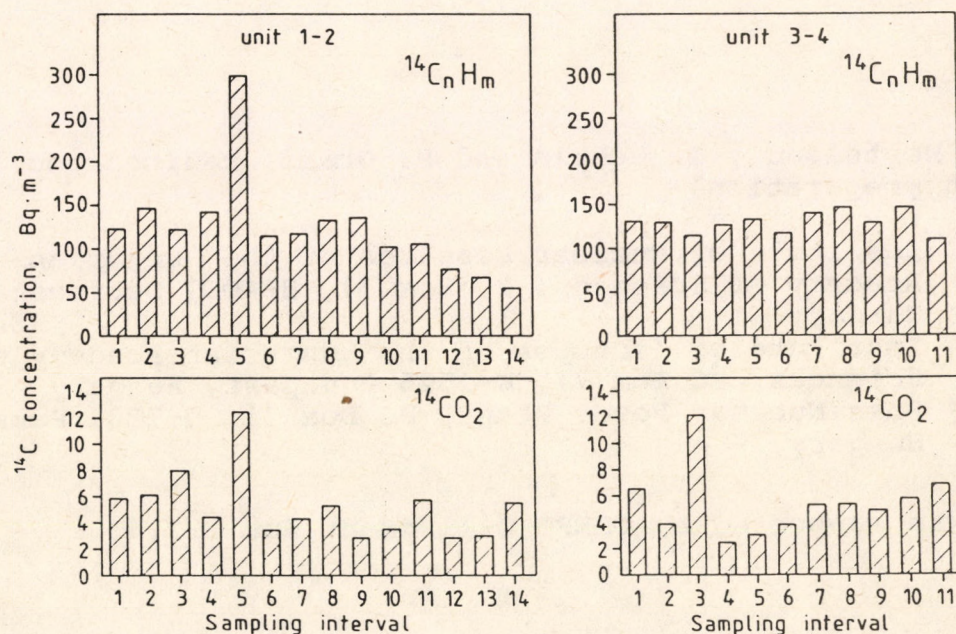


Fig.1. Weekly average ^{14}C concentrations of discharged air in $^{14}\text{CO}_2$ and $^{14}\text{C}_n\text{H}_m$ chemical forms.

Sampling intervals; unit 1-2: 24.02.-01.06.87,

unit 3-4: 10.03.-01.06.87.

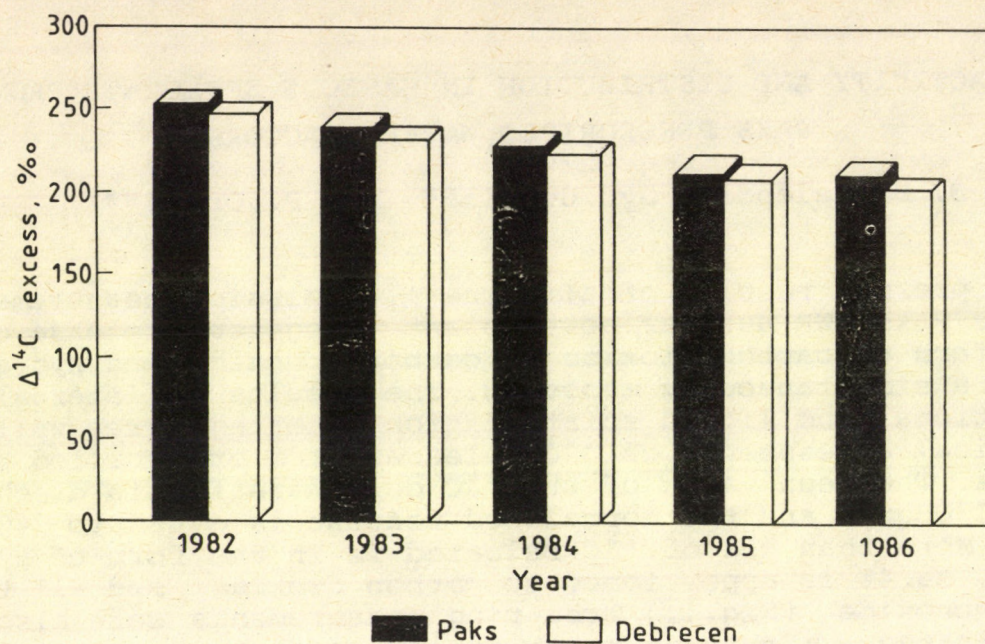


Fig 2. ^{14}C excess in tree rings at Paks NPP and at a reference point, Debrecen, Hungary

REFERENCES

- [1] E. Hertelendi, G. Uchrin and P. Ormai, Radiocarbon 1989 (in preparation)

* Institute of Nuclear Research of the Hungarian Academy of Sciences, PO Box 51, H-4001 Debrecen Hungary

** Institute of Isotopes of the Hungarian Academy of Sciences, PO Box 77, H-1525 Budapest, Hungary

*** Paks Nuclear Power Plant, PO Box 71, H-7031 Paks, Hungary

+ Work was supported by OKKFT G-11 grant No. 2.2.4.

DEVELOPMENT OF A PERSONNEL NEUTRON DOSIMETER

L. Medveczky

The neutron sensitivity of a dosimeter consisting of fission foils as radiator-converters and solid state nuclear track detector was studied [1]. The radiator-converters used in pairs were the following alloys: a.) Th-232 (99.5%)+ U-nat (0.5%) made by ÚJP (Zbraslav, ČSSR) and b.) Al+U made by Nukem GmbH (Hanau, FRG). This type of dosimeter was irradiated in free air with Am-Be and Pu-Be neutron sources and also with 14 MeV energy neutrons. The dosimeter was exposed also to moderated fission spectrum on the surface of a phantom. The sensitivity data of this dosimeter are given in Table I.

Table I.

Neutron source	Sensitivity of dosimeter		μSv track/cm ²
	0.5 eV - 10 MeV energy range of neutrons	1.4 - 10 MeV	
reactor	832 ⁺⁹⁵	218 ⁺²⁵	
Am-Be	55.2 ⁺⁵	14.4 ^{+1.2}	
Pu-Be	37.5 ⁺⁴	9.9 ⁺¹	
14 MeV	72 ⁺¹⁶	23.8 ⁺³	

The dosimeter is used as an emergency dosimeter as well as an area dosimeter [2].

For the purpose of obtaining information about the registering-limit of this dosimeter, of thermoluminescence dosimeters and also a dosimeter consisting of allyl diglycolcarbonate (Cr-39) track detector with a polyethylene radiator, a comparison was began exposing simultaneously [3] these dosimeters to mixed neutron-gamma field at the MGC type cyclotron in the ATOMKI.

References

- [1] Medveczky L. Zsolnay Á.: Izotóptechnika, 32 /1989/ to be published in Hungarian.
- [2] L. Medveczky, E. Horváth: Kernenergie, to be published
- [3] L. Medveczky, I. Uray, G. Dajkó: in preparation

DEVELOPMENT OF AN AUTOMATIC SAMPLE CHANGER EQUIPMENT TO SI(LI) X-RAY SPECTROMETERS

J. Bacsó, I. Uzonyi

For the time being, in most of the XRF (X-ray fluorescence) laboratories the automatization of the entire measurement procedure becomes more and more imperative in order that the effectiveness of analytical work and reliability of results can be improved further. In order to accomplish a computer controlled and all day long operation of our Si(Li) X-ray spectrometer without any necessary supervision, an automatic sample changer equipment was developed for XRF analytical purposes [1].

The sample changer (see Fig. 1) can be attached to vertical dipstick X-ray spectrometers, especially to NZ 860 (ATOMKI-type) [2] in the present form. The samples are placed in bores of 13mm diameter on the outer surface of a cylinder-shaped and turnable drum made of 5N Al which is fastened in the vacuum chamber in a detachable way (see Fig.1 and Fig.2). Simultaneously 50 pellets made from various kinds of biological, geological, etc. materials or batches of hair strands can be placed in. For the excitation of characteristic X-ray lines annular radioisotope sources (e.g. ^{55}Fe , ^{109}Cd , ^{125}I , ^{241}Am) can be placed in the vacuum chamber in a generally used, optimized geometrical arrangement [3].

The electronic unit of the sample changer makes both automatic and manual control possible by using the control signals of a multichannel analyzer (MCA) (in our lab. CANBERRA S 35 Plus is applied) and/or by setting the following switches placed on the front panel of this unit: "MCA/LOCAL": manual control selection of MCA; "FORWARD/BACKWARD": selection of a clockwise/counter-clockwise turning direction of the sample holder drum which means the positioning of samples in increasing/ decreasing serial number order; "STEP": manual control of one by one sample changing; "RESET": system reset means that the first sample is set into measurement position. In both cases the instantaneous serial sample number (1..50) is shown continuously on two of 7 segment LED displays. The timing diagram of automatic control with MCA is shown on Fig. 3. Sample changing is started in the previously set direction for the "SCADV" ("Sample Changer Advance") TTL pulse received from the MCA through the J112 External Control connector [4]. At the same time the controller sends a busy signal to the MCA on the "BSYIN" ("Device Busy In") line until the sample changing process is completed. For control any MCA can be used which can receive and provide the two TTL pulses mentioned above.

References:

- [1] J. Bacsó, I. Uzonyi, *Isotopenpraxis* 24 (1988) 72
- [2] J. Bacsó, G. Kalinka, Zs. Kertész, P. Kovács, T. Lakatos, *ATOMKI Report* 24 (1982) 133
- [3] M. Kis-Varga, J. Bacso, *Journal of Radioanalytical Chemistry* 31 (1976) 407.
- [4] CANBERRA Series 35 Plus Operator's Manual (1985)

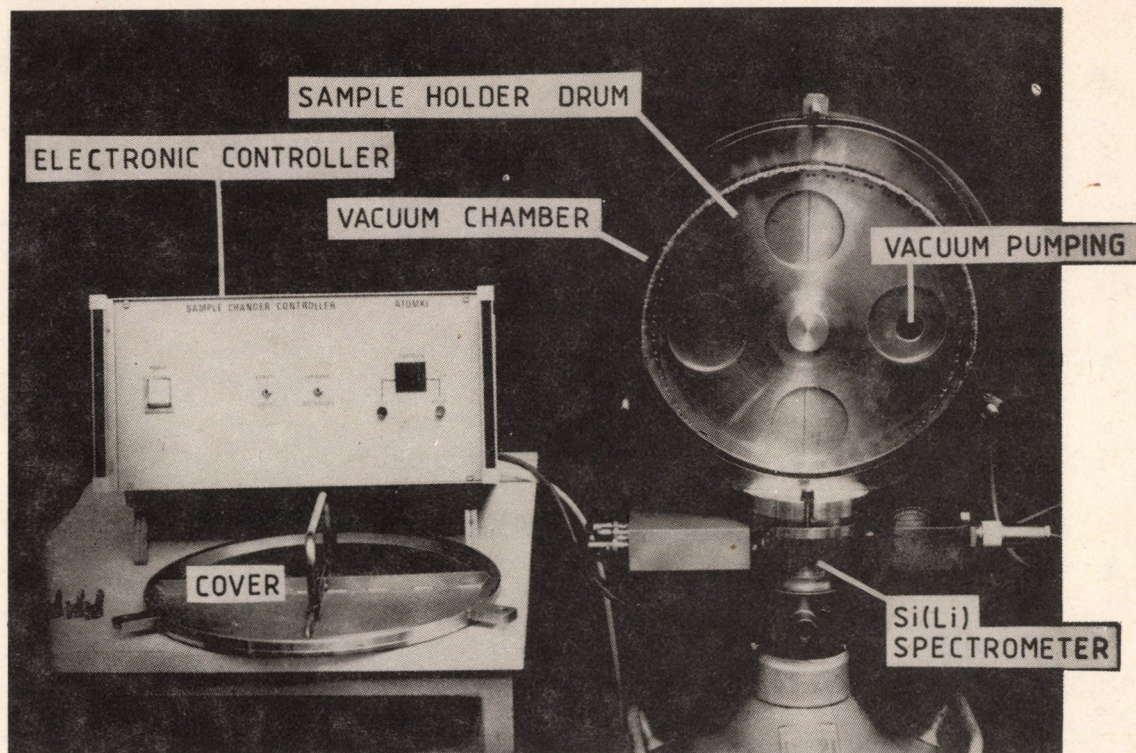


Fig. 1. Photograph of the sample changer equipment.

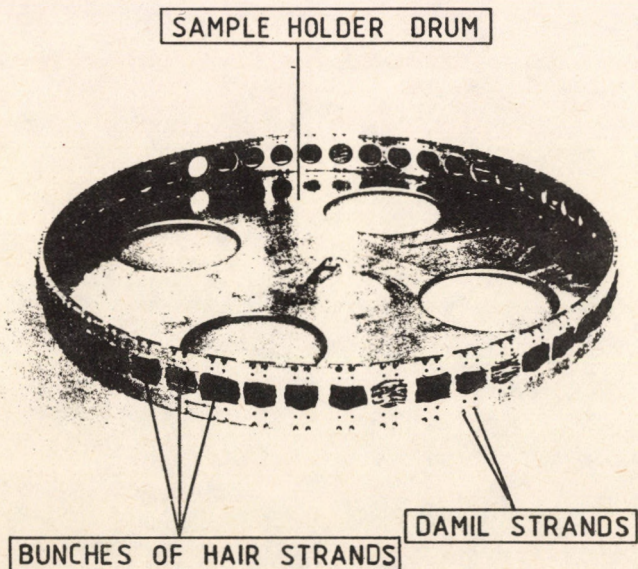


Fig. 2. Photograph of the sample holder drum filled with bunches of hair strands.

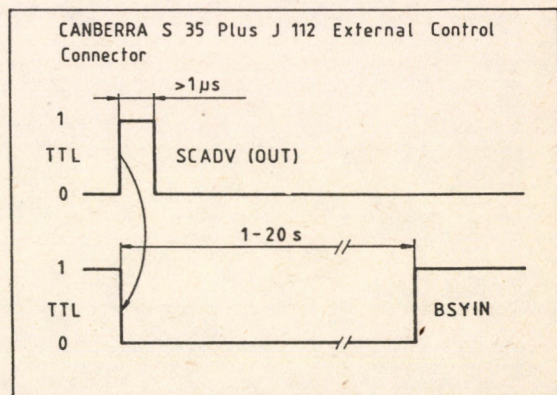


Fig. 3. Timing diagram of the automatic sample changing process controlled by MCA. Sample changing will start for the "Sample Changer Advance" TTL pulse received from the MCA. Spectrum collection can start only when BSYIN "Device Busy In" signal is at TTL 1 level indicating that the sample changing has been finished.

**DEVELOPMENT OF METHODS
AND INSTRUMENTS**

SOME STEPS TOWARDS AN INCREASED STABILITY
QUADRUPOLE MASS SPECTROMETER

László Kiss

One of the main direction of the development of quadrupole mass spectrometers is achieving increased peak stability. Instabilities of the mass peaks are caused first of all by changes in the environmental and internal temperature conditions. This phenomenon is more pronounced in the range of higher atomic masses (e.g. 300 or 500 u).

The shape and the stability of the peaks are mainly determined electrically by the parameters of the RF/DC unit. If these parameters depend on the temperature, the peaks of the mass spectrum also will change by influence of the temperature.

Some years ago a method was worked out for the temperature-separated measurement of certain parts of the RF/DC unit, by which one was able to determine those circuits and components which are especially responsible for the temperature stability of the RF/DC unit.

In the present article only two significant phases of stability-improving development are treated in brief.

The iron-powder transformers formerly applied in the tuned RF power stage had significant losses at the given RF power level (at 300 u). These losses resulted in warming up the iron-powder core. The increasing temperature caused a mistuning of the output resonant circuit which led to further heat generation. (See figure 1.)

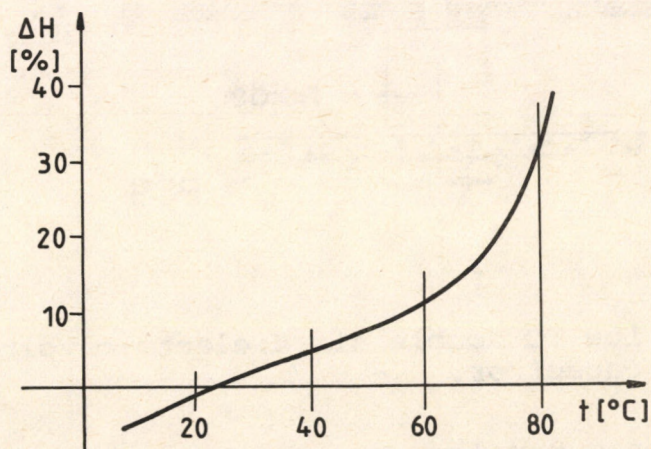


Figure 1. Relative mistuning as a function of temperature of iron-powder toroidal core.

We did not intend to apply forced air cooling of the toroidal core because low voltage, small-sized ventilators are rather expensive. In addition, the inner part of the RF/DC unit will

get dirty with the dust carried by the ventilator during its operation.

Instead, to avoid losses a high Q air core coil has been developed. Its geometrical sizes were optimized by computer aid. This "home-made" coil wound onto a light plastic form well met our requirements.

The other component in the RF part, which significantly determines the temperature stability of the unit, is the RF voltage divider capacitor.

In the previous versions we used low Temperature Coefficient (TC) tubular ceramic capacitors (e.g. $TC = +15 \div 30 \text{ ppm}/^\circ\text{C}$) for this purpose in well-matched pairs for the sake of good temperature stability. However, there is a well-known problem: the thermal response of a compensating capacitor will not always perfectly track the capacitor that is being compensated. Because of the mentioned drawbacks we developed an air dielectric double voltage divider capacitor.

During the development we had the primary aim to produce the lowest TC high-voltage divider capacitor possible. For the plates of the double divider condensator the low TC alloy invar (Fe64Ni36 , $TC = 1 \text{ ppm}/^\circ\text{C}$) superior to aluminium, steel, copper etc. has been chosen. The distance-holder rings made of quartz glass have as very low TC as the invar plates. (See figure 2.)

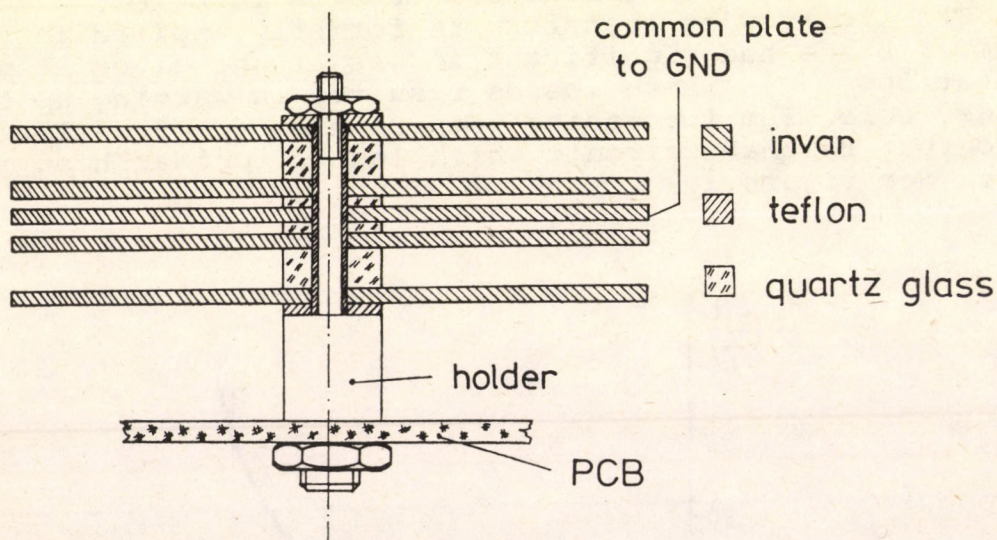


Figure 2. Low TC double air dielectric voltage divider capacitor.

The mentioned developments and some other changes in the RF/DC unit brought significant improvement of the mass peak stability. The development of RF/DC unit and other parts of quadrupole mass spectrometer is a continuous process and it is going on for the moment too.

VACUUM TREATMENT OF CR-39 FOR THE REDUCTION
OF BACKGROUND IN NEUTRON INDUCED AUTORADIOGRAPHY

K. Freyer*, H.C. Treutler*, K. Dietze*, I. Hunyadi,
I. Csige, G. Somogyi

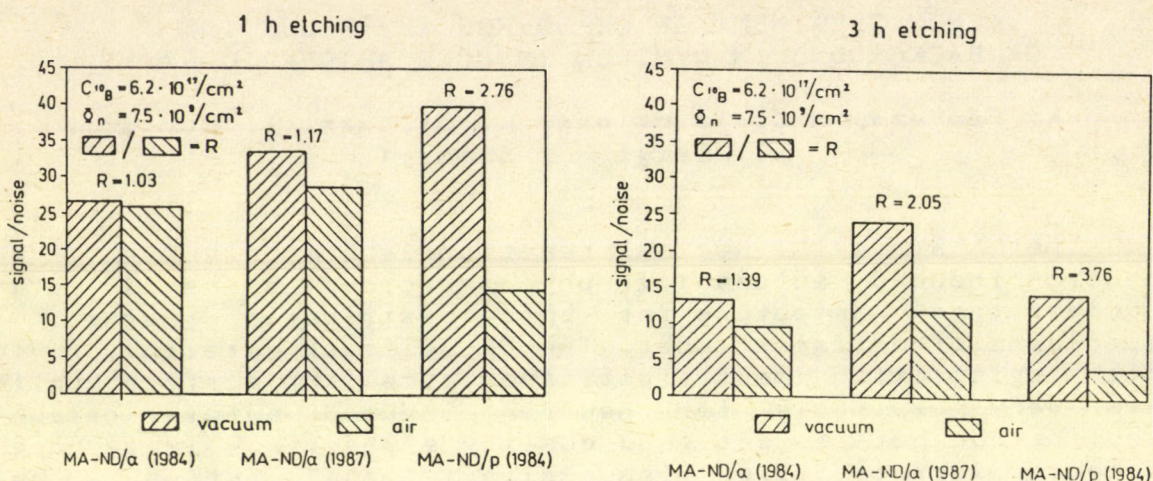
The $^{10}\text{B}(n,\alpha)^7\text{Li}$ nuclear reaction is commonly used in the neutron induced autoradiography performed by solid state nuclear track detectors for boron distribution mapping in specimens of different sort. The CR-39 track detectors having high registration sensitivity and excellent surface quality are very suitable for neutron induced autoradiographic application but to get good quality alpha track image on the detector surface (i.e. high "signal/noise" ratio) a well thermalized neutron beam is required above all. Such irradiation facilities are operating only in a few big institutes, while more or less thermalized neutron sources are available in many places. Therefore we have made efforts to elaborate a simple and effective method for boron concentration and distribution measurement at such irradiation conditions where the thermalization degree of the neutron source is not favorable.

Based on previous results obtained from systematic studies of the vacuum effect on the detection sensitivity of CR-39 [1,2] joined experiments have been performed to reduce the neutron induced background on the autoradiograms. The main components of this background are proton tracks originating, on one hand, from the $^{14}\text{N}(n,p)^{14}\text{C}$ thermal neutron induced reaction on the nitrogen present in the ambient air and diffused into the detector and, on the other hand, from the $^1\text{H}(n,n')p$ energetic neutron scattering on the hydrogen content of the detector material [3].

Boron doped silicon samples in contact with Hungarian made CR-39 detectors (trade mark: MA-ND) were irradiated in air and in vacuum (1kPa) using a special irradiation chamber at the Cf-252 fission neutron source of the Central Institute of Isotope and Radiation Research in Leipzig [4]. In the case when the irradiation was performed in vacuum, 8 hours outgassing was applied prior to and 1 hour after the irradiation for stabilizing the effect of vacuum. After a short (1 hour) and a longer (3 hours) etching in 6.25M NaOH solution at 70°C the track density over the sample (g_0) and without sample (g_B) were measured by manual scanning. The "signal/noise" ratios, corresponding to $(g_0 - g_B)/(g_B)$ are presented on Figs. 1-2 for neutron irradiation performed both in vacuum and air. The numbers above the paired columns represent the vacuum data relative to the air ones.

Due to the selective desensitization effect of the properly chosen vacuum treatment, the neutron induced proton background has been reduced to 0.7-0.3 of that measured in air for the

* Central Institute of Isotope and Radiation Research,
Leipzig, GDR



Figs. 1-2 The "signal/noise" ratio in boron determination at a Cf-252 fission neutron source obtained with MA-ND detectors of different type and production year. The left columns refer to the case, when the irradiation was performed in vacuum conditions.

most sensitive detectors (MA-ND/α -87 and MA-ND/p -84), while the registration sensitivity of the charged particles from the $^{10}B(n,\alpha)^7Li$ reaction has been suffered only about 20% reduction. It can be seen also from the figures that the value of the "signal/noise" ratio and also the effect of the vacuum treatment depend on the etching time, too. Further experiments are in progress to define the optimal parameter values of vacuum treatment and etching.

References

- [1] Fujii M., Csige I., Somogyi G., 20th Int. Cosmic Ray Conf., Moscow, Aug.2-15, 1987. Vol.2, pp. 414-417. Eds. Kozyarivsky et al. NAUKA, Moscow, 1987.
- [2] Csige I., Hunyadi I., Somogyi G., Fujii M., Proc.of 14th Int. Conf. on SSNTDs, Lahore. April 2-6,1988. To be published in Nuclear Tracks in 1989.
- [3] Somogyi G.,Varga Zs.,Hunyadi I.,Freyer K.,Tretler H.C. Nuclear Tracks, Vol. 12, Nos 1-6, pp. 949-952, 1986.
- [4] Freyer K., Tretler H.C., Geisler M., J. Radioanal Nucl. Chem., Articles 83/1, pp. 31-38, 1984.

ADAPTIVE DIGITAL FILTERING FOR X-RAY SPECTROMETRY

T. Lakatos

An adaptive signal processing system was developed for high count rate high resolution spectrometry, which is based on the fully digital filtering of preamplifier output signals. The system provides the maximum possible throughput rate at a fixed shaping time. In adaptive mode of operation the throughput rate is much higher than in the case of traditional systems.

The resolution in amplitude measurements on pulse signals from nuclear detectors with respect to noise, high rate effects and detector collection time is determined by weighting function of the whole signal processing system [1]. The above holds true for the throughput rate, too.

Our intention was to realise a system with a finite weighting time interval to eliminate the high rate effects and with a weighting function which is symmetrical with respect to the time of pulse appearance providing simultaneously high resolution and higher throughput rate than the traditional systems give [2]. Theoretical considerations and results of computer simulation showed that digital realisation of the aim would be expedient [3]. This choice has many advantages. The biggest of them is that we can realise the adaptive mode of operation, too.

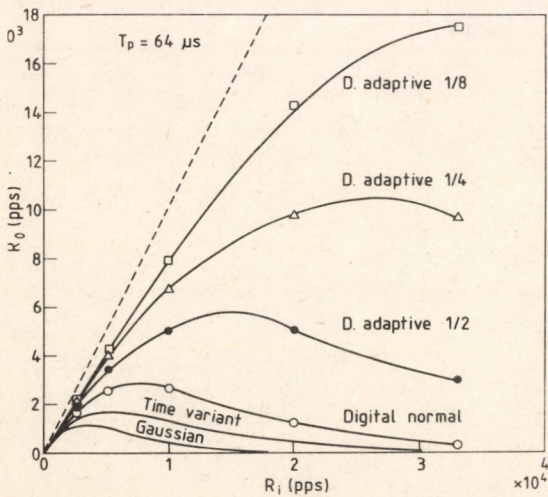


Fig. 1. The Throughput Rate

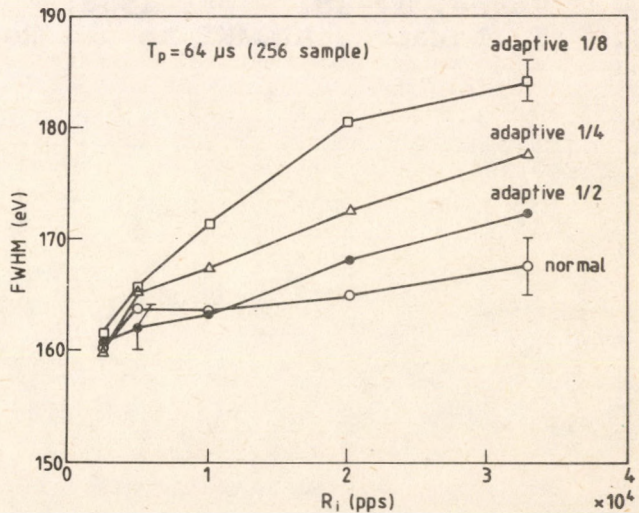


Fig. 2. Resolution as a Function of Input Count Rate

Having a true step input pulse from the pulsed reset preamplifier, a very useful output response can be realised:

$$S_0 = \frac{\sum W_i (J_i - A_{-i})}{\sum W_i}$$

Where W_i is the i -th weight J_i is the i -th sample after and A_{-i} is the $-i$ -th sample before the pulse arrival.

Applying a finite semi-cusp-like weighting function a high resolution system was developed. If the number of samples is fixed the resolution is theoretically independent of the count rate because of the finite weighting interval.

Because the S_0 value is independent of the sample number, the system is suitable for adaptive operation. If a second pulse appears during the shaping time the output word is immediately sent. The minimum adaptive shaping time and the optimum peaking time are set in the same time by the user.

The Fig.1. gives comparison between the measured throughput rates of the system and the idealised one of the semi-Gaussian and time-variant filters.

The resolution (measured at 5.9 keV) as a function of the input count rate in different modes of operation is given in Fig.2.

References

1. V. Radeka, Proc. Int. Symp. Nucl. Electronics Versailles, 10-13. Sept. 1968. p. 61.
2. T. Lakatos, XIII. Int. Symp. Nucl. Electronics Varna, 12-18. Sept. 1988.
3. T. Lakatos, ATOMKI Annual Rep. 1987.

A NEW VERSION OF THE COMPUTER PACKAGE "PIXASE"

L. Zolnai, Gy. Szabó

Our computer package for evaluation of PIXE spectrum series has recently been published [1,2]. Nevertheless some improvement has been done compared to the published version for the convenience of the users using the possibilities of the IBM-PC/AT computers:

- Now both codes (ASELES and PIXASE) satisfy the strict requirements of the standard FORTRAN'77.
- The maximum number of the pile-up channels has been increased to 64 (previously it was 32)
- The code can be optionally augmented with a simple graphical output giving possibility of a quick checking of the results (see fig. 1.)

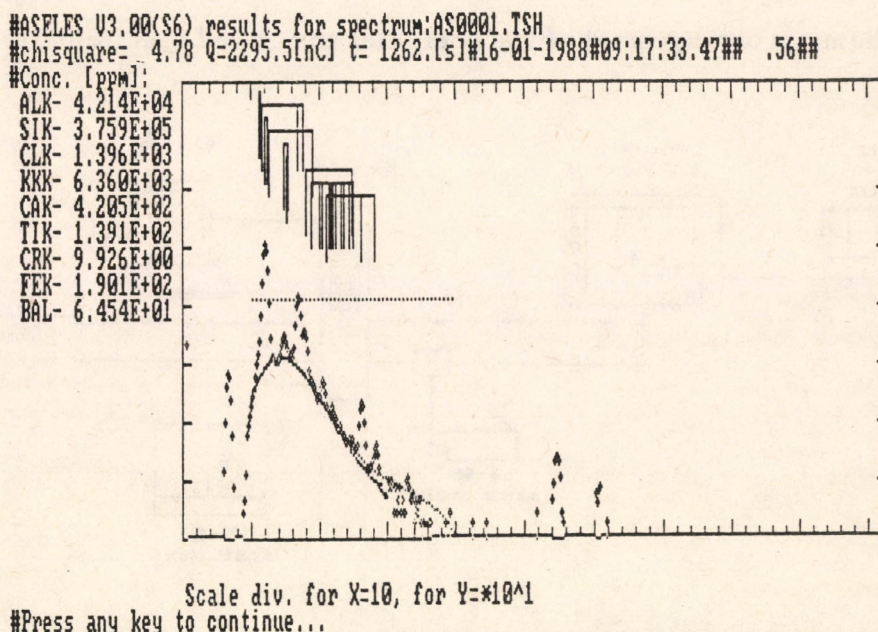


Fig.1. Example for the graphical output of the results of the code ASELEX.

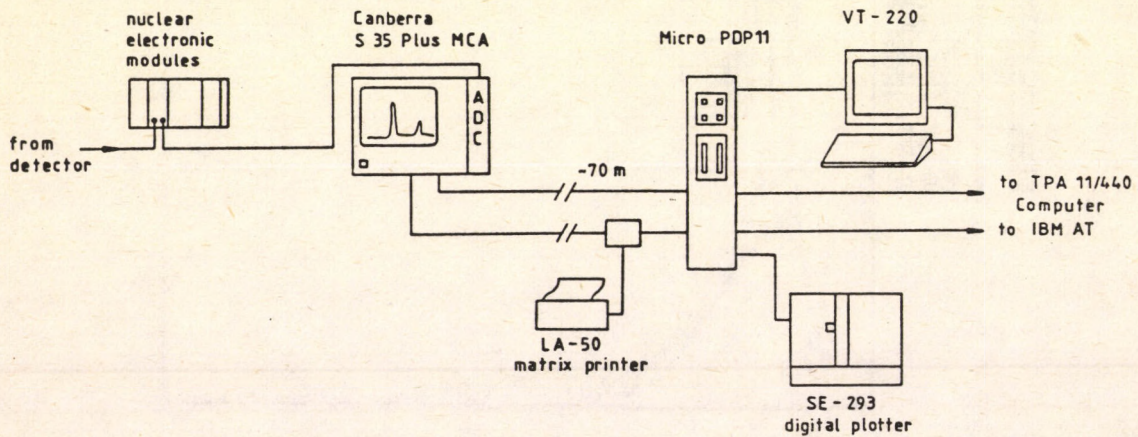
References

- [1] L. Zolnai and Gy. Szabó, Nucl. Instr. and Meth. B34(1988) 118
- [2] Gy. Szabó and L. Zolnai, Nucl. Instr. and Meth. B in press

Communication Software between a Micro PDP-11 Computer and a Canberra S35-Plus Multichannel Analyzer

F. Ditrói, S. Takács

A series of computer codes is developed making possible the data transfer between a Canberra S35-Plus MCA and a DEC Micro PDP-11 computer. The programs also provide the remote control of the analyzer. The programs contain both FORTRAN and MACRO routines. The speed of data transfer is up to 19.2 kbaud through RS-422 interfaces. It is also possible to plot the acquired spectra or calculated curves on a digital plotter. The programs run under RSX-11M operating system. The transfer time of a 4096 channel spectrum is about 15 seconds. The transferred spectra can be evaluated either on the semigraphic terminal of the TPA 11/440 computer, or on an IBM compatible AT. The Figure shows the schematic arrangement of the computer controlled spectrometer facility.



- [1.] F. Ditrói, S. Takács, Program Package for Micro PDP-11 Computer for Interfacing, Data Transfer and Remote Control of a Canberra S35-Plus Multichannel Analyzer, submitted to Nucl. Instr. Meth.

A HORIZONTAL BEAM-LINE FOR PRACTICAL IRRADIATIONS

F. Szelecsényi, F. Tárkányi

The charged particle irradiation is one of the main tools for the use of cyclotrons on applied fields. For better organisation of the preparations and irradiations, and to reduce the radiation exposure dose of the staff, besides of our vertical beam-line a horizontal one has also been constructed for both low and high intensity irradiations [1].

The new beam-line and the targets are located at 22.5° at right to the direction of unbended beam after the first switching magnet close to the cyclotron. The beam-line is composed of the usually applied beam forming, diagnostic, current measuring and vacuumtechnical devices in accordance with Fig.1.

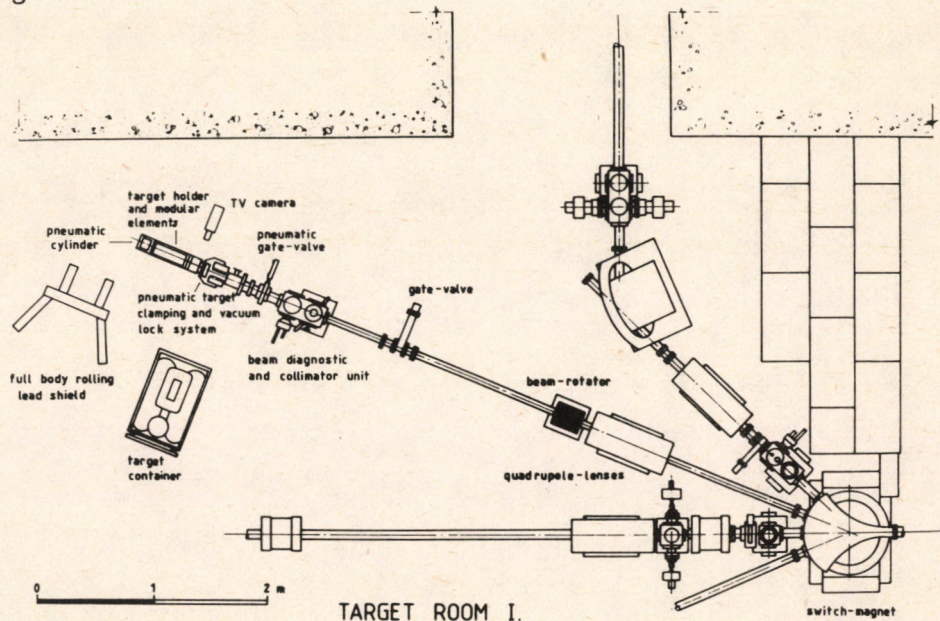


Fig.1. Horizontal beam-line for practical applications

To avoid the hot-spots on the surface of the target, a three-phase motor stator is used as a charged particle beam rotator, located at 4 m away from the target position. The target holder, the modular elements, the modular frame, the current measuring devices, the water cooling system are similar to ones used at our vertical beam-line. A target support table is mounted to the beam-line for external irradiations of special targets. The horizontal beam-line and the target system are operated from a remote operating console. The system is used for irradiations of solid, liquid and gas targets both in vacuum and in the air.

REFERENCES

- [1] L. Andó et al., ATOMKI Report X/32 (1987)

THE NEW CENTRAL GEOMETRY OF THE CYCLOTRON MGC-20

Z. Kormány, I. Szücs and A. Valek

Beam dynamical study of the third harmonic mode acceleration [1] revealed that the significant intensity loss observed in this mode of operation was due to the dee geometry in the centre. To improve the third harmonic characteristics of the cyclotron, a new central arrangement has been designed and new dee inserts (Fig.1) have been manufactured and installed.

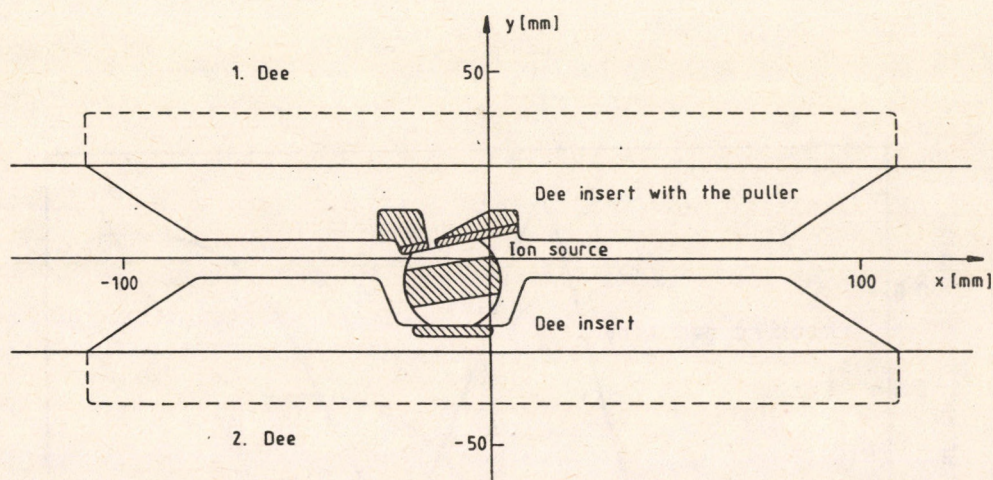


Fig. 1. The new central arrangement of the cyclotron

As a result of the modification, the MGC cyclotron produces the required alpha beam intensities both in the first and third harmonic modes of operation. The current values in Table 1 were measured at about 400 W of arc power (2A, 200V) in the ion source. The ratio of intensities achieved in the two modes is two-three times lower now than that was with the original geometry. As a basic requirement, the good first harmonic features of the machine have been preserved as well.

Fig. 2 shows a further advantage of the modified geometry: the maximum intensity is achieved at considerably lower dee voltage, resulting in more stable work of the RF system. It is especially important at frequencies above 22 MHz, where the obtainable dee voltage amplitude begins to drop. Furthermore the orbit centering is better in the new geometry, as it is shown by the decrease of the required inner harmonic coil currents at optimum settings and it yields higher extraction efficiency than that was earlier.

Table 1. Measured alpha beam intensities in the new geometry

Mode of operation	third					first
	Energy /MeV/	5.3	6.	7.4	8.9	10.6
Frequency /MHz/	17.	18.	20.	22.	24.	11.
Max. external beam / μ A/	14.	19.	22.4	11.2 ⁺	14. ⁺	48.

⁺ at frequencies above 20 MHz, only pulsed mode can be used

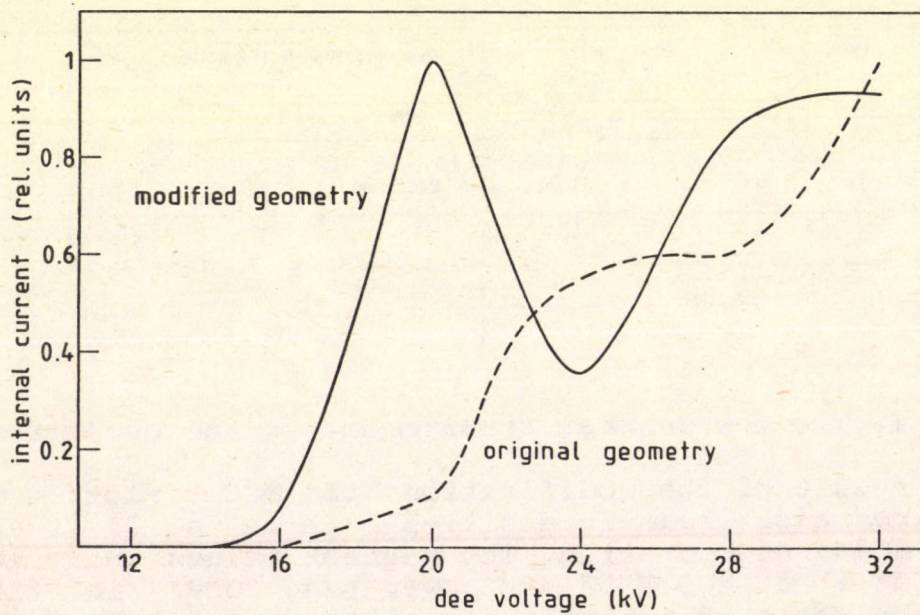


Fig. 2. Internal current vs. dee voltage amplitude

References

- [1] Z. Kormány, ATOMKI Annual Report (1987) 94

CHARGED PARTICLE IRRADIATIONS AT THE CYCLOTRON

Z. Kormány, I. Szücs, A. Valek, J. Vámosi

For charged particle irradiations various experimental set-ups have been developed at the cyclotron MGC-20.

The experimental arrangement designed for irradiations with elastically scattered particles and/or nuclear reaction products from the target is shown in Fig. 1. It is built on the basis of a standard vacuum chamber of the beam transport system of the cyclotron. Connecting a pipe or a second vacuum chamber to its exit hole, the sample can be irradiated in vacuum, replacing this with a foil covered exit window, the irradiation can be carried out in atmosphere. The beam probe, the diaphragm, the target holder and the Faraday cup can be cooled by water. The system was used to irradiate solid state track detector foils with alpha particles, protons and fission fragments.

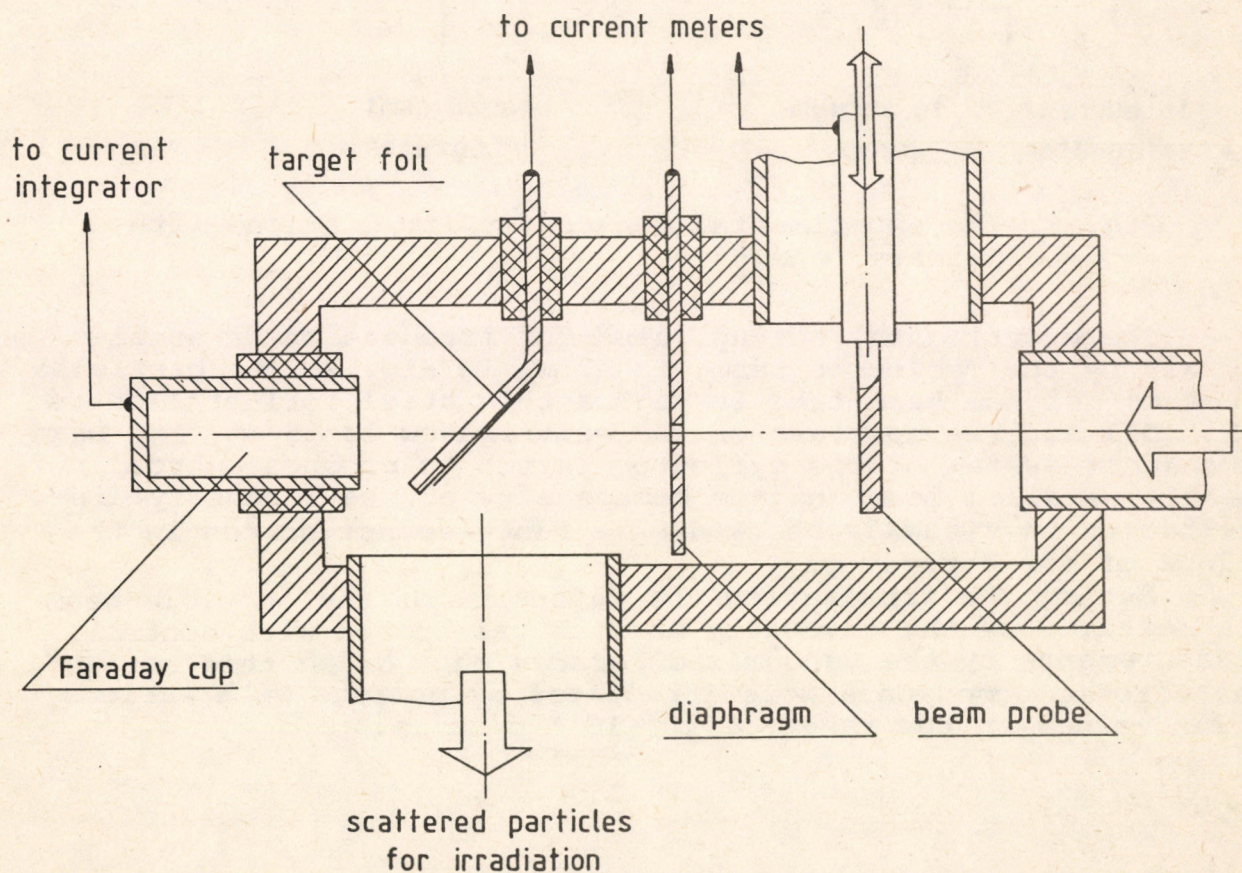


Fig. 1. The experimental set-up for irradiations with secondary particles

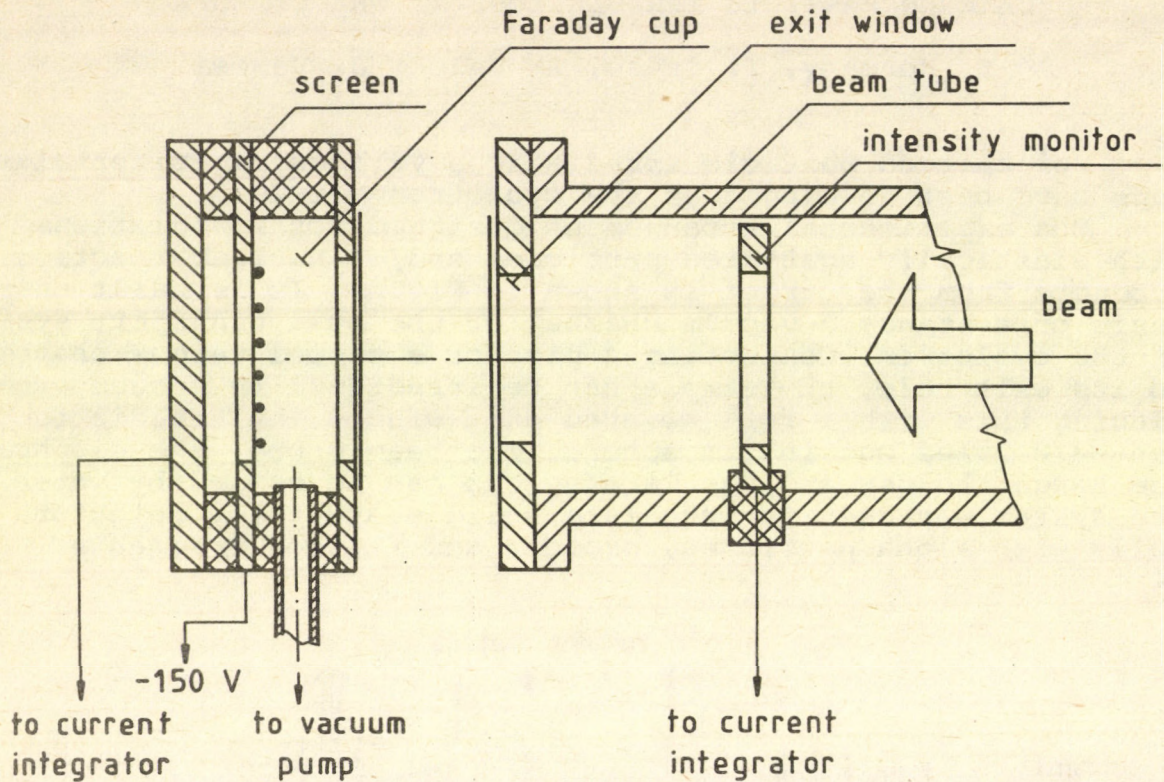


Fig. 2. The experimental set-up for irradiations with primary beam

The experimental set-up, used for irradiation of samples in air by the cyclotron beam, is shown in Fig. 2. The particles come out of the beam tube through a thin steel foil of thickness of 0.021 mm. The aperture of the exit window is 35 mm. The beam transport system of the cyclotron is set to produce a broad, nearly parallel beam and the homogeneity of the intensity distribution is visually checked on a fluorescence screen in the place of the Faraday cup.

During the irradiation the intensity of the particle beam is measured by the intensity monitor calibrated with control measurements by the vacuumized Faraday cup. Using this set-up electronic components were irradiated by protons with various flux values in the range of 10^7 - 10^{10} p/cm².s.

A NEW TYPE OF ELECTROSTATIC ELECTRON ANALYZER

K. Tökési, L. Kövér, D. Varga

Different types of electron spectrometers have been constructed for atomic and surface physics research in ATOMKI. One of them is a "box"-type distorted field cylindrical mirror electron spectrometer (ESA-13, Fig. 1), the calculated parameters of which were presented in earlier papers (1, 2).

Some advantageous properties of this spectrometer are: modular construction (more analyzer modules can be placed along a spectrometer axis), the positions of the electron source and of the focus are outside the spectrometer. This geometry, however, contains still severe limitation regarding the irradiation of the sample, therefore we replaced the endings of

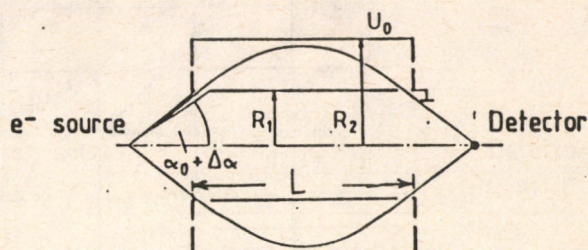


Fig. 1 Schematic diagram of the "box"-type distorted field cylindrical mirror electron spectrometer

the analyzer by conically shaped electrodes ensuring a better accessibility from the point of view of excitation.

The present calculations have been made for a "box"-type distorted field cylindrical mirror electron spectrometer with similar geometrical parameters (R_2/R_1 , L/R_1 are the same, see Fig. 1) as in the case of ESA-13, having conically shaped ends of 45° half angle.

Figure 2 shows the calculated electron trajectories in the analyzers with 43° degree entrance angle, and the respective calculated functions describing the dependence of the focal length on the entrance angle of the electrons are shown in Fig. 3.

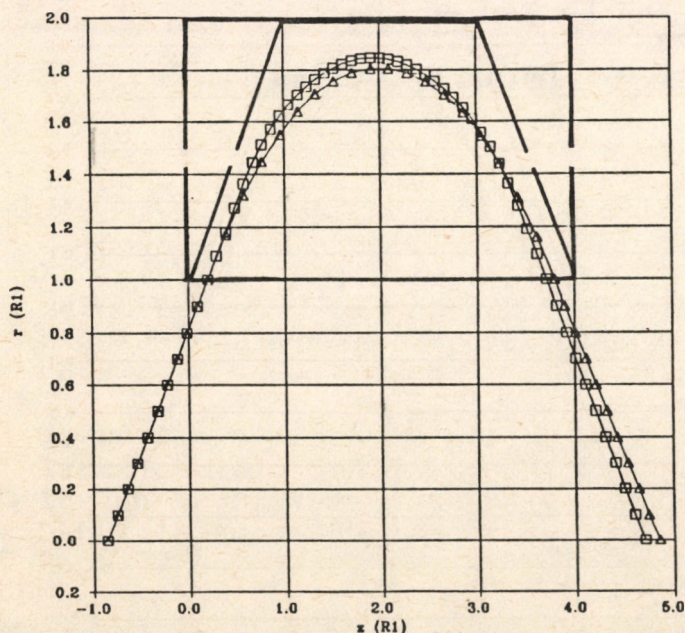


Fig. 2 The calculated electron trajectories with 43° entrance angle Δ in the "box"-type distorted field cylindrical mirror electron spectrometer, \square in the "box" type distorted field cylindrical mirror electron spectrometer having conically shaped ends of 45° half angle.

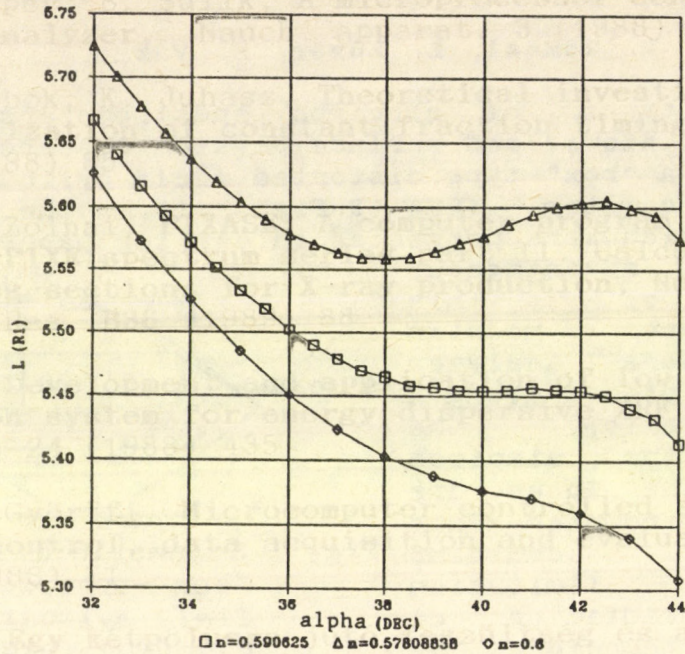


Fig. 3 The calculated functions describing the dependence of the focal length on the entrance angle of the electrons at several different spectrometer constants ($n=U_0/E_{kin}$)

These latter results demonstrate that the modified distorted field spectrometer with conical endings has second order focusing properties.

References

1. D. Varga, A. Kövér, L. Kövér, and L. Redler, Nucl. Instrum. Meth. A238(1985)393.
2. A. Kövér, D. Varga, E. Szmola, Gy. Mörlik, L. Gulyás K. Tökési, to be published

THE OPERATION OF THE VAN DE GRAAFF ACCELERATORS IN 1988

L. Bartha, Á.Z. Kiss, E. Koltay, A. Nagy, Gy. Szabó

The operation time of the 5 MV Van de Graaff accelerator amounted to 1079 hours this year. The machine time was distributed mainly among atomic physics, nuclear physics, analytical studies, accelerator physics and machine tests, as shown in Table 1. In most cases protons (91%) were accelerated, only

Table 1

Field	Hours	%
Atomic physics	313	28
Nuclear physics	279	26
Analytical studies	338	31
Accelerator physics	46	4
Machine test	103	10
Total	1079	100

short measurements were performed with alpha particles (1.5%). Some test runs were made with light heavy ions and molecular beam components (7.5%). For a period of three months the machine was closed. As part of a reconstruction activity planned for a few years period the whole insulator stack and acceleration tube has been dismantled for a careful cleaning, repair and for the replacement of some insulator and tube units.

The 1 MV Van de Graaff accelerator found an intense application in ion-atom collision research in the joint regime of the accelerator and the electrostatic cylindrical mirror spectrometer ESA-13. We succeeded in lowering the minimum available bombarding energy to a value as low as 70 keV. Total measuring time amounted to 1118 beam hours.

In order to broaden the selection of ion species available from the 5 MV machine several experiments were made. In the first case test runs were made with Li beams extracted from the regular rf-ion source in a regime when the internal surface of the discharge tube was coated with a layer of LiF deposited by vacuum evaporation. In these runs analyzed Li^+ and Li^{++} beams available with the intensity of 20 nA disappeared after a running time of the order of 10-20 hours due to the instability of the deposited layer. In other experiments N^{2+} beam component was produced under optimized ion source conditions. Up till now the practical intensity of 40 nA was obtained after the analy-

zing magnet.

Special investigations could be performed in the field of ion-atom collision physics by using molecular beams. Searching for a possible source of simple light molecular beam components experiments were made with the use of methane as discharge gas in the ion source. As shown in Fig.1 several molecular components of practical intensities were obtained in the analyzed beam. The development work will be continued according to the needs of our users in atomic physics.

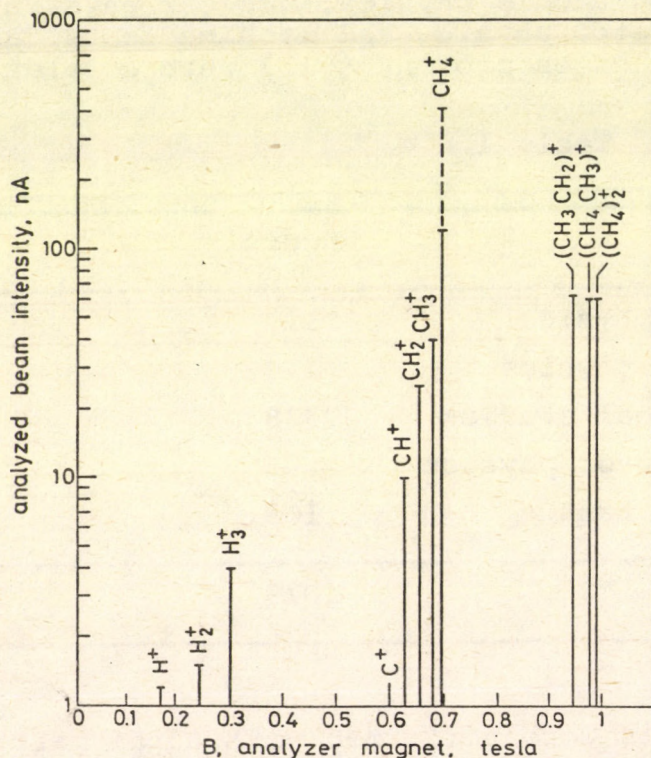


Fig. 1.

Reference

Á.Z. Kiss, E. Koltay, I. Papp, Gy. Szabó, J. Félserfalvi, I. Nyilas, Nucl. Instr. Meth. A268 (1988) 382

STATUS REPORT ON THE CYCLOTRON

Z. Kormány and A. Valek

The operation of the cyclotron MGC-20 and the measuring centre met the requirements of the users in 1988. Because of a budget cut the utilization was concentrated to 8 months and the remaining part of the year was reserved for maintenance and developments. The overall working time at the cyclotron was almost 3500 hours with monthly distribution shown in Figure 1. The cyclotron was available for the users 1935 hours; the effectively used beam time is summarized in Table 1.

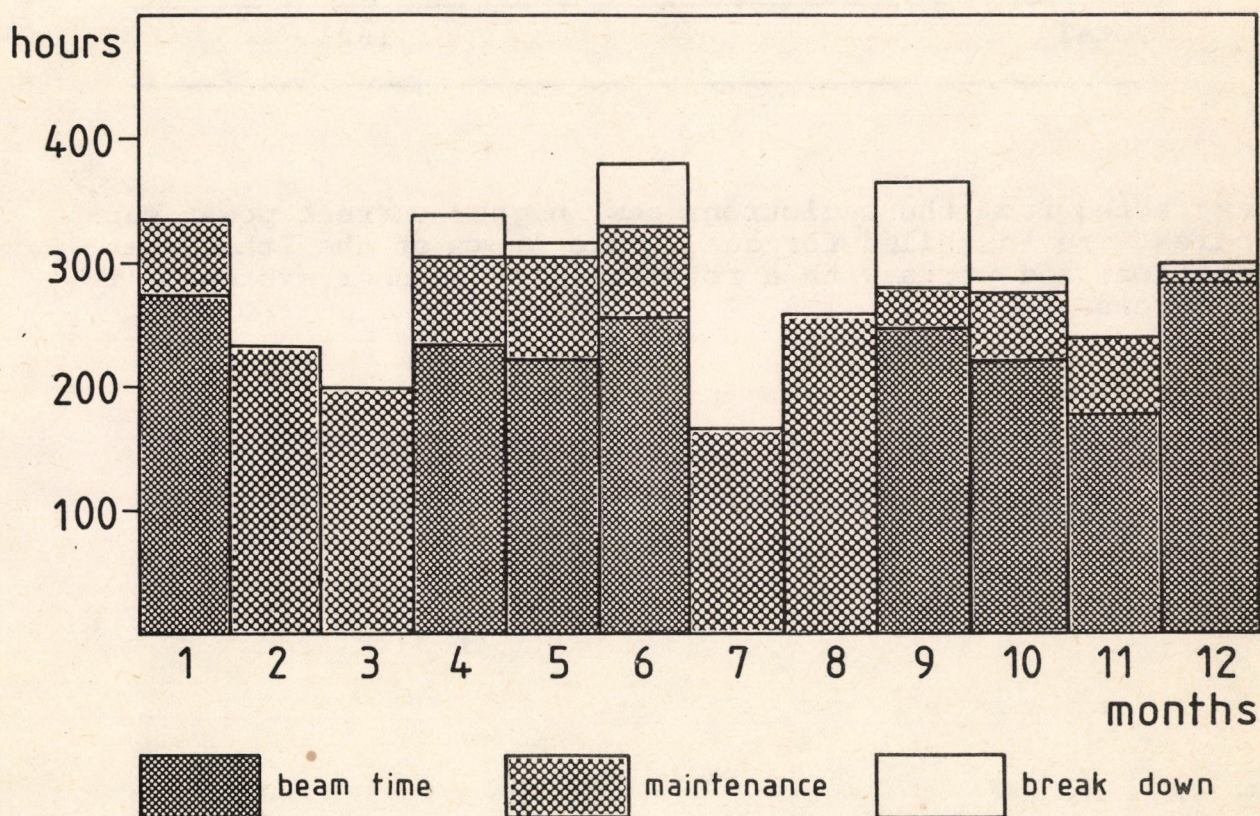


Fig. 1. Operation time distribution in 1988

In the maintenance period, besides the regular repairs and tests, the RF control system and the tuning capacitor block of the dees were completely changed in cooperation with the manufacturer. As developments, new dee inserts were built into the cyclotron centre, ensuring higher beam intensities in the third harmonic mode of acceleration (reported separately); the optimum setting of the cyclotron was systematically investigated at various energy protons and diagrams were prepared for quicker and better tuning of the machine; 20 MeV energy protons were

Table 1. Effectively used beam time

Project	Beam time in hours
Nuclear spectroscopy	535
Nuclear reaction studies	332
Nuclear life-time studies	31
Isotope production	356
Neutron source	188
Material investigations	91
Charged particle irradiations	88
Total	1621

extracted from the cyclotron; new, higher current power supplies were installed for quadrupole lenses of the 7th target station; and works with a rotating wire scanner system is in progress.

PUBLICATIONS

AND

SEMINARS

PAPERS PUBLISHED

(* denotes co-author from another establishment)

Nuclear Physics

J. Cseh, G. Lévai, **Core-plus-alpha-particle states of ^{20}Ne and ^{16}O in terms of vibron models**, Phys. Rev. C38 (1988) 972

J. Cseh, M. Józsa, A. Z. Kiss, E. Koltay, E. Somorjai,
*J. Keinonen, **The reaction $^{36}\text{S}(\alpha, \gamma)^{40}\text{Ar}$: gamma-transition properties of resonance and bound states in ^{40}Ar** , Nucl. Phys. A489 (1988) 225

T. Kibédi, Zs. Dombrádi, T. Fényes, A. Krasznahorkai, J. Timár, Z. Gácsi, *A. Passoja, *V. Paar, *D. Vretenar, **Structure of ^{112}In nucleus**, Phys. Rev. C37 (1988) 2391

A. T. Kruppa, R. G. Lovas, B. Gyarmati, **Complex scaling in the cluster model: resonances in ^8Be** , Phys. Rev. C37 (1988) 383

G. Lévai, J. Cseh, **Distribution of alpha-particle strength in light nuclei**, Journal of Physics G14 (1988) 467

*J. P. Martin, *V. Barci, *H. El-Samman, *A. Gizon, *J. Gizon, *W. Klamra, B. Nyakó, *F. A. Beck, *T. H. Byrski,
*J.C.Merdinger, **Collective band structures and particle alignments in ^{124}Ba , ^{125}Ba and ^{125}Cs** , Nucl. Phys. A489 (1988) 169

*A. Mushtaq, F. Tárkányi, *M. S. Sutisna, *B. Scholten,
*S. M. Qaim, **Charged particle data for radioisotope production**, Progress Report on Nuclear Data Research in the FRG. for the Period Apr. 1. 1987 to March 31. 1988, Ed.: S. Cierjacks, Neandc (E)-292 vol. V. Indc (Ger) -32LN+ Special

Z. Papp, **Potential separable expansion approach to scattering on Coulomb like potentials**, Phys. Rev. C38 (1988) 2457

*M. S. Rouabah, *T. H. Byrski, *A. F. Beck, *D. Curien,
*B. Haas, *J. C. Merdinger, *J. P. Vivien, *J. Gizon, B. Nyakó,
High spin bands in ^{120}Xe , Zeitschrift für Physik A238 (1987) 493

*N. Rowlei, K. F. Pál, *M. A. Nagarajan, **Diaboloic pair transfer between states of good particle number**, Physics Letter B201 (1988) 187

F. Tárkányi, *S. M. Qaim, *G. Stocklin, **Excitation functions of ^3He - and alpha-particle induced nuclear reactions on natural krypton: production of ^{82}Sr at a compact cyclotron**, Int. Journal of Radiation, Applications and Instrumentation A39 (1988) 135

F. Tárkányi, *S. M. Qaim, *G. Stocklin, **Excitation functions of ^3He -particle induced nuclear reactions on enriched ^{82}Kr and ^{83}Kr** , *Radiochimica Acta* **43** (1988) 185

K. Varga, R. G. Lovas, **Eigenvalue problem of the resonating-group norm operator with mixed cluster states**, *Phys. Rev. C* **37** (1988) 2906

T. Vertse, *P. Curuchet, *O. Civitarese, *L. S. Ferreira, *R. J. Liotta, **Application of Gamow resonances to continuum nuclear spectra**, *Phys. Rev. C* **37** (1988) 876

*C. H. Yu, *M. A. Riley, *J. D. Garrett, *G. B. Hagemann, *J. Simpson, *P. D. Forsyth, *A. R. Mokhtar, *J. D. Morrison, B. Nyakó, *J. F. Sharpey-schafer, *R. Wyss, **Proton band crossings and electromagnetic transition probabilities in ^{161}Lu** , *Nucl. Phys.* **A489** (1988) 477

J. Cseh, M. Józsa, *J. Keinonen, A. Z. Kiss, E. Koltay, E. Somorjai, **^{40}Ar nucleus studied by the reaction ^{36}S (α , γ) ^{40}Ar** , Proceedings of the 6th Conf. on Capture Gamma-Ray Spectroscopy Leuven, Belgium, 31 Aug -4 Sep 1987, Eds.: K. Abrahams, P Van Assche, Bristol and Philadelphia, 1988, Institute of Physics, Institute of Physics Conference Series Number 88.

J. Cseh, **Application of the algebraic cluster model to light nuclei**, 5th Int. Conf. on Clustering Aspects in Nuclear and Subnuclear Systems, Kyoto, Japan, 25-29 Jul 1988, Contributed Paper, Eds.: Y. Sakuragi, T. Wada, Y. Fujiwara, Kyoto, 1988

*S. M. Qaim, F. Tárkányi, *A. Mustaq, *G. Stocklin, **Excitation functions for the production of positron emitting radionuclides ^{82}Sr (^{82}Rb) and ^{73}Se** , Proceedings of the Int. Conf. on Nuclear Data for Science and Technology, 30 May-3 Jun 1988, Mito

G. Lévai, J. Cseh, **Distribution of alpha-particle strength in light nuclei**, Proceedings of the 5th Int. Conf. on Nuclear Reaction Mechanism, Varenna, 13-18 Jun 1988, Milan, Italy

D. Berényi, F. Szelecsényi, **Analysis of the cross section data for the production of short-lived light positron emitter with the Debrecen cyclotron**, Proceedings of the IAEA Consultants' Meeting on Data Requirements for Medical Radioisotope Production, 20-24 Apr 1987, Ed.: K. Okamoto, Tokyo

Atomic Physics

*B. B. Bandong, *R. L. Watson, J. Pálinkás, *C. Can, **K X-ray spectra of highly charged recoil ions produced by heavy-ion impact on oxygen**, *Journal of Physics* **B21** (1988) 1325

D. Berényi, **High-energy ion-atom collisions**, Comments on Atomic and Molecular Physics 21 (1988) 169

D. Berényi, G. Hock, **Proceedings of the High-Energy Ion-Atom Collisions, 1987, Debrecen, Hungary**; in Lecture Notes in Phys. Eds.: H. Araki, J. Kyoto, J. Ehlers et al, 1988, Berlin, Heilderberg, New-York, etc., Springer Ver.

*O. Heil, *J. Kemmler, *K. Kroneberger, A. Kövér, Gy. Szabó, L. Gulyás, *R. De Serio, *S. Lencinas, *N. Keller, *D. Hofmann, *H. Rothard, D. Berényi, *K. O. Groeneveld, **Electron loss and capture to continuum from He and Ne atoms bombarded with He⁺ ions**, Zeitschrift für Physik D9 (1988) 229

*J. Kemmler, *S. Lencinas, *P. Koschar, *O. Heil, *H. Rothard, *K. Kroneberger, Gy. Szabó, *K. O. Groeneveld, **Production and transport of electrons in thin carbon foils**, Nucl. Instr. and Meth. in Phys. Res. B33 (1988) 317

A. Kövér, Gy. Szabó, L. Gulyás, K. Tökési, D. Berényi, *O. Heil, *K. O. Groeneveld, **The electron loss process at backward observation angles in collision systems He⁺ (2MeV) - He, Ne, Ar**, Journal of Phys. B21 (1988) 3231

*T. Mukoyama, L. Sarkadi, **Relativistic Coulomb continuum wave function at zero kinetic energy in ion-atom collisions**, Bull. of the Inst. for Chem. Res. Kyoto Univ. 66 (1988) 11

T. Papp, J. Pálinkás, **Measurement of the M2-E1 mixing in L X-ray transitions**, Phys. Rev. A38 (1988) 2689

L. Sarkadi, *T. Mukoyama, **Subshell coupling effects in L-shell ionization of gold by proton impact**, Phys. Rev. A37 (1988) 4540

E. Vatai, **Energy dependence of electron shake up/off calculation with realistic potential change**, Phys. Rev. A38 (1988) 3777

L. Végh, **Scattering correlation in double ionization of helium by fast antiprotons and protons**, Phys. Rev. A37 (1988) 992

L. Végh, **Stopping powers calculated from empirical electron-ejection cross sections**, Phys. Rev. A37 (1988) 1942

Materials Science and Analysis

F. Ditrói, I. Mahunka, S. Takács, **Ciklotron az iparban**, Korszerű Technológiák 16 (1988) 23

*L. Költő, M. Kiss-Varga, **Composition analysis of Roman age enamelled bronze objects**, in Archeometrical Research in Hungary, Eds.: M. Járó, L. Költő, Központi Múzeumi Igazgatóság, Budapest, 1988., p. 141

Earth and Cosmic Science, Environmental Research

I. Borbély-Kiss, *L. Haszpra, E. Koltay, S. László, *A. Mészáros, *E. Mészáros, Gy. Szabó, **Elemental concentrations and regional signatures in atmospheric aerosols over Hungary**, Physica Scripta 37 (1988) 299

I. Borbély-Kiss, E. Koltay, E. Mészáros, Gy. Szabó, **Trace elements in atmospheric aerosols over Hungary**, Proceedings of the 12th Int. Conf. on Atmospheric Aerosols and Nucleation, Held at the University of Vienna, 22-27 Aug 1988, Vienna, Eds.: P. E. Wagner, G. Vali, Lecture Notes In Phys. 309, Berlin, ... 1988, Springer Verl.

Biological and Medical Research

J. Bacsó, I. Uzonyi, *B. Dezső, **Determination of gold accumulation in human tissues caused by gold therapy using X-ray fluorescence analysis**, Int. Jour. of Rad. Appl. and Instr. Part "A" Appl. Rad. and Isot. 39 (1988) 323

F. Tárkányi, *S. M. Qaim, *G. Stocklin, **Production of ^{82}Sr via the ^{82}Kr (^3He , ^3N) Process at a compact cyclotron**, Proceedings of the 7th Int. Symposium on Radiopharmaceutical Chemistry, 4-8 Jul 1988, Groningen, The Netherlands

Z. Kovács, I. Mahunka, *J. Környei, **MGC type cyclotron in the nuclear medicine in Hungary**, *ibid.*

I. Mahunka, F. Tárkányi, L. Andó, F. Szelecsényi, A. Fenyvesi, F. Ditrói, S. Takács, **Medical project at the GC cyclotron in Debrecen**, Proceedings of the 4th Symposium on the Medical Appls. of Cyclotron, 28-31 May 1988, Turku, Finland

Development of Methods and Instruments

É. Csongor, *L. Wilhelmova, *Z. Dvorak, *P. Povinec, *M. Grgula, **Inter-laboratory comparison of atmospheric ^{85}Kr concentration measurements**, Int. Journ. of Rad. Appl. and Instr. A39 (1988) 401

J. Bacsó, I. Uzonyi, **Development of an automatic sample changer equipment for XRF measurements**, *Isotopenpraxis* 24 (1988) 72

I. Uzonyi, **A new XRF method for the analysis of biological samples**, *Isotopenpraxis* 24 (1988) 79

*Gy. Bagi, P. Bornemissza-Pauspertl, *E. Hidvégi, **Inverst correlation between growth and degrading enzyme activity of seedling after gamma and neutron irradiation of pea seeds**, *Int. Journ. of Rad. Biology* 53 (1988) 507

*N. G. Zaitseva, *Kim Sen Khan, *O. Knotek, P. Mikecz, *V. A. Khalkin, **Radiochemical separation of radiothallium from proton irradiated lead**, *Journ. of Radioanal. and Nucl. Chem. Articles* 121 (1988) 307

Cs. Ujhelyi, **Comparison of three procedures for determining true count-rates with "proportional" sources of a radioisotope**, *Int. Journ. of Rad. Appl. and Instr.* A39 (1988) 631

L. F. Gáll, P. Mikecz, T. Papp, **Preparation of uranium targets by a chemical method**, *Nucl. Instr. and Meth. in Phys. Res.* A270 (1988) 248

L. Zolnai, Gy. Szabó, **PIXASE: A computer program package for evaluation of PIXE spectrum series, Part 1 spectrum evaluation**, *Nucl. Instr. and Meth. in Phys. Res.* B34 (1988) 118

L. Kiss, **Szenzoros RH/KH konverter**, *Rádiótechnika* 37 (1988) 466

J. Környei, I. Mahunka, P. Mikecz, M. Lakatos, F. Kecskés, L. Andó, **Iodobell in vivo készletek a felhasználás helyszínén történő jódjelzésre**, *Izotóptechnika* 31 (1988) 57

M. Horváth, A. Pszota, J. Környei, M. Lakatos, I. Mahunka, P. Mikecz, **Hazai ^{123}I -dal, hazai módszerrel jelzett heptadekánsav (HDS) a humán diagnosztikában**, *Izotóptechnika* 31 (1988) 61

J. Nagy, K. Juhász, **Rendszerek megbízhatósági vizsgálata I.: soros rendszerek**, *Járművek, Mezőgazdasági gépek* 35 (1988) 113

S. Mészáros, G. Halász, K. Vad, *F. J. Kedves, Sz. Balanyi, **Magnetic field dependence of I-V characteristics of high T_c superconducting ceramics**, *Physica* C153 (1988) 1529

J. Végh, **The analytical form of the Shirley-type background**, *Journ. of Elect. Spectrosc. and Rel. Phenom.* 46 (1988) 411

G. Langer, I. Berecz, S. Bohátka, F. Sági, L. Mózsik, **Tömegspektrométeres mérési módszer növényi gázanyagcsere "in vivo" vizsgálatára**, *Mezőgazdaság gépesítése* 6 (1988) 54
Szerkeszti: Bánházi Gy. és mások (VI. szekció: Mezőgazdasági elektronizálás és mérés technika) MTA-MEM Agrár Műszaki Bizottság kutatási és fejlesztési tanácskozása, Gödöllő

A. Paál, K. Sepsy, B. Sulik, **A microprocessor controlled multichannel analyzer**, Nauch. apparat. 3 (1988) 95

J. Gál, Gy. Bibók, K. Juhász, **Theoretical investigation and practical realization of constant fraction timing**, Nauch. apparat. 3 (1988) 85

Gy. Szabó, L. Zolnai, **PIXASE: A computer program package for evaluation of PIXE spectrum series part II. Calculation of the effective cross sections for X-ray production**, Nucl. Instr. and Meth. in Phys. Res. B36 (1989) 88

M. Kis-Varga, **Development and application of low power X-ray tube excitation system for energy dispersive XRF analysis**, Isotopenpraxis 24 (1988) 435

J. Molnár, M. Györffi, **Microcomputer controlled systems for measurements control, data acquisition and evaluation**, Nauch. apparat. 3 (1988) 71

L. Záborszky, **Egy kétpólusra jutó feszültség és a rajta folyó áram egymástól független, egyidejű, pontos mérése**, Mérés és Automatika 36 (1988) 106

CONFERENCE CONTRIBUTIONS AND TALKS

(* denotes co-author from another establishment)

Nuclear Physics

J. Cseh, **Analysis of molecular excitations in light nuclei**, Univ. of Arizona, 6 Jan 1988

J. Cseh, **Application of the vibron model in nuclear physics**, Univ. of Tokyo, Physics Dept., 11 Aug 1988, Tokyo

J. Cseh, **The algebraic cluster model**, Hokkaido University, Physics Dept., 5 Aug 1988, Japan

Zs. Dombrádi, **Kölcsönható bozon-fermion modell**, 1988. ápr. 20., KLTE (Kossuth Univ.), Debrecen

T. Fényes, **Magspektroszkópiai kutatások**, Három éves a magyarországi ciklotron c. tudományos ülészek, 1988. dec. 14., ATOMKI, Debrecen

T. Fényes, **Atommag spektroszkópiai kutatások az ATOMKI ciklotronnál**, 1988. febr. 10., KFKI (Centr. Res. Inst. of Phys.), Budapest

I. Hunyadi, **Low energy charged particle nuclear reaction studies with SSNTDs**, 1st Yugoslavian Symposium on Solid State Nuclear Track Detectors, 28-30 Sep 1988, Beograd

T. Kibédi, **Structure of ^{112}In nucleus**, Dept. of Nucl. Phys. of Australian National Univ., 1988, Canberra, Australia

A. Z. Kiss, E. Somorjai, *J. Räsänen, *E. Rauhala, **Stopping powers of 1.9-7 MeV ^4He ions in havar, nickel, kapton and mylar**, 6th Int. Conf. on Ion Beam Modification of Materials 12-17 Jun 1988, Tokyo

Z. Kovács, L. Andó, I. Mahunka, P. Mikecz, F. Szelecsényi, F. Tárkányi, **Proizvodstvo izotopov s pomoshchyu MGC tsiklotrona v Debrecene**, Mezhdunarodnoe Soveshchanie po Obmenu Opytov Ekspluatatsii Tsiklotronov MGC-20, 24-26 Maj 1988, Leningrad, USSR

G. Lévai, J. Cseh, **Distribution of alpha-particle strength in light nuclei**, 5th Int. Conf. on Nuclear Reaction Mechanism, 13-18 Jun 1988, Varenna, Italy; and Osaka University, Nucl. Phys. Lab., 18 Aug 1988; and Tokyo Metropolitan University, Phys. Dept, 9 Aug 1988, Japan

- R. G. Lovas, **Microscopic versus three-body description of ${}^6\text{Li}$** , Nationaal Instituut Voor Kernfysica en Hoge-Energiefysica, Sectie-Kernfysica, 25 Feb 1988, Amsterdam, The Netherlands
- R. G. Lovas, **Clustering in ${}^6\text{Li}$** , Rijksuniversiteit Utrecht, Fysisch Laboratorium, 24 Feb 1988, Utrecht, The Netherlands
- R. G. Lovas, **Cluster structure of ${}^6\text{Li}$** , 5th Int. Conf. on Clustering Aspects in Nuclear and Subnuclear Systems, 25-29 Jul 1988, Kyoto, Japan
- R. G. Lovas, A. T. Kruppa, **Consistent cluster model description of A=2 to 8 nuclei**, Int. Symposium on Developments of Nuclear Cluster Dynamics, 1-3 Aug 1988, Sapporo, Japan
- B. Nyakó, **Experimental studies of superdeformed nuclei**, ISN, 19 Oct 1988, Grenoble, France
- B. Nyakó, *A. Gizon, *J. Gizon, *M. Józsa, *W. Klamra, **Collective band structure in the odd-odd nucleus ${}^{126}\text{La}$** , 3rd Int. Conf. on Nucleus-Nucleus Collisions, 6-11 Jun 1988, Saint-Malo, France
- J. Cseh, **Application of the algebraic cluster model to light nuclei**, *ibid.*
- J. Cseh, **Algebraic approach to the molecular resonances**, *ibid.*
- *O. Dragun, *R. J. Liotta, T. Vertse, **Makroszkópikus formfaktorok használata részecskeátadó reakciókban**, IX. Magyar Magfizikus Találkozó, 1988. okt. 20-23., Visegrád, Hungary
- L. Zolnai, Z. Máté, S. Szilágyi, *A. Bredbacka, *M. Brenner, *K. M. Kallman, *P. Manngard, **Alfa rugalmas szórás ${}^{34}\text{S}$, ${}^{50}\text{Cr}$, ${}^{62}\text{Ni}$ magokon**, *ibid.*
- M. Józsa, J. Cseh, A. Z. Kiss, E. Koltay, E. Somorjai, *J. Keinonen, **Rezonancia gamma-átmenetek vizsgálata a ${}^{36}\text{S}$ (alfa-gamma) ${}^{40}\text{Ar}$ reakcióban**, *ibid.*
- Zs. Dombrádi, **Törzspolarizációs jelenségek páratlan-páratlan In magokban**, *ibid.*
- F. Szelecsényi, **A ${}^{67}\text{Ga}$ előállítására vonatkozó hatáskeresztmetszet mérések a debreceni ciklotronnál**, *ibid.*
- A. Krasznahorkai, J. Timár, J. Gulyás, T. Kibédi, Z. Gácsi, T. Fényes, Zs. Dombrádi, *A. Passoja, *R. Julin, *J. Kumpulainen, *V. Paar, *D. Vretenar, **Proton-neutron multiplett állapotok a Z 50 magtartományban**, *ibid.*
- T. Fényes, **A magfizikai kutatások fejlődési irányai néhány környező országban, gyorsítók**; *ibid.*
- T. Fényes, **Zárszó**, *ibid.*

*S. M. Qaim, F. Tárkányi, *A. Mustaq, *G. Stocklin, **Excitation functions for the production of positron emitting radionuclides ^{82}Sr (^{82}Rb) and ^{73}Se** , Int. Conf. of Nuclear Data for Science and Technology, 30 May-3 Jun 1988, Mito, Japan

Atomic Physics

T. Papp, J. Pálinkás, L. Sarkadi, **On the M2/E1 mixing in L3 X-ray transitions**, 11th Int. Conf. of Atomic Physics, 4-8 Jul 1988, Paris

T. Papp, J. Pálinkás, L. Sarkadi, *C. Neelmeijer, *K. Brankoff, *D. Grambole, *C. Heiser, *F. Herrmann, *W. Rudolph, **Experimental study of the L3-subshell alignment of multiply ionised atoms**, *ibid.*

A. Kövér, Gy. Szabó, L. Gulyás, K. Tökési, D. Berényi, *O. Heil, *K. O. Groeneveld, **Problems in the evaluation procedure of the electron loss peak in light ion-atom collision systems at backward observation angles**, *ibid.*

A. Kövér, **ECC cusp at structured projectiles**, Oak Ridge National Labs., 24 Oct 1988, Oak Ridge, TN, USA

A. Kövér, **Atomic physics and biological research at the Institute of Nuclear Research in Debrecen**, *ibid.* and in Battelle Pacific NW Labs, Richland, WA, USA, 17 Oct 1988

*R. D. Dubois, A. Kövér, **Single and double ionization of helium by hydrogen atom impact**, 10th Conf. on Appl. of Accelerators in Research and Industry, 7-9 Nov 1988, Denton, TX, USA

*Y. Watanabe, L. Végh, **Scattering correlation in multiple ionization by proton, antiproton and multicharged ion impact**, *ibid.*

A. Kövér, L. Sarkadi, J. Pálinkás, D. Berényi, Gy. Szabó, T. Vajnai, *O. Heil, *K. O. Groeneveld, *J. Gibbons, *I. A. Sellin, **The contribution of the ECC to the forward electron cusp in 50-150 keV/u He⁺-He and He⁺-Ar collisions**, *ibid.*

L. Végh, **Critical angle in double ionization**, *ibid.*

*Y. Awaya, *Y. Kanai, *T. Mizogawa, *A. Hitachi, B. Sulik, **Multiple innershell ionization of 0.8-26 MeV/u heavy ion impact**, *ibid.*

I. Kádár, S. Ricz, B. Sulik, J. Végh, D. Varga, D. Berényi, **High resolution target Auger spectroscopy at the impact of energetic heavy ions on Ne**, *ibid.*

L. Végh, B. Sulik, **Independence of the recoil ion velocity on the screening effect of the target electrons**, Spectroscopy and Collisions of Few Electron Ions, 29 Aug-2 Sep 1988, Bucharest

I. Kádár, D. Berényi, S. Ricz, B. Sulik, D. Varga, J. Végh, **High resolution target Auger spectroscopy of heavy ion-atom collisions**, *ibid.*

B. Sulik, *T. Kambara, *Y. Kanai, *T. Mizogawa, *Y. Awaya, **Binary encounter approximation in the geometrical space and its application in X^{q+} -Ca collisions**, *ibid.*

A. Kövér, L. Sarkadi, J. Pálincás, D. Berényi, Gy. Szabó, T. Vajnai, *O. Heil, *K. O. Groeneveld, *J. Gibbons, *I. A. Sellin, **Ionizációs és elektronbefogási folyamatok elektron spektroszkópiai vizsgálata**, IX. Magyar Magfizikus Találkozó, 1988. okt. 20-23., Visegrád, Hungary

T. Papp, J. Pálincás, L. Sarkadi, **Röntgenátmenetek multipól-szerkezetének vizsgálata**, *ibid.*

S. Ricz, I. Kádár, J. Végh, B. Sulik, D. Varga, D. Berényi, **Auger-elektronok nagy energiájú nehéz ion-Ne ütközésekből**, *ibid.*

D. Berényi, **Recent results on heavy ion induced Auger-electron spectroscopy and on "cusp" studies in ATOMKI**, Nucl. Phys. Inst. of the Czechoslovakian Acad. of Sci., 13 Apr 1988, Rez (near Prague), Czechoslovakia

D. Berényi, **Ion-atom collisions study at accelerators in ATOMKI**, Dept. of Phys., Univ. of Varna, 11 May 1988, Varna, Bulgaria

D. Berényi, **ECC and ELC contribution to the cusp and its shape at the impact of light ions with accompanying electrons**, 4th Int. Workshop on Cross Sections for Fusion and Other Appl., 3 Nov 1988, Texas A and M Univ., College Station, TX, USA

D. Berényi, **Some recent results on cusps and Auger electrons studies in ion-atom collisions**, Seminar, IKF, 11 Nov 1988, Frankfurt/M., FRG

*O. Heil, *J. Kemmler, *K. Kroneberger, *A. Kövér, *Gy. Szabó, L. Gulyás, *R. De Serio, *S. Lencinas, *N. Keller, *D. Hofmann, *H. Rothard, D. Berényi, *K. O. Groeneveld, **Cuspelekttronen von He^+ -He, Ne-stossystemen**, Arbeitstagung über "Energieriche Atomare Stosse", 24-30 Jan 1988, Tiefenbach, FRG

Materials Science and Analysis

F. Ditrói, I. Mahunka, S. Takács, **Ciklotronra alapozott analitikai módszerek**, Csepel Művek Anyagvizsgáló és Gépipari Minőségellenőrző Intézete, 1988. ápr. 19.

*J. Gómőri, *E. Gegus, M. Kis-Varga, **A hasfalvi bronzkorong vizsgálata**, A Veszprémi Akadémiai Bizottság Archeometriai és Iparrégészeti Munkabizottságának Ülése, 1988. máj. 18-19., Veszprém, Hungary

S. Takács, F. Ditrói, I. Mahunka, **Investigation of bulk oxygen concentration in high purity aluminium**, Analysis of High Purity Substances, 30 May-3 Jun 1988, Rockova Dolina, Czechoslovakia

*J. Kispéter, *J. Beczner, I. Borbély-Kiss, *L. Horváth, *L. Kiss, *Z. Rózsa, **The effect of ionizing radiation on some physical properties of lactalbumin**, XIX. Annual Meeting of ESNA (European Society of Nuclear Methods in Agriculture), 29 Aug-2 Sep 1988, Vienna

I. Borbély-Kiss, **PIXE (Proton Indukált Röntgen Emisszió) módszer és alkalmazása az élelmiszeriparban és a mezőgazdaságban**, A Debreceni Akadémiai Bizottság Agrofizikai Munkabizottságának és a Magyar Biofizikai Társaság Agro- és Élelmiszerfizikai Szekciójának tudományos Ülése, 1988. szept. 21., Szeged, Hungary

I. Borbély-Kiss, E. Koltay, Gy. Szabó, L. Zolnai **Applications of PIXE analytical method in the Van de Graaff Laboratory of the ATOMKI**, seminar lecture, 12 Oct 1988, Ustav Jaderne Fysiky CSAV, Rez (near Prague), Czechoslovakia

S. Takács, F. Ditrói, I. Mahunka, **Investigation of aluminum made by powder metallurgy by using CPAA method**, 10th Conf. on Appl. of Accelerators in Research and Industry, 7-9 Nov 1988, Denton, TX, USA

I. Mahunka, S. Takács, F. Ditrói, **Ciklotronra alapozott nukleáris módszerek és alkalmazásaik**, Felületvizsgálatok és Alkalmazásuk Fémeken és Ötvözeteken c. tudományos ülés, MTESZ Csepeli Szervezetének Műszaki Klubja, 1988. okt. 25., Csepel, Hungary

A. Fenyvesi, **A debreceni ciklotron a gyakorlat szolgálatában**, IX. Magyar Magfizikus Találkozó, 1988. okt. 20-23., Visegrád, Hungary

F. Tárkányi, **A debreceni ciklotron alkalmazási lehetőségei**, Három éves a magyarországi ciklotron c. tudományos ülés, 1988. dec. 14., ATOMKI, Debrecen

S. Mészáros, G. Halász, K. Vad, *F. J. Kedves, Sz. Balanyi, **Magnetic field dependence of I-V characteristics of high T_c superconducting ceramics**, Int. Conf. on High Temperature Superconducting Materials and Mechanism of Superconductivity, 29 Feb-4 Mar 1988, Interlaken, Switzerland

I. Cserny, **Mikroszámítógépes adatgyűjtőrendszerek elektron-spektróméterekhez**, MTA Automatikus Elemzési Munkabizottsága és a Debreceni Akadémiai Bizottság Analitikai Kémiai Munkabizottság előadói ülése, 1988. ápr. 28-29., Debrecen

D. Varga, L. Kövér, **Fotoelektron-spektroszkópia: újabb eredmények fémek és ötvözetek vizsgálatában**, Felületi Vizsgálatok és Alkalmazásuk Fémeken és Ötvözeteken c. szeminárium (Magyar Kémikusok Egyesülete), Csepeli Műszaki Klub, 1988. okt. 25., Csepel, Hungary

Earth and Cosmic Sciences, Environmental Research

K. Balogh, **A nemesgáz tömegspektrometria hazai alkalmazási lehetőségei**, Magyarhoni Földtani Társulat, 1988. szept. 2., Budapest

K. Balogh, **K/Ar dating of post-sarmatian basalts in the Carpathian basin**, Geochronologisches Kolloquium, 27-28 Oct 1988, BVFA Arsenal, Wien

K. Balogh, **K/Ar vozrast postsarmatskih bazaltov v Vengrii**, Geological Institute of Georgian Acad. of Sci., 21 Jun 1988, Tbilisi, USSR

I. Csige, *K. Péntek, *M. Veress, **Felszíni karsztos formák fejlődésének modellezése**, Radon a Környezetben, ATOMKI, 1988. máj. 27., Debrecen

*G. Géczy, I. Csige, **A barlangi légcseré egyszerű modellje a szemlőhegyi-barlangban végzett radon mérések alapján**, ibid.

I. Csige, Gy. Somogyi, I. Hunyadi, *A. M. Marenny, *G. P. Herten, **Cosmic-ray heavy ion measurements on the board of COSMOS-1468, -1514, -1667, -1837, -1887 satellites with solid state nuclear track detectors**, 11th European Cosmic-ray Symposium, 21-27 Aug 1988, Balatonfüred, Hungary

I. Csige, Gy. Somogyi, I. Hunyadi, *A. M. Marenny, *G. P. Herzen, **Cosmic-ray jet-spectra measurement on the board of COSMOS satellites**, Simposium po podvedeniyu tistogov eksperimentalnyh issledovaniy na biosputnike "Kosmos-1887", 29 Nov-1 Dec 1988, Moskva

I. Csige, **A new high resolution charge and energy determination method for energetic heavy ions in SSNTD stacks**,
1st Yugoslavian Symposium on Solid State Nuclear Track
Detectors, 28-30 Sep 1988, Beograd

J. Hakl, **The radon profile in a 270 m deep drilled well**,
ibid.

A. Kovách, **Geochronologische Daten zur Entwicklungs-geschichte des Kristallins von Sopron**, ibid.

J. Hakl, *L. Lénárt, **Radoneloszlás a miskolci egyetemi fúrt kútban**, "Bemutatózik az NME Hidrogeológiai-Mérnökgeológiai Tanszéke", Magyar Hidrológiai Előadónap, 1988. máj. 10., Miskolc, Hungary

A. Kovách, **Rb-Sr Altersbestimmung an Gesteinen der Sopron-Gebirge in NW-Ungarn**, Isotopenkolloquium Freiberg, 6-9 Sep 1988, Freiberg, DDR

*K. Szende, *M. J. Gömöri, *J. Ivancsics, *J. Verő, É. Csongor, **Une mine de fer et des fournaeux médiévaux sur le territoire de Kopháza**, 113 Congr. Nat. des Sociétés Savantes, Comité des Travaux Historiques et Scientifiques, 5-9 Apr 1988, Strasbourg, France

*A. Várhegyi, *I. Baranyi, *I. Gerzson, Gy. Somogyi, J. Hakl, I. Hunyadi, **Application of underwater radon measurements in geology**, 14th Int. Conf. on SSNTDs, 2-6 Apr 1988, Lahore, Pakistan

*I. Törőcsik, J. Hakl, **Radon mérések a Baradla barlangban**, Radon a környezetben, 1988. máj. 27., ATOMKI, Debrecen

*L. Lénárt, J. Hakl, *F. Szolga, **Radon mérések az Albaregia barlangban**, ibid.

*L. Lénárt, J. Hakl, **Radonmérések a Miskolc környéki barlangokban**, ibid.

J. Hakl, *L. Lénárt, **Radon mérések a mélyfúrású kutakban, forrásokban, talajban**; ibid.

*B. Paripás, *I. Nikl, I. Csige, I. Hunyadi, **Hogyan éljünk együtt a radonnal?**, ibid.

Gy. Somogyi, *I. Nikl, I. Csige, I. Hunyadi, **Radon aktivitás koncentrációk meghatározása hazai lakások légterében**, XIII. Sugárvédelmi Továbbképző Tanfolyam, 1988. máj. 8-10., Balatonkenese, Hungary

*I. Nikl, *I. Végvári, I. Hunyadi, I. Csige, *M. Gallyas, *Z. Gémesi, **Mátrai gázbeton blokkból épült lakások sugár-egészségügyi vizsgálata**, ibid.

I. Borbély-Kiss, E. Koltay, E. Mészáros, Gy. Szabó, **Trace elements in atmospheric aerosols over Hungary**, 12th Int. Conf. on Atmospheric Aerosols and Nucleation, 22-27 Aug 1988, Univ. of Vienna, Vienna

I. Hunyadi, Gy. Somogyi, *F. Körösi, **Neutron induced radiography with SSNTDs and its use for element micromapping in biological specimens**, 16th Int. Symposium on Autoradiography, 21-26 Aug 1988, Ulan-Ude, USSR

I. Hunyadi, Gy. Somogyi, M. Tóth-Szilágyi, **Alpha-radioactivity distribution of environmental samples measured by SSNTD technique**, *ibid.*

J. Hakl, *L. Lénárt, Gy. Somogyi, **Radon concentration in the caves of Bükk Mountains**, 1st Yugoslavian Symposium on Solid State Nuclear Track Detectors, 28-30 Sep 1988, Beograd

J. Tóth, L. Kövér, J. B. Schág, I. Borbély-Kiss, **Urban aerosol investigations using XPS**, 7th Seminar of Socialist Countries on Electron Spectroscopy, 20-24 Sep 1988, Bourgas, Bulgaria

A. Kovách, **Környezeti aktivitásszintek Debrecenben**, DOTE-ATOMKI-DAB XII. évi együttes tudományos ülése, 1988. dec. 15., Debrecen

E. Hertelendi, *G. Uchrin, *P. Ormai, **A paksi atomerőmű ¹⁴C környezeti szennyezésének mérése**, IX. Magyar Magfizikus Találkozó, 1988. okt. 20-23., Visegrád, Hungary

*G. Uchrin, *P. Ormai, E. Hertelendi, **A paksi atomerőműből a levegővel kibocsátott trícium és radiokarbon mérése**, Vegyészkonferencia, 1988. júl. 13-16., Pécs, Hungary

E. Hertelendi, *G. Uchrin, *P. Ormai, **¹⁴C released in various chemical forms with gaseous effluents from Paks nuclear power plant**, 13th Int. Radiocarbon Conf., 20-25 Jun 1988, Dubrovnik, Yugoslavia

Biological and Medical Research

I. Hunyadi, **Neutron induced autoradiography with SSNTDs and its use for element micromapping in biological specimens**, *ibid.*

L. Medveczky, J. Hakl, A. Fenyvesi, **Neutron beam depth-dose dosimetry in water phantom using ionization chamber and SSNTDs**, *ibid.*

*Cs. Béres, A. Fenyvesi, *P. Jakucs, I. Mahunka, Z. Kovács, *T. Molnár, *L. Szabó, F. Ditrói, **Application of an MGC-20 cyclotron and methods of radioecology in solution of problems of forestry and wood industry**, 10th Conf. on Appl. of Accelerators in Research and Industry, 7-9 Nov 1988, Denton, TX, USA

Z. Kovács, I. Mahunka, *J. Környei, **MGC type cyclotron in the nuclear medicine in Hungary**, 7th Int. Symposium on Radiopharmaceutical Chemistry, 4-8 Jul 1988, Groningen, The Netherlands

F. Tárkányi, *S. M. Qaim, *G. Stöcklin, **Production of ^{82}Sr via the $^{82}\text{Kr}(^3\text{He}, 3n)$ process at a compact cyclotron**, *ibid.*

P. Mikecz, Z. Kovács, *Gy. Tóth, L. Andó, F. Szelecsényi, **$^{67}\text{GaCl}_3$, $^{111}\text{InCl}_3$ intermedierek előállítására humáncélokra az ATOMKI ciklotronjával**, Debreceni Akadémiai Bizottság Kémiai Szakbizottsága Komplexkémiai Munkabizottságának tudományos ülése, 1988. ápr. 29., Debrecen

*J. Környei, *M. Horváth, *A. Pászota, *M. Lakatos, *L. Szirtes, P. Mikecz, I. Mahunka, **Iodobell kits "on the spot" labelling with ^{123}I** , Radioactive Isotope in Klinik und Forschung Symposium, 11-15 Jan 1988, Badgastein, Austria

P. Mikecz, **Polucheniya ^{123}I , ^{67}Ga , ^{111}In izotopov na MGC-20 tsiklotrone**, Metody Polucheniya Tsiklotronnykh Radioizotopov Meditsinskovo Naznacheniya Stran-Chlenov Sev. Obninka, 10-15 Oct 1988, Fei, USSR

J. Tóth, L. Kövér, J. B. Schág, I. Borbély-Kiss, **Urban aerosol investigations using XPS**, 7th Seminar of Socialist Countries on Electron Spectroscopy, 20-24 Sep 1988, Bourgas, Bulgaria A. Kovách, **Környezeti aktivitásszintek Debrecenben**, DOTE-ATOMKI-DAB XII. évi együttes tudományos ülése, 1988. dec. 15., Debrecen E. Hertelendi, *G. Uchrin, *P. Ormai, **A paksi atomerőmű ^{14}C környezeti szennyezésének mérése**, IX. Magyar Magfizikus Találkozó, 1988. okt. 20-23., Visegrád, Hungary *G. Uchrin, *P. Ormai, E. Hertelendi, **A paksi atomerőműből a levegővel kibocsátott trícium és radiokarbon mérése**, Vegyészkonferencia, 1988. júl. 13-16., Pécs, Hungary E. Hertelendi, *G. Uchrin, *P. Ormai, **^{14}C released in various chemical forms with gaseous effluents from Paks nuclear power plant**, 13th Int. Radiocarbon Conf., 20-25 Jun 1988, Dubrovnik, Yugoslavia

*A. Csejtej, *T. Márián, *T. Molnár, A. Fenyvesi, **Neutron-terápiás besugárzási lehetőségek a debreceni ciklotronnál az eddigi sugárbiológiai tapasztalatok tükrében**, Három éves a magyarországi ciklotron c. tudományos ülészak, 1988. dec. 14., ATOMKI

I. Mahunka, **Cyclotron neutron sources for medical use at ATOMKI**, Seminar talk, Institute für Nuklearmedizin, DKFZ, 8 Jun 1988, Heidelberg, FRG

*A. Csejtei, *T. Molnár, A. Fenyvesi, **A debreceni ciklotron neutronforrás sugárbiológiai jellemzői**, Fiatal Onkológusok Fóruma, 1988. jún. 17-18., Miskolc, Hungary

L. Medveczky, **Orvosi- és anyagvizsgálati képalkotások fizikai alapjai**, XIII. Sugárvédelmi Továbbképző Tanfolyam, 1988. máj. 8-10., Balatonkenese, Hungary

G. Langer, I. Berecz, S. Bohátka, *F. Sági, *L. Mózsik, **Tömegspektrométeres mérési módszer növényi gázanyagcsere "in vivo" vizsgálatára**, Mezőgazdaság gépesítése (VI. szekció: Mezőgazdasági Elektronizálás, Méréstechnika) MTA-MÉM Agrár-Műszaki Bizottság Kutatási és Fejlesztési Tanácskozása, 1988. jan. 19-20., Gödöllő, Hungary

*F. Sági, G. Langer, *L. Mózsik, F. Gáll, **A hőmérséklet és a fény-intenzitás hatása a gáz komponensek változására a búza szárának üregében**, III. Növényélettani Kongresszus, 1988. júl. 5-7., Szeged, Hungary

G. Langer, I. Berecz, S. Bohátka, S. Fekete, I. Gál, **Ten channel inlet system for MS measurements**, Yugoslavian-Austrian-Hungarian 4th Joint Vacuum Conf., 20-23 Sep 1988, Portoroz, Yugoslavia

Development of Methods and Instruments

Bacsó J., Uzonyi I., **Automatikus mintaváltó mérésvezérlés és kiértékelés REA spektrométerhez**, MTA Automatikus Elemzési Munkabizottság és a Debreceni Akadémiai Bizottság Analitikai Kémiai Munkabizottság közös előadói ülése, 1988. ápr. 29., Debrecen

E. Hertelendi, E. Csongor, L. Záborszky, J. Molnár, J. Gál, M. Györffi, S. Nagy, **Counter system for high precision ^{14}C dating**, 13th Int. Radiocarbon Conf., 20-25 un 1988, Dubrovnik, Yugoslavia

*K. Freyer, *H. C. Treutler, *K. Dietze, I. Hunyadi, Gy. Somogyi, I. Csige, **Vacuum treatment of CR-39 for the reduction of background in neutron induced autorad-iography**, 4th Conf. of Radioisot. Appl. and Radiation Processing in Industry, 19-23 Sep 1988, Leipzig, DDR and 16th Int. Symposium on Autoradiography, 21-26 Aug 1988, Ulan-Ude, USSR

L. Medveczky, J. Hakl, A. Fenyvesi, **Fast neutron radiation field measurements with SSNTDs**, *ibid.*

- I. Csige, *L. Nádor, J. Hakl, **Computer simulation for coincidences of etched nuclear particle tracks**, *ibid.*
- Z. Kormány, **Sistema programm dlya izucheniya dinamiki puchka ciklotrona MGC**, Informacionnoe Soveshchanie po Obmenu Opitom Ekspluatatsii Ciklotrona MGC-20, 24-26 May 1988, Leningrad, USSR
- A. Valek, **Opyt ekspluatatsii ciklotrona v iyai van v Debrecene**, *ibid.*
- T. Lakatos, **Adaptive digital filtering for X-ray spectrometry**, XIII. Mezhdunarodnij Simpoziya po yadernoj Elektronike, 12-18 Sep 1988, Varna, Bulgaria
- Z. Kormány, A. Valek, **Test results of the new central geometry of MGC**, 25th European Cyclotron Progress Meeting, 21-24 Sep 1988, Uppsala, Sweden
- Z. Diós, J. Gál, L. Kiss, J. Molnár, G. Pintér, I. Szabó, J. Szádai, **Quadrupole mass spectrometer for science and industry**, Adriatico Conf. on the Impact of Digital Microelectronics and Microprocessors in Particle Physics, 28-30 Mar 1988, Trieste, Italy
- I. Csige, M. Tóth-Szilágyi, *L. Nádor, *Z. Weil, J. Hakl, *I. Molnár, I. Hunyadi, **Some properties of etched alpha particle tracks in CR-39**, 1st Yugoslavian Symposium on Solid State Nuclear Track Detectors, 28-30 Sep 1988, Beograd
- L. Medveczky, **Calibration of and measurements with a neutron dosimeter consisting of fission foils and SSNTD**, *ibid.*
- F. Ditrói, S. Takács, **Program package for micro PDP-11 computer for interfacing data transfer and remote control of a CANBERRA S35-PLUS multichannel analyser**, 10th Conf. on Appl. of Accelerators in Research and Industry, 7-9 Nov 1988, Denton, TX, USA
- I. Mahunka, **Ciklotronok és alkalmazásaik**, 1988. okt. 14., Kossuth Univ., Debrecen
- J. Végh, **An XPS data evaluation program for IBM-PC**, 7th Seminar of Socialist Countries on Electron Spectroscopy, 20-24 Sep 1988, Bourgas, Bulgaria
- L. Kövér, J. Tóth, I. Cserny, *A. Itoh, **An experimental method for resolution calibration of electron spectrometers**, Yugoslavian-Austrian-Hungarian 4th Joint Vacuum Conf., 20-23 Sep 1988, Portoroz, Yugoslavia
- Cs. Trajber, I. Szabó, Z. Árvay, **A program for the control of a multiple inlet quadrupole mass spectrometer system**, *ibid.*
- S. Fekete, G. Langer, S. Bohátka, I. Gál, J. Gál, K. Sepsy, J. Szádai, **Intelligent vacuum system controller**, *ibid.*

- S. Bohátka, I. Berecz, I. Gál, G. Langer, M. Simon, **Investigation on pre- and post-filters in Quadrupole MS**, *ibid.*
- I. Berecz, S. Bohátka, I. Futó, I. Gál, G. Langer, **Gas penetration between the stages of diffusion pumps**, *ibid.*
- L. Kövér, J. Tóth, I. Cserny, **Resolution calibration in XPS using Rh metal**, 5th Int. Conf. on Quantitative Surface Analysis (QSA-5), 15-18 Nov 1988, Nat. Phys. Lab., London
- I. Valek, **Beszámoló az ATOMKI ciklotron laboratóriumának munkájáról**, IX. Magyar Magfizikus Találkozó, 1988. okt. 20-23., Visegrád, Hungary
- E. Hertelendi, É. Csongor, L. Záborszky, J. Molnár, J. Gál, M. Györffi, S. Nagy, **Sokcsatornás radiokarbon mérőrendszer**, *ibid.*
- A. Valek, **Researches and applications at the MGC in Debrecen**, Faculty of the Heavy Ions of the Univ. of Warsaw, 10 Nov 1988, Warsaw
- A. Valek, **Cyclotron in the ATOMKI: researches, applications, operation and developments**, Jefremov Scientific Research Institute of Electrophysical Apparatures, 23 Nov 1988, Leningrad, USSR
- A. Valek, **A 103 cm-es ciklotron és üzemeltetésének tapasztalatai**, Három éves a magyarországi ciklotron c. tudományos Ülésszak, 1988. dec. 14., ATOMKI, Debrecen
- G. Dajkó, **Nukleáris szűrők előállítási lehetőségének vizsgálata ciklotronon**, *ibid.*
- Z. Kormány, A. Valek, **Recent developments at the MGC of the ATOMKI**, XI. Svesoyuznoe Soveshchanie po Uskoritelyam Zaryazhnyh Tsastic, 25-27 Oct 1988, Dubna, USSR
- L. Szabó, G. Dajkó, S. Nagy, **1. Magyar Membranológiai Konferencia**, 1988. nov. 3., Tatabánya, Hungary
- I. Berecz, K. Balogh, S. Bohátka, E. Hertelendi, L. Kövér, G. Langer, **Tömegspektrometriai és elektron-spektrometriai fejlesztések**, XXXI. Magyar Színképelemző Vándorgyűlés, 1988. ján. 27-30., Szolnok, Hungary
- I. Csige, I. Hunyadi, Gy. Somogyi, *M. Fujii, **Vacuum effect on etch induction time and registration sensitivity of polymer track detectors**, 14th International Conference on SSNTDs, 2-6 Apr 1988, Lahore, Pakistan

I. Berecs, S. Bohátka, I. Gál, G. Langer, *L. Mózsaik, *F. Sági,
**Mass spectrometric analyser system for measurement of plant
gases**, 11th International Mass Spectrometry Conf., 29 Aug-2 Sep
1988, Bordeaux, France

A. Paál, K. Sepsy, B. Sulik, **Development a multichannel
analyser in eurocard system using single board microcomputer**,
Adriatico Conf. on the Impact of Digital Microelectronics and
Microprocessors in Particle Physics, 28-30 Mar 1988, Trieste,
Italy

THESES COMPLETED

Candidate of Physical Science Degree

A. Kruppa, Generalization of the GCM descripton; the cluster model of ${}^6\text{H}$ and ${}^8\text{Be}$

T. Papp, Higher order processes in ion-atom collisions

PhD in Physics

F. Szelecsényi, Production of ${}^{67}\text{Ga}$ at the MGC-20 cyclotron, Supervisor: I. Mahunka

M. Józsa, Alpha particle excited resonances in the nucleus ${}^{40}\text{Ar}$, Supervisor: E. Somorjai

Diploma works

Gy. Kiss, Development of a measuring system and a computer program for measuring and displaying the beam profile of the MGC-20 cyclotron, Supervisor: T. Lakatos

K. Varga, Observance of the Pauli-principle in the description of the $\alpha+d$ system, Supervisor: R. G. Lovas

A. Csejtei, Investigation of characteristics of cyclotron neutron sources from the point view of biomedical applications, Supervisor: I. Mahunka

SEMINARS IN THE ATOMKI

January 14

Experimental evidence for nonseparability of quantummechanical systems in irreversible processes

E. Vatai

January 28

Image of radiation field obtained by directional detection

I. Petr, Technical University of Prague, Prague

February 4

Resonances excited by alpha particles in nucleus ^{40}Ar

M. Józsa

February 11

Electron loss at large angles

A. Kövér

February 18

E2 and M2 components in X-ray transitions

T. Papp

February 25

Software systems for acquisition and evaluation of data

J. Végh

March 2 *

Heavy-ion reactions in particle physics

J. Zimányi (Central Research Institute of Physics, Budapest)

March 17

Generalization of the GCM descripton; the cluster model of ^6H and ^8Be

A. Kruppa

March 24

The evidence of the nonseparability of quantummechanical systems

R. G. Lovas

March 31

Miniature gas-expansion cooling system for semiconductors

Gy. Máthé

April 6

Some recent nuclear chemistry work at KFA Jülich, with special emphasis on the production of cyclotron radioisotopes
S. M. Qaim, KFA, Jülich, FRG

April 12 **

Photoelectron spectroscopy of adsorbed xenon (PAX) as a local work function probe
K. Wandelt, Fritz-Haber Inst., West Berlin

April 12 **

Quantitative aspects of PAX
A. Jablonski, Inst. of Phys. Chem. of the Polish Acad. of Sci., Warsaw

April 13 **

Electron transport in the surface region of solids
A. Jablonski, (see Apr 12)

April 14

Production of isotope ^{67}Ga with small cyclotron
F. Szelecsényi

April 21

The application of algebraic cluster model for light nuclei
J. Cseh and G. Lévai

April 22 **

Microprobe applications in the biomedical science
R. D. Vis, Vrije Univ., Amsterdam, The Netherlands

April 28

Computer physics
Zs. Dombrádi

May 3 **

Interaction and dynamics of composite particles
E. Schmid, Inst. für Teoretische der Univ. Tübingen, FRG

May 4 *

Microwave methods in solid-state physics
S. Bódi, Kossuth University, Debrecen

May 12
Radiative capture in light nuclei
A. Kiss

May 18 **
Description of the giant multipole resonances in a resonant RPA
T. Curuchet, Res. Inst. of Phys., Stockholm

May 19
Current Status of Solid State Nuclear Track Detectors
R. Ilic, Ljubljana, Yugoslavia

May 26
The publications and the citation index of the ATOMKI
L. Zolnai

June 2
The complex program of the JINR, Dubna till 2000
T. Fényes

June 8
Multiphoton ionization in strong electromagnetic fields
T. Aberg, Helsinki Lab. of Phys., Univ. of Technol., Espoo,
Finland

June 9
X-ray and Auger processes in high-energy heavy-ion collisions
S. Ricz

June 16
The plans and possibilities of the ATOMKI
D. Berényi

June 20 **
Electron capture processes by ion-atom collisions

June 22 **
Radiative processes induced by ion-atom collisions
T. Watanabe, Inst. of Phys. and Chem. Res. (RIKEN), Wako,
Saitama, Japan

June 22 **
Lev Landau. A portrait of a theoretical physicist
F. Janouch, Res. Inst. of Phys., Stockholm

June 22

Higher order processes in ion-atom collisions

T. Papp

June 29

System project for computerization of the administration in our institute

G. Székely

July 1 **

Ion-atom/surface collisions relevant for plasma edge studies

H. Winter, Inst. für Allgemeine Phys., TU, Wien

August 12 **

Electron rearrangement in non-relativistic and relativistic atomic collisions

R. D. Rivarola, Inst. de Fisica Rosario, Argentina

September 8

High-temperature superconductivity with Y-Ba-Cu-O ceramics

K. Vad

September 11 **

Level structure of neutron-deficient Sm, Nd and Ce isotopes and the IBA O(6) approximation

B. D. Kern, Univ. of Kentucky, Lexington, KY, USA

September 12 **

A review of the GSI e⁺e⁻ experiments and the Stanford gamma-gamma experiment

W. E. Meyerhof, Stanford Univ., Stanford, CA, USA

September 15

pn multiplett states in nucleus ¹⁰⁸In

A. Krasznahorkay

September 17 **

Development of all-aluminium alloy ultra high vacuum systems

H. Ishimaru, Nat. Lab. for High Energy Phys., Ohio-machi, Tsukuba-gun, Tokyo

September 19 **
Zero degree Auger spectroscopy
September 22
Electron correlations in heavy-ion collisions
N. Stoterfoht, Hahn-Meitner Institute (HMI), West-Berlin

September 28 *
Trends and results in the Laboratory of Neutron Physics in the JINR in Dubna
I. M. Frank (Dubna)

October 6
Cluster Conference in Kyoto 88
J. Cseh

October 13
Results with a fast, adaptive X-ray spectrometer
T. Lakatos

October 26
Electron capture to the continuum and electron loss processes
L. Gulyás

November 3
Corepolarization in odd-odd In nuclei
Zs. Dombrádi

November 10
Ionization and electron capture at low projectile energy
L. Sarkadi

November 16 *
The education of exact sciences in the Calvinist College of Debrecen
B. Szénássy (Kossuth University, Debrecen)

November 28 **
Enhanced double ionization of the 3dσ molecular orbital
V. Zoran, Centr. Inst. of Phys., Bucharest

November 25 **
Coupled channel calculations of the ionization probabilities in a relativistic, dynamic basis
I. C. Legrand, Centr. Inst. of Phys., Bucharest

November 28 **

Some recent experimental results on three-body Coulomb systems
M. G. Menendez, Univ. of Georgia, Athens, GA, USA

December 1

On the qualification of research topics and research workers
E. Koltay

December 8

The Stockholm-Debrecen collaboration
A. Paál and G. Székely

December 13 **

The interacting boson model of light nuclei
P. Van Isacker, Daresbury Lab., UK

December 22

The development of the quadrupole mass spectrometer produced by ATOMKI
J. Gál and G. Langer

Comments:

1. unindexed: hebdomadal seminars
2. * denotes: seminars at the Physical Centre of Debrecen
(which consists of Kossuth Univ., Medical Univ., ATOMKI)
3. ** denotes: seminars at the divisions and sections

AUTHOR INDEX

- Andó L. 3, 76
András L. 100
André S. 16
- Arva-Sós E. 84
- Bacsó J. 92, 94, 106
Bakulin V. A. 94
Balogh K. 84
Bang J. 36
Barneoud D. 15, 16
Bartha L. 123
Beck F. A. 13, 15, 16
Berényi D. 43, 53, 55
Borbély-Kiss I. 101
Brakoff K. 47
Brant S. 9
Bredbacka A. 20
Brenner M. 20
- Curutchet P. 36, 37
- Cseh J. 31, 33
Cserny I. 80
Csige I. 77, 87, 110
Csótó A. 35
- Dezsö B. 92
Dietze K. 110
Ditrói F. 71, 72, 73, 74, 75, 115
Dombi I. 71
Dombrádi Zs. 5, 6, 9, 22, 25
- El-Nasir S. Seif 74
El-Samman H. 16
Engstler S. 39, 41
- Fekete S. 86
Fenyvesi A. 96
Fényes T. 5, 6, 22, 25
Foin C. 16
Freyer K. 110
Fujii M. 77
- Gácsi Z. 9, 11
Genevey J. 16
Gémesi Z. 75
Gibbons J. 53
Gizon A. 13, 15, 16
Gizon J. 13, 15, 16
Grambole D. 47
Greife U. 41

Groeneveld K. O. 53, 55
Gulyás J. 5, 6
Gulyás L. 53, 55

Gyarmati B. 35
Györffi M. 86

Hakl J. 88
Halász G. 69
Heil O. 53, 55
Heiser C. 47
Herrman F. 47
Hertelendi E. 86, 103
Hunyadi I. 77, 87, 100, 110

Józsa M. 13, 16, 17, 18
Julin R. 5, 9

Kalinka G. 78
Kallman K. M. 20
Kádár I. 43
Kedves F. J. 69
Keinonen J. 1
Kibédi T. 9
Kiss A. Z. 1, 123
Kiss J. 86
Kiss L. 108
Kiss-Varga M. 78
Klamara W. 13, 15
Kochbach L. 47
Koltay E. 1, 101, 123
Kormány Z. 117, 119, 125
Kovács A. 82
Kovács P. 78
Kovács Z. 3, 98
Körösi F. 100
Kövér A. 53, 55
Kövér L. 51, 90, 121
Krasznahorkay A. 6, 9
Krauss A. 39
Kruppa A. T. 35
Kumpulainen J. 5, 6, 9

Lakatos T. 112
Langanke K. 39
Lénárt L. 88
Lévai G. 29
Liotta R. J. 36, 37
Lovas R. . 27
Lusztig G. 92

Mahunka I. 71, 72, 74, 75, 76, 96
Manngard P. 20
Máté Z. 17, 18, 20
Medveczky L. 105

Merdinger J. C. 13, 15, 16
Mészáros S. 69, 86
Mikecz P. 98
Molnár T. 96

Nagy A. 123
Neelmeijer C. 47
Neldner K. 39
Nikl I. 87

Nyakó B. M. 13, 15, 16

Oganov V. S. 94
Ormai P. 103

Paar V. 9
Papp T. 45, 47
Passoja A. 5, 9
Pálinkás J. 45, 47, 53
Pécskay Z. 84
Pintér G. 78
Pintye E. 1

Rachmanov A. S. 94
Ricz S. 43
Rolfs C. 39, 41
Rudolf W. 47

Sarkadi L. 45, 47, 53
Schröder U. 39, 41
Sellin I. A. 53
Somogyi G. 77, 87, 88, 100, 110
Somorjai E. 39
Sudár S. 3
Sulik B. 43, 57
Svingor E. 82

Szabó Gy. 53, 55, 101, 114, 123
Szelecsényi F. 3, 76, 116
Szigeti I. 92
Szilágyi S. 20
Szűcs I. 117, 119

Takács S. 71, 72, 73, 74, 75, 115
Tárkányi F. 3, 116
Tikkanen P. 1
Timár J. 5, 6, 9
Tóth Gy. 98
Tóth J. 90
Tökési K. 80, 121
Török I. 49
Treutler H. C. 110

Uchrin Gy. 103
Uzonyi I. 92, 94, 106

Vad K. 69
Vajnai T. 53
Valek A. 117, 119, 125
Varga D. 43, 80, 121
Varga K. 27
Vatai E. 63, 65, 67
Vámosi J. 119
Veress Z. 17, 18, 36
Verho E. 6
Vertse T. 18, 36, 37
Végh J. 43
Végh L. 57, 59, 61

Watanable T. 59

Zolnai L. 16, 17, 18, 19, 20, 114

Kiadja a
Magyar Tudományos Akadémia
Atommagkutató Intézete
A kiadásért és szerkesztésért felelős
Dr. Berényi Dénes, az Intézet igazgatója
Készült a Piremon kisvállalat nyomdájában
Törzsszám: 65780
Debrecen, 1989. március

